PAUL SCHERRER INSTITUT

PSI

Paul Scherrer Institut, 5232 Villigen PSI, Switzerland
Tel. +41 (0)56 310 21 11, Fax +41 (0)56 310 21 99
www.psi.ch

u b

b
UNIVERSITÄT
BERN

LABOR FÜR RADIO- UND UMWELTCHEMIE
DER UNIVERSITÄT BERN UND
DES PAUL SCHERRER INSTITUTS

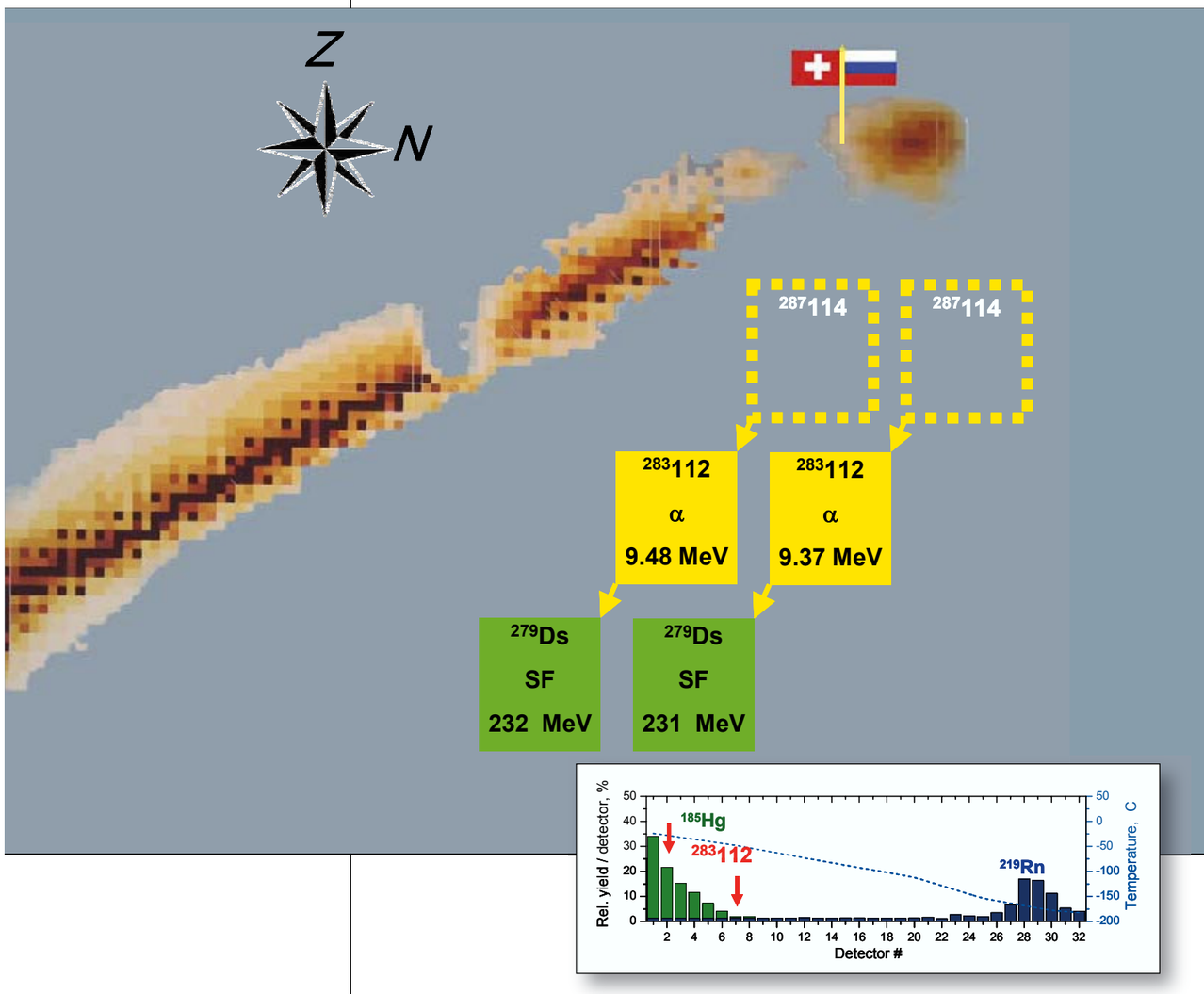

Annual Report 2006

January 2007

TABLE OF CONTENTS

Analytical Chemistry

Radwaste Analytics

Geochemistry Universität Bern

EDITORIAL

Expertise in radiochemistry can attract considerable interest caused by actual politics: the recent awareness to society that ^{210}Po may serve as radiotracer to kill people initiated some interest in this very nuclide. By chance it turned out that our laboratory has gained a lot of experience in the chemistry and spectroscopy of ^{210}Po. For dating of ice cores over the past century we usually analyse ^{210}Po to determine via the secular equilibrium the total amount of ^{210}Pb. In addition, in our research activities with superheavy elements ^{210}Po has been widely used since many years as a model for future studies of element 114!

The year 2006 was exceptional, a real *annus mirabilis*. Not only has our laboratory been successfully evaluated but also our publication record as well as our experimental activity was above average. This found its expression in three press releases from PSI and one by Bern University.
The list of outstanding events includes

- an audit on 7–9 June by an international team of experts that stressed the importance of radiochemical and environmental research currently being conducted in our laboratory. The audit team also pointed to the *win-win* situation of PSI and Bern University which in their view both profit from the synergisms between programs, facilities and personnel,

- a publication in the prestigious journal Nature on *Photosensitized reduction of nitrogen dioxide on humic acid as a source of nitrous acids*, by Konrad Stemmler et al. from the surface chemistry group, nicely showing the importance of humic acid in the atmospheric nitrogen cycle (HONO formation),

- a successful field campaign, jointly organized by Margit Schwikowski with colleagues from Chile in the extremely harsh environment of Patagonia, to retrieve in this area of the globe an ice core for climate study,

- a first ever successful chemical study of an element from the island of superheavies, Z = 112, conducted with only two observed atoms at the Flerov Laboratory of Nuclear Reactions in Dubna as a joint experiment between PSI, Bern University and FLNR,

- the organisation of a very successful European Science Foundation workshop on Exotic Radionuclides from Accelerator Waste for Science and Technology from 15–17 November, organized by Dorothea Schumann, that discussed new perspectives for future use of rare isotopes formed in spallation reactions at our 590 MeV ring machine,

- the very successful application of ^{14}C measurements in organic and elemental carbon as a tool for source apportionment in atmospheric aerosols by Soenke Szidat and his group, and last but not least, if not most important,

- the unbowed interest of students to join our laboratory for research. In the year 2006 we supervised the hitherto unrivalled number of four summer students and three diploma students.

The Bologna reform at Bern University caused a change from a diploma to the Bachelor/Master system. Therefore, we had to implement several new courses on the Master level. These extensions were only possible thanks to the help of personnel from PSI.

Heinz W. Gäggeler

CHEMICAL PROPERTIES OF ELEMENT 112

R. Eichler for a PSI-Univ. Bern-FLNR-ITE collaboration

Here we present the results of a chemistry experiment aimed at the investigation of chemical properties of element 112. The observation of two decay chains of the isotope ^{283}112 in this experiment allows for the first time an unambiguous distinction between a Rn-like and a Hg-like behaviour of element 112. Furthermore the experimental result confirms for the first time the production of elements 112, 114, and 116 in the nuclear fusion of ^{48}Ca with actinide targets as reported from the DGFRS experiments at FLNR Dubna.

1 INTRODUCTION

Since 1999 the production of about 30 new isotopes of super heavy elements (SHE) have been reported at FLNR in ^{48}Ca induced nuclear fusion reactions with actinides (see e.g. [1]) Some isotopes of the elements 112 and 114 have half-lives allowing for their chemical investigation by gas phase chemical means. There have been several attempts to investigate the isotope ^{283}112, that can be produced in the nuclear reaction ^{238}U(^{48}Ca,3n). All these attempts were not able to reproduce the results from FLNR Dubna and some of the results are contradicting (see [2-4] and references therein). The largest production cross section for the isotope ^{283}112 was reported via the nuclear fusion reaction ^{242}Pu(^{48}Ca,3n)^{287}114 [1] and the subsequent alpha decay of the short-lived primary product.

2 EXPERIMENTAL

The In-situ Volatilization and On-line detection (IVO) setup connected to the Cryo-On-Line Detector (COLD) described in [4] was used to investigate the adsorption properties of element 112 on gold simultaneously with Hg and Rn. Therefore, a stationary grid supported 1.4 mg/cm^2 ^{242}Pu target was irradiated by about 3*10^{18} particles ^{48}Ca at a center-of-target energy of 237±3 MeV. The overall efficiency estimated for a Hg-like and a Rn-like species with a half-life of about 4 s were about 11% and 9%, respectively. Additional losses may occur due to the unknown behaviour of the primary product ^{287}114 in the setup. The experiment was devided into two parts using two different temperature gradients in the COLD: A -24 to -186°C, and B: +35 to -180 °C.

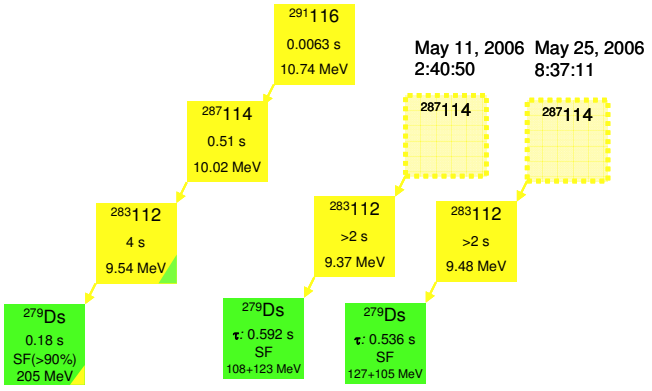

Fig. 1: Comparison of the two decay chains observed in this experiment (right chains) with the decay properties of ^{291}116, ^{287}114, ^{283}112, and ^{279}110 reported by FLNR (left chain) [1].

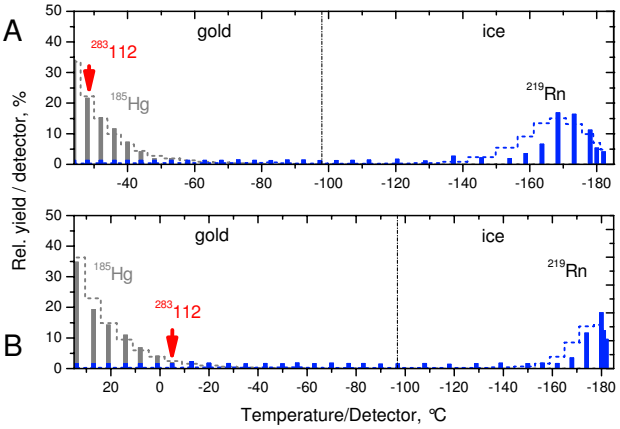

Fig. 2: Thermochromatograms of ^{185}Hg, ^{219}Rn, and ^{283}112 measured in the two applied temperature regimes A and B during the irradiation of ^{242}Pu with ^{48}Ca. The solid lines represent the Monte-Carlo simulation results [5] using $-\Delta H_{ads}^{Au}$(Hg)= -98 kJ/mol and $-\Delta H_{ads}^{Au}$(Rn)= -20 kJ/mol.

3 RESULTS

During the experimental part A for the first time in a chemistry experiment an unambiguous decay pattern attributed to ^{283}112 was observed on detector #2 (T=-28°C) (see Fig. 1). The statistical treatment of this observation based on Monte-Carlo techniques [5] revealed a clearly stronger interaction of element 112 with the gold surface compared to the noble gas radon (see Fig. 2, A). However, no distinction from Hg was possible. Therefore, in the experimental part B the temperature at the inlet of the COLD was increased. Indeed, another decay chain attributed to ^{283}112 was observed on detector #7. Only 5 % of the entire Hg was able to reach this detector. A statistical treatment allowed for the first time to determine a chemical property of element 112, namely its adsorption enthalpy on gold surfaces - $\Delta H_{ads}^{Au}(112) = 52^{+46}_{-7}$ kJ/mol, which indicates a metallic interaction of element 112 with gold comparable to its homologue Hg [6]. Beside this chemical observation, the confirmation of the decay properties of ^{283}112 and ^{279}110 anchors nuclear charges Z of the members of the decay chains observed for the isotopes ^{287}114 and ^{291}116 [1].

REFERENCES

[1] Y.T. Oganessian et al., Phys. Rev. C70, 64609 (2004).
[2] A.B. Yakushev et al. Radiochim. Acta 91, 433 (2003).
[3] K.E. Gregorich et al. Phys. Rev. C72, 14605 (2005).
[4] R. Eichler et al. Radiochim. Acta 94, 181(2006).
[5] I. Zvara Radiochim. Acta 38, 95 (1985).
[6] R. Eichler et al., Nature, submitted (2006).

SEARCH FOR ^{283}112 IN THE REACTION ^{238}U(^{48}Ca,3n)

R. Eichler for a PSI-Univ. Bern-FLNR-ITE collaboration

Here we present the results of a chemistry experiment aimed at the chemical search for ^{283}112, produced in the nuclear fusion reaction ^{238}U(^{48}Ca,3n). No decays attributed to ^{283}112 were observed in this thermochromatography experiment performed using the IVO technique. Production cross section limits were estimated and compared to data available in literature.

1 INTRODUCTION

In 1999 the production of the isotope ^{283}112 decaying by SF with a half-life of about 3-5 min was reported from the Vassilissa separator experiments using the nuclear reactions ^{48}Ca with ^{238}U and ^{242}Pu [1-3]. First gas phase chemical attempts sensitive to investigate this long-lived isotope using the ^{238}U-based reaction seemed to confirm this observation [4,5]. However, the detection of the very unspecific SF-decay as an unambiguous identification of a species is problematic. Furthermore, the energy distribution of the observed high energy events in both experiments did not show a pattern expected for the SF decay of a super heavy nucleus. Moreover, new experiments using the Dubna Gas-Filled Recoil Separator (DGFRS) at FLNR observed other decay properties of ^{283}112 [6] decaying by alpha particle emission with a half-life of about 4 s. This observation queried all previous results. There have been several attempts in various laboratories to reproduce the findings from either the Vassilissa or the DGFRS experiments using the nuclear reaction ^{238}U(^{48}Ca,3n) (see [7-9] and references therein). All these attempts did not resolve the contradicting results from FLNR. In spring 2006 a new series of experiments aiming at the gas phase chemical identification of ^{283}112 using the ^{238}U(^{48}Ca,3n) reaction was started.

2 EXPERIMENTAL

A grid supported stationary 1.4 mg/cm^2 ^{238}U target was irradiated for about 4 weeks with a total beam dose of $4.5*10^{18}$ particles ^{48}Ca at a center of target energy of 237 MeV. ^{nat}Nd (15 μg/cm^2) was added to the target in order to produce the α-decaying ^{185}Hg, which has a half-life of 49 s. The collimator grid supporting the 4 μm Ti vacuum window had a transmission for the beam of about 55%. The uranium target was mounted on a copper cooling grid and faced the incident beam. The recoiling products had to pass the 1.5 μm Ti target backing and subsequently this grid. An average loss of 20% due to the target grid was determined. The volatile products were transported by a 900 ml/min carrier gas mixture of He/Ar 70%/30% through a quartz tube, containing a quartz wool plug and Ta metal, held at 850ºC by a tubular oven. This arrangement ensured the removal of the aerosol particles produced by beam induced sputtering on the beam dump and the removal of traces of oxygen and water from the carrier gas. The volatile atomic and molecular species were transported through an 8 m long PFA capillary to the thermochromatography detector COLD. The COLD detector provided an on-line event-by-event spectroscopy of adsorbed volatile species, covering a temperature gradient of -5ºC/cm from -24ºC down to -184ºC. A transport time of 3.6 s was measured for ^{185}Hg. The decay losses during the transport account for a transport efficiency of about 54% for a volatile species having a half-life of 4 s. The deposition efficiency was 100% for ^{185}Hg. The detection efficiency for a ^{283}112(α)-^{279}Ds(SF) correlation was 75%. The effective target thickness was assumed to be about 1.0 mg/cm^2 with respect to the shape of the excitation function of the reaction ^{238}U(^{48}Ca,3n)^{283}112 as reported in [4]. Target material losses of 44% per week due to beam induced sputtering were estimated using the absolute yield drop of ^{185}Hg during the irradiation. Therefore, the target was changed once in a week. The overall efficiency of the experiment was estimated for a Hg-like ^{283}112 to about 10% [10,11].

3 RESULTS

No decays attributed to ^{283}112 were observed in this experiment. From two gas phase chemical experiments, which were sensitive to detect a 4 s α-decay of ^{283}112 followed by 0.2 s SF-decay of ^{279}Ds ([9] and this work) it is possible to give an upper limit cross section of about 1.3 pb (95% c.i.) for the nuclear reaction ^{238}U(^{48}Ca,3n)^{283}112, that is statistically not in contradiction to the results reported from the DGFRS experiments [6]. All three thermochromatography experiments performed using the same nuclear reaction ([9] and this work) were sensitive to a 5-min SF-decaying ^{283}112. Hence, a production cross section limit of <0.4 pb (95% c.i.) can be deduced from the non observation of any SF in these experiments [9,11]. This limit points to a significantly lower production cross section compared to the value reported from the Vassilissa experiments [1-3]. The production cross section limits were calculated assuming no additional loss of element 112 due to its unknown chemical behaviour in the experimental setups, e.g., retention on quartz, Teflon, or tantalum. To resolve the unclear situation regarding the nuclear reaction ^{238}U(^{48}Ca,3n)^{283}112 further experiments using the Vassilissa separator or the TASCA separator [12] are required.

REFERENCES

[1] Y.T. Oganessian et al., Nature 400, 242 (1999).
[2] Y.T. Oganessian et al., Eur. Phys. J. A5, 63 (1999).
[3] Y.T. Oganessian et al., Eur. Phys. J. A19, 3 (2004).
[4] A.B.Yakushev et al. Radiochim. Acta 91, 433 (2003).
[5] H.W. Gäggeler et al., Nucl. Phys. A734 , 208 (2004).
[6] Y.T. Oganessian et al., Phys. Rev. C70, 64609 (2004).
[7] K.E. Gregorich et al., Phys. Rev. C72, 014605 (2005).
[8] S. Hofmann et al., Proc. of the Carpathian Summer School of Physics 2005, Romania 2005, eds. S. Stoica, L. Tracht, R.E. Tribble, World Scientific.
[9] R. Eichler et al., Radiochim. Acta 94, 181(2006).
[10] R. Eichler et al., Nature, submitted (2006).
[11] R. Eichler et al., Nucl. Phys. A (2006) in press.
[12] http://www-win.gsi.de/tasca/

LONG-TERM MEASUREMENTS OF SAMPLES FROM THE 115/Db EXPERIMENT

R. Dressler, D. Schumann (PSI), R. Eichler (PSI & Univ. Bern), S.V. Shishkin (FLNR)

Long-term measurements of the Db sample #4 from the 115/Db experiment in 2004 were performed. In this sample the highest SF activity assigned to ^{268}Db or ^{268}Rf was measured. Our measurements bolster the exceptional quality of the separation of the Db containing fraction from heavy actinides.

1 INTRODUCTION

In 2004 an independent confirmation of the formation of element 115 in nuclear fusion reactions using ^{48}Ca [1] was obtained in chemistry experiments performed at FLNR Dubna [2-4]. The products of the nuclear reaction ^{48}Ca(^{243}Am,3n)^{288}115 were collected for about 24 h in a copper catcher. A fraction containing Db was chemically separated. Subsequently, the α- and SF-decays of the samples were measured time resolved for up to 957 h. In nine separate experiments a total of 15 SF events were registered within the first 175 h of the measurement. These SF-decays were attributed to ^{268}Db (or to ^{268}Rf, the possible short-lived EC-decay daughter of ^{268}Db). The measurement of the non-specific SF-decay only requires the verification of an exceptional separation of other SF-activities, such as heavy actinides. Unfortunately, it was not possible to obtain significant information about the separation factor of heavy actinides from the α-spectra measured during the experiments due to vast amounts of β-decaying by-products (e.g. Sc, Nb), passing the chemical separation. Therefore, additional long-term measurements of the sample #4 obtained in this experiment [2] were performed. This sample contained the highest SF activity per beam dose. Three SF-events assigned to ^{268}Db or ^{268}Rf were registered during the first 51 h of measurement, and no additional events in the remaining 304 h registration period. This sample was selected as the most valuable candidate to proof the quality of the actinide separation.

2 EXPERIMENTAL DETAILS

The α-spectroscopic measurement of sample #4 was started on May 23, 2006, about 2 years after its preparation. The used detector (600 mm^2 PIPS) was slightly contaminated with ^{239}Pu, ^{241}Am, and ^{244}Cm from standard calibration sources. Additionally, the whole detector chamber was contaminated with ^{236}Pu and ^{232}U from previous measurements. These contaminations are clearly seen in the spectra of a 100 h background (BG) blank measurement shown in Fig. 1 (blue line). Beside these contaminations, the spectrum of the 348 h measurement of sample #4 (Fig 1. red bars) contains traces of the sputtered target material ^{243}Am and target like transfer products as ^{237}Np, $^{238\text{-}240}$Pu, and ^{244}Cm. The spontaneous fission (SF) activity of sample #4 was measured in a second setup using two detectors (2 x 300 mm^2 PIPS) in 4π counting geometry for 3600 h. No real SF events were recorded during this measurement. There were 13 single events detected in the energy range from 15 MeV to 33 MeV, which were attributed to high energetic cosmic BG. The energy calibration of this setup was done afterwards using a ^{148}Gd and ^{244}Cm source. In addition a ^{252}Cf sample was measured for several hours proofing the detection of real SF-events. The sum spectra of both detectors (blue) together with the sum of the measured SF-fragment energy distribution of ^{252}Cf (cyan) are shown in Fig. 2. The previously measured events attributed to ^{268}Db from this sample [2] are indicated too (red).

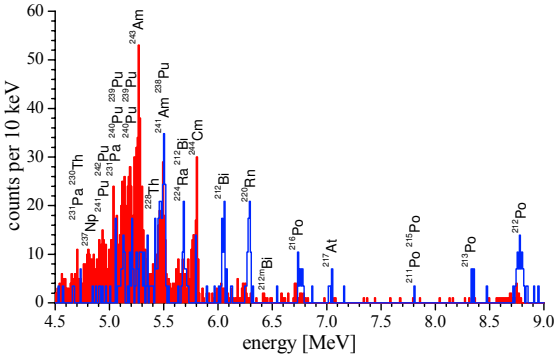

Fig. 1: α-spectrum of sample #4 measured during 348 h (red), 100 h blank spectrum (detector contamination) scaled to the same measurement time (blue).

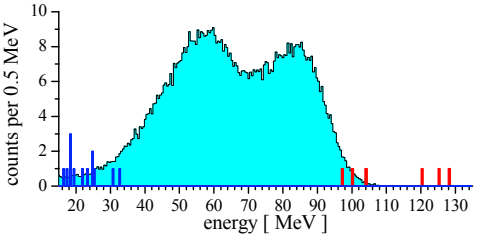

Fig. 2: SF-spectra of sample #4 measured in 4π counting geometry: originally measured SF events during 358 h (red) [2]; high energetic events measured 2 years later during 3600 h (blue); ^{252}Cf calibration spectrum (cyan).

3 RESULTS

No α-lines of heavy actinides (e.g. ^{252}Es, ^{252}Cf) are present in the BG spectrum. The original measurement [2] was divided into a part of 100 h (containing the three SF-events), and the remaining 258 h (part of the BG measurement). From the observed ^{243}Am and ^{244}Cm activities in the recent α-BG measurement (Fig. 1) $3.6\cdot10^{-6}$ and 0.043 SF-events, respectively, would be expected within 100 h. In the entire BG-measurement of sample #4 during 3858 h no additional SF-event was observed, i.e. on a 2σ level the activity of long-lived SF-decaying nuclei is $< 7.8\cdot10^{-4}$ per hour. The probability to measure one SF-event within 100 h from the identified isotopes is < 7.2%, for two and three SF-events we obtain < 0.28%, and $< 7.3\cdot10^{-3}$%, respectively. Therefore, we conclude that there is no evidence for SF- decay attributed to heavy actinide isotopes in sample #4 from the 115/Db chemistry experiment [2].

REFERENCES

[1] Y. Oganessian et al., Phys. Rev. C69, 21601(R) (2004).
[2] S. Dmitriev et al., Mendeleev Commun. 1 (2005).
[3] D. Schumann et al., Radiochim. Acta 93, 1 (2005).
[4] Y.Oganessian et al., Phys. Rev. C72, 34611 (2005).

TRANSPORT TIME OPTIMISATION OF IVO: PART I: EXPERIMENTAL RESULTS

R. Dressler, D. Piguet (PSI), A. Serov, R. Eichler (PSI & Univ. Bern)

The transport time behavior of the IVO system was optimized. A mean transport time of about 1 s is feasible.

1 INTRODUCTION

A decisive parameter of the experimental chemical investigations of transactinides is the time needed to transport nuclear reaction products from the irradiation position to the chemistry apparatus. Future experiments with ^{289}114 ($T_{1/2} \approx 2.5$ s) produced in the ^{244}Pu(^{48}Ca,3n) reaction require a speed optimization of the IVO system.

2 EXPERIMENTAL DETAILS

The transport time of ^{219}Rn emanating from an ^{227}Ac source and of short-lived Hg-isotopes (half-lives from 3.6 s to 10.8 s) produced in the nuclear reactions ^{nat}Sm(^{40}Ag, xn) $^{192-x}$Hg in the IVO system was investigated. The gas loop system [1] consists of a metal bellow pump, an expansion vessel (10 l), a 6 mm i.d. transport capillary of 10 m length to the recoil chamber, the recoil chamber (44 ml), a transport capillary of 10 m length from the recoil chamber, and the COLD detector. The carrier gas mixture of 70% He and 30% Ar is optimised to stop nuclear reaction products of ^{40}Ar or ^{48}Ca induced reactions within the small recoil chamber volume. The inner diameter as well as the temperature of the second capillary was changed during the experiment. In a first experiment series multiply the carrier gas was flushed for 1 s through the ^{219}Rn source directly before entering the recoil volume and subsequently, the source was bypassed for 20 s. The repetition pattern was controlled by the data acquisition system via an electropneumatic valve to pass or to bypass the ^{227}Ac source. The time spectra were constructed from the event by event recorded in-flight α–decays of ^{219}Rn and ^{215}Po from 6.75 MeV to 7.75 MeV (Fig. 1.). The experimental data were normalized and the 2σ counting errors indicated.

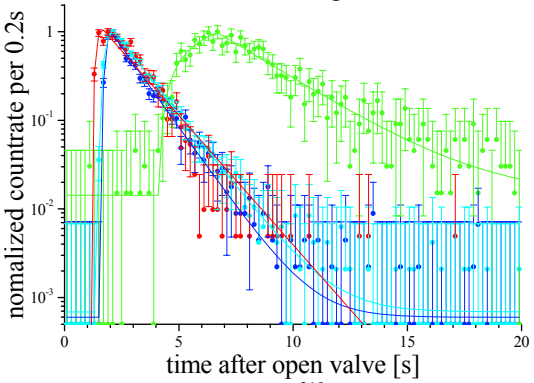

Fig. 1: Transport time spectra of ^{219}Rn (capillary at room temperature i.d. 1 mm (green), 1.56 mm (cyan), 2.00 mm (blue), capillary at 80°C (red) i.d. 1.56 mm), dots experimental, lines model fits.

The experimental parameters are compiled in Tab. 1 and 2: inner diameter of the transport capillary (i.d.), applied gas flow (Φ), as well as the deduced transport time in the capillary (τ_c), and mean flush out time of the recoil chamber (τ_r) For a description of the fit model see [2].

Tab. 1: System parameters and transport time determined in the ^{219}Rn measurements ([a] increased pump power, [b] heated column)

i.d. [mm]	Φ [l/min]	τ_c [s]	$_r$ [s]
1.00	0.460	4.15	5.19
1.56	1.739	1.49	1.72
2.00	1.849	1.62	1.52
1.56[a]	1.950	1.28	1.28
1.56[b]	2.000	1.21	2.01

In a second experiment series the production of short-lived Hg isotopes was controlled by the data acquisition system switching the beam on and off for 1 s and for 60 s, respectively. The transport time spectra were constructed from the α–events of $^{181-183}$Hg (5.65 -6.15 MeV) deposited on the gold covered detectors in the COLD. Fig. 2 shows the time spectra obtained at optimum conditions with and without heating of the transport capillary. The used transport models as well as the transport time versus capillary diameter dependency are discussed in [2].

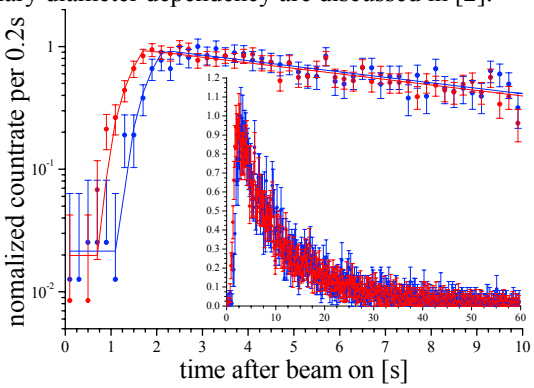

Fig. 2: Transport time spectra of Hg (capillary at room temperature (blue), at 80°C (red) i.d. 1.56 mm), dots experimental data, lines represent model fits.

Tab. 2: System parameter and transport time determined in the Hg measurements. ([a] increased pump power, [b] heated column).

i.d. [mm]	Φ [l/min]	τ_c [s]	$_r$ [s]
1.56	1.728	1.14	0.31
2.00	2.050	1.13	0.31
1.56[a]	1.875	1.03	0.31
1.56[b]	1.966	0.71	0.31

3 RESULTS

Transport times of 1.0 s – 1.3 s (50% – 75% flush-out of the recoil chamber) can be achieved for nuclear reaction products with the presently used IVO system under optimal conditions.

REFERENCES

[1] R. Eichler et al., Radiochim. Acta 94, 181(2006).
[2] R. Dressler et al., this report p. 7 (2007).

TRANSPORT TIME OPTIMISATION OF IVO: PART II: MODEL CALCULATIONS

R. Dressler, D. Piguet (PSI), A. Serov, R. Eichler (PSI & Univ. Bern)

A gas flow model was developed to describe transport time spectra measured with the IVO system as well as to understand the dependence of the transport time on the inner diameter of the transport capillary.

1 INTRODUCTION

In part I [1] the experimental data were presented obtained in the speed optimization experiments with the IVO system, which is described in detail in [2]. A theoretical model is required to determine the transport time from the experimentally measured time distributions.

2 FLOW MODEL

The transport time behaviour of the IVO system depends mainly on the effective volume of the recoil chamber in which the nuclear reaction products are thermalized and of the inner diameter (i.d.) of the transport capillary to the measurement system. In reality the flow inside the transport capillary is laminar with a parabolic velocity profile. For simplification it can be described as a plug flow, since the diffusion coefficients of the transported trace amounts of the nuclear reaction products Hg or Rn are quite high (about 10-20 mm^2/s). The flushing process of the recoil chamber can be described as an ideally mixed steering reactor. The convolution of the plug flow and the steering reactor together with the production source term and the radioactive decay is given in Eq. 1. Here $\dot{n}$ is the production rate, t_{prod} the production time, λ the decay constant, τ_r the mean time to sweep out the recoil chamber, and τ_c the plug flow time through the capillary. In addition a constant background term was used to fit the transport time spectra.

Eq. 1 was used to describe the Rn experiments (see [1]). Only the decay constant of ^{219}Rn was fixed in the fitting procedure. The production time t_{prod} was taken variable, because due to mechanical reasons the opening and closing times of the used valve was not equal. Furthermore, the flushing of the bypass capillary takes variable time in dependence of the established flow conditions. The results obtained with this model for the experiments with ^{219}Rn are given in Tab. 1 and Fig. 1 of [1].

In the case of the experiments using Hg isotopes, the activity growth and the decay of the nuclides inside the detector must be taken into account. This is done in Eq. 2. In the fitting procedure a fixed effective half-life of 6.44 s (mean value of ^{180}Hg-^{183}Hg) was introduced. Additionally, the production time had to be increased to 1.3 s to take the heating of the recoil chamber due to the Ar beam into account. The recoil range of the nuclear reaction products in the recoil chamber is well defined. Therefore, the mean time to sweep out the recoil chamber τ_r was fixed to 0.31 s. This is about 1/5 of the time determined with ^{219}Rn, which flushes through the entire chamber. The results of fitting the Hg experiments with this model are given in Tab. 2 and Fig. 2 of [1]. A qualitative description of the transport time as a function of i.d. of the used capillary can be obtained: first, the back pressure of the whole gas loop is calculated as a function of i.d. using the Hagen-Poiseuille law. Subsequently, with the flow-to-pressure characteristics of the used metal bellows pump the volume flow and the mean transport time is calculated.

The limiting cases of the experiment - only transport through the capillary (green) and sweeping out the whole recoil chamber and the capillary (red) - are plotted in Fig. 1. As expected, the experimental data are mostly in between both cases.

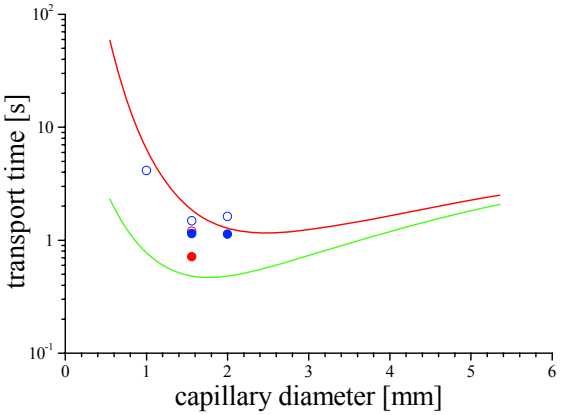

Fig. 1: Dependence of the transport time on capillary diameter: pure capillary (green line), capillary together with recoil chamber (red line), open symbols Rn, closed symbols Hg measurements, unheated capillary (blue), heated (red).

REFERENCES

[1] R. Dressler et al., this report p. 6.
[2] R. Eichler et al., Radiochim. Acta 94, 181(2006).

$$p_{transp}(t) = \frac{\dot{n}\,\mathrm{Exp}[-\tau_c\lambda]}{1+\tau_r\lambda}\begin{cases} 0 & \text{if } t<\tau_c \\ 1-\mathrm{Exp}[-(t-\tau_c)\cdot(\lambda+1/\tau_r)] & \text{if } t<t_{prod}+\tau_c \\ \mathrm{Exp}[-(t-\tau_c)\cdot(\lambda+1/\tau_r)]\cdot\left(\mathrm{Exp}[t_{prod}\cdot(\lambda+1/\tau_r)]-1\right) & \text{if } t>t_{prod}+\tau_c \end{cases} \qquad \textbf{Eq. 1}$$

$$p_{decay}(t) = \frac{\dot{n}\,\mathrm{Exp}[-\tau_c\lambda]}{1+\tau_r\lambda}\begin{cases} 0 & \text{if } t<\tau_c \\ 1+\mathrm{Exp}[-(t-\tau_c)\cdot(\lambda+1/\tau_r)]\cdot\tau_r\lambda-\mathrm{Exp}[-(t-\tau_c)\cdot\lambda]\cdot(1+\tau_r\lambda) & \text{if } t<t_{prod}+\tau_c \\ \mathrm{Exp}[-(t-\tau_c)\cdot\lambda]\cdot\left(\mathrm{Exp}[-t_{prod}\lambda]+\mathrm{Exp}[-t_{prod}/\tau_r]\cdot\tau_r\lambda-(1+\tau_r\lambda)\right) & \text{if } t>t_{prod}+\tau_c \end{cases} \qquad \textbf{Eq. 2}$$

ANION EXCHANGE SEPARATION OF Pa, Nb AND Ta IN AQUEOUS MINERALIC ACID SOLUTIONS

H. Bruchertseifer (PSI), H.W. Gäggeler (Univ. Bern & PSI), E.E. Tereshatov, N.V. Aksenov, S.V. Shishkin, G.A. Bozhikov, G.K. Vostokin, G.Y. Starodub, S.N. Dmitriev (FLNR Dubna)

A procedure to separate Pa, Nb, and Ta was developed based on strongly basic anion exchangers for application in experiments to chemically identify Dubnium. Immediately after separation from lanthanides by cation exchange the group 5 elements were fixed from aqueous fluoride solutions on top of the anion exchanger column and eluted in mineral acid fractions. This method can be used for fast preparation of sources of high purity for α-spectroscopy.

1 INTRODUCTION

The radiochemical separation of the group 5 elements can be performed on a standard cation exchange column using hydrofluoric acid solutions, which achieve excellent separations from Ln and An [1]. Nb is eluted first using very dilute fluoride solutions. The separation from Pa is complicated, due to its rapid hydrolysis in acidic solutions and competing fluoride complex formation. Adsorption losses of Nb and low distribution coefficients of their fluorides as well as impurity effects are uncertain features in this first step of the separation procedure, especially for its use on the one-atom-at-a-time limit in heavy ion irradiation experiments. A combination of cation and anion exchange separation techniques should then be a good approach to solve the above mentioned problems.

2 EXPERIMENTAL

The tracers ^{92m}Nb, ^{177}Ta, and ^{175}Hf, were produced via (α, xn) reactions using the Cyclotron U-200 at FLNR [1]. ^{233}Pa was obtained from a Np/Pa generator [2]. These nuclides were mixed with 1μg of carrier of each element and 1mg La (as $La(NO_3)_3$) and dissolved in a few ml of conc. HNO_3/HCl before solvent evaporation in a Teflon cup. The dry residue was re-dissolved in 0.2M HCl and adsorbed on a Dowex 50x8 column. The anion exchange behaviour of Nb, Ta, and Pa was investigated by loading them on a Dowex 1x8 column. Their concentrations in the eluted fractions were determined by γ- and X-ray spectrometry using standard HPGe γ- and X-ray detectors, respectively.

3 RESULTS AND CONCLUSION

The results of the experiments show that the group 5 elements in HF solutions, starting from concentrations of 5 x 10^{-4}M HF /0.2M HCl (not shown) and 1M to 7M HF (see Fig. 1) were strongly retained on an anion exchange resin. Impurities, appearing in the reagents, such as elements of the alkaline and alkaline earth groups, pass through the column without retention. Thus, efficient source purification for α-spectrometry is achieved. Subsequently, by elution with 3M HCl/1.5M HF Pa and Hf were separated from Nb. Nb can be eluted in a smaller volume (<1 ml) substituting HCl by HNO_3 in the eluent mixture (see Fig.2). Finally, Ta was desorbed with solutions not containing HF to exclude its strong adsorption on the anion exchanger (see Fig. 2). Summarizing the results of the anion exchange behaviour of the investigated fluoride complexes, two approaches can be proposed for application in experiments to characterize Db as a group 5 element of the periodic table.

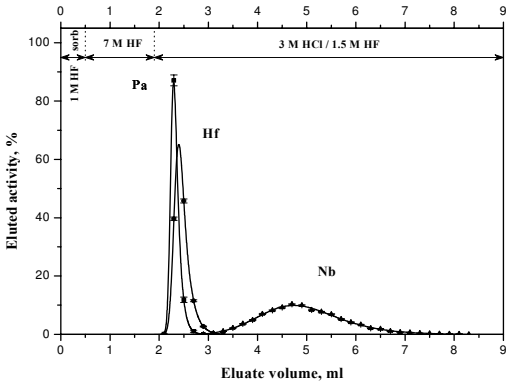

Fig. 1: Pa, Hf and Nb sorption and separation with HCl/HF solutions (Dowex 1x8, 6x10mm, 200-400 mesh)

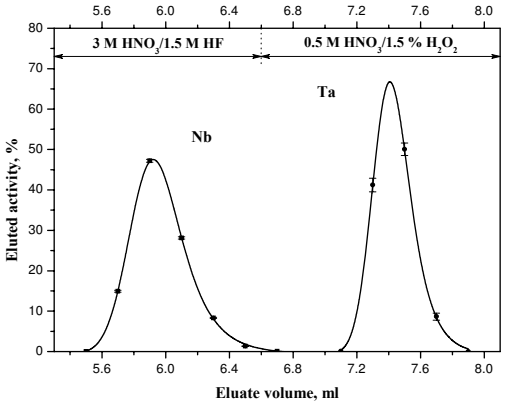

Fig. 2: Nb and Ta separation with HNO_3 /HF, H_2O_2 solutions (Dowex 1x8, 6x10mm, 200-400 mesh)

1. Separation of the three fractions of Nb/Pa , Zr/Hf, and Ta from actinides on a cation exchange column [1], followed by sorption and separation on a Dowex 1 resin column;
2. Separation of Nb, Pa, and Ta together in one fraction from the actinides on a cation exchange column with 1M HF, followed by sorption, purification, and single element desorption on a Dowex 1 resin column.

Finally, α- and SF-spectroscopic measurements can be used to identify Db in one of the separated fractions to single out its chemical properties.

REFERENCES

[1] H.Bruchertseifer et al., Ann. Rep. Labor Radio- & Umweltchemie 05, 8-9 (2006).
[2] L.I. Guseva et al. Radiochemistry **2**, 103 (1993).

IONIZATION EFFICIENCIES FOR CARBON AND NITROGEN MOLECULES IN AN ELECTRON CYCLOTRON RESONANCE ION SOURCE

H. Frånberg (Univ. Bern, PSI and ISOLDE/CERN), H. W. Gäggeler (Univ. Bern & PSI), M. Ammann (PSI), U. Köster (ILL, Grenoble), F. Wenander (ISOLDE/CERN)

Ionization efficiencies of carbon and nitrogen with a MiniMono Electron Cyclotron Resonance ion source were measured. Significantly higher ionization efficiencies were achieved than with other ion sources.

INTRODUCTION

Within the EU-RTD project TARGISOL the most suitable materials for the target and ion source unit at ISOL (Isotope Separation On-Line) facilities for the production of beams of short-lived radioactive carbon isotopes with half-lives of minutes down to ms have been investigated. Experiments have been performed at three different laboratories in Europe, PSI (Switzerland), GANIL (France) and ISOLDE (CERN). The isotopes are produced in an ISOL target by a 1.4 GeV incoming proton beam. The target (see Fig. 1) can be heated up to 2000˚C to assist the product in effusing out of the target. The atoms are transported (by diffusion) through a transfer-line and into an ion source, where they are singly ionized and extracted into a beam line for physics experiments. Carbon and nitrogen are very reactive elements and are, in elementary form, subject to losses on their way from the target to the ion source, leading to low yields for the experiments. Previous work concentrated on production, release and migration along the transfer line [1]. In this work, we report on a test of the ion source, a 1^+ electron cyclotron resonance (ECR) ion source.

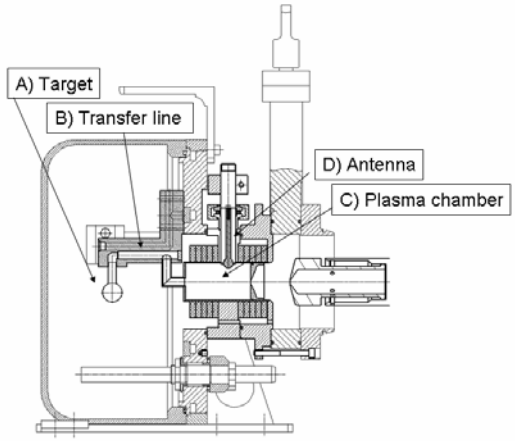

Fig. 1: MiniMono ECR ion source coupled to an ISOLDE target.

MINIMONO ECR ION SOURCE

The ECR ion source is a cold ion source, i.e., there is no hot surface inside the plasma chamber (as compared to a FEBIAD ion source) and is expected to avoid the ionization losses that were previously observed in the target and ion source unit [2]. The electrons are coming from a buffer gas which is excited with a RF field. A magnetic field around the plasma chamber is confining the plasma in the source. The radioactive atoms coming from the target are ionized in the plasma by collisions with the excited electrons. There are several different ECR ion source types with different performance to achieve ionization from 1^+ to n^+. ECR ion sources are outstanding when it comes to ionization of noble gases. At GANIL, a design for the 1^+ ECR source has been optimized with respect to efficiency and ionization rate by P. Jardin [3]. The adaptation and first experiments of ionization of noble gases with the MiniMono ECR model ion source have been performed by Gaubert et al. [4] and Wenander et al. [5]. The MiniMono ECR is constructed with mirror symmetry of two permanent magnet coils around the plasma chamber (see Fig. 1). Between the magnets there is an antenna providing a microwave frequency of 2.45 GHz for ionization of the buffer gas. The only adjustable parameters in this type of source are the RF power and the flow of the buffer gas into the source.

The tests were performed at the ISOLDE offline separator. The ionization efficiencies for He, N_2, CO and CO_2 were measured with Argon as buffer gas.

RESULTS

As the results presented in Table 1 show, ionization efficiencies of several % were achieved for carbon and nitrogen isotopes, while ionization efficiencies that were measured with an ISOLDE FEBIAD ion source were < 0.1%. Therefore, these results are very promising for future on-line experiments at ISOLDE.

Tab. 1: Measured ionization efficiencies for He, N_2, CO and CO_2 in the MiniMono ECR ion source. I_{fc} denotes the extracted current, ε_t the transmission efficiency and ε_i the ionization efficiency.

Source gas	Ion	I_{fc}	RF power	ε_t	ε_i
		μA	W	%	%
He	$^4He^+$	170	75	80	5.7
CO	$^{13}CO^+$	80	30	26	18.3
CO_2	$^{13}CO_2^+$	80	30	26	3.5
N_2	$^{14}N^{15}N$	100	30	26	5.3

REFERENCES

[1] H. Franberg et al., submitted to Radiochim. Acta.
[2] H. Franberg et al., Rev. Sci. Instrum. 77, 03A708 (2006.
[3] P. Jardin et al., Nucl. Instrum. Meth. B 204, 377 (2003).
[4] G. Gauberg et al., Rev. Sci. Instrum. 74 (2), 956 (2003).
[5] F. Wenander et al., Nucl. Phys. A 746, 659 (2004).

SYNTHESIS OF NITROGEN PEROXIDES FOR USE IN TRACER EXPERIMENTS

T. Bartels-Rausch, T. Huthwelker, M. Ammann (PSI)

HO_2NO_2 was synthesized in the gas phase by photolysis of water in presence of NO_2. To further characterize and optimize the synthesis, an existing mass spectrometer was modified and a chemical box model was developed.

INTRODUCTION

Surprisingly high concentrations of nitrogen peroxides in the air, especially HO_2NO_2, have been found in cold regions [1,2]. This is of importance, because HO_2NO_2 has the potential to impact the oxidative capacity of the atmosphere. Yet, as of today only little is known about the fate of this chemical species and its role in atmospheric chemistry. Especially, its partitioning behaviour to ice in the arctic snow pack or in cirrus clouds is not known und should therefore be investigated in the laboratory. The tracer methods used in our laboratory require a stable, clean source of HO_2NO_2 in the gas phase through a synthesis method that allows online production starting from nitrogen monoxide (NO).

For this, we intend to use UV photolysis of a humidified mixture of nitrogen dioxide in O_2 / N_2. For product identification, a new ionization procedure was implemented at our mass spectrometer to facilitate the quantification of HO_2NO_2 and several potential by-products in the gas phase simultaneously. Additionally, a chemical box model is currently developed to assist in the optimization of the HO_2NO_2 production.

MEASUREMENT OF PRODUCTS

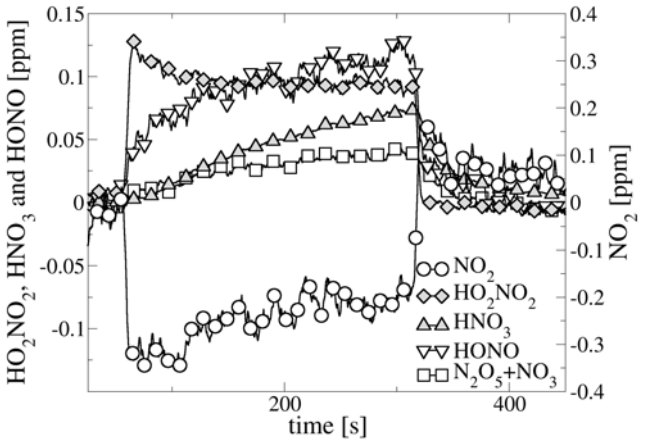

Fig. 1: Simultaneous detection of several nitrogen oxides exiting the HO_2NO_2 source.

Fig. 1 shows the change in concentrations of products exiting the HO_2NO_2 source. It can be clearly seen that in this particular run HO_2NO_2 is among the main products, but that the by-products are similar in concentration. The different nitrogen oxides were detected by the mass spectrometer after their reaction with SF_6^- at a pressure of 1 to 2 mbar. At these low pressures fragmentation of HO_2NO_2 is minimized [2]. Fragmentation results in incorrect estimates of HONO, N_2O_5 and NO_3 concentrations, because the HO_2NO_2 fragment ions are identical in mass to the products of reactions of HONO, N_2O_5 and NO_3 with SF_6^-.

MODELING THE SOURCE CHEMISTRY

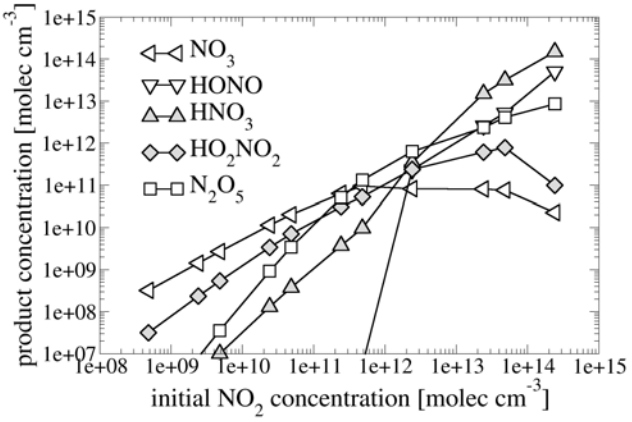

Fig. 2: Dependence of the product distribution on the initial NO_2 concentration as simulated by a chemical box model.

To further optimize the HO_2NO_2 synthesis, a simple chemical box model is currently developed. The model uses the rates of about 60 reactions to predict the concentrations of 17 species that play a role in the photolysis and in the gas phase reactions of the HO_2NO_2 source. Preliminary model runs indicate that the yield of HO_2NO_2 relative to the by-products depends on the initial NO_2 concentration. The result shown in Figure 1 was based on the reaction of 1.5 ppm initial NO_2 (app. 1e+13 molecules cm^{-3}), 23 % relative humidity, and 1 % oxygen in the gas flow through the UV excimer lamp with irradiation at 172 nm. Lowering the initial NO_2 concentration to below 10 ppb (10^{11} molecules cm^{-3}) should reduce the HNO_3 and HONO production (Fig. 2). However, the model still needs to be tuned to and compared with measurements, as for example wall losses of species are not included in the parameterisation.

In summary, we have now two tools to optimize and characterize a gas phase HO_2NO_2 source. This source will then be used to investigate the interaction of HO_2NO_2 with surfaces relevant to the atmosphere, such us ice and snow, using our radioactive tracer techniques.

REFERENCES

[1] Talbot et al., Geophys. Res. Let., 26, 3057 (1999).

[2] Slusher et al., Geophys. Res. Let., 28, 3875 (2001).

NITROGEN DIOXIDE UPTAKE KINETICS ON BASIC HYDROQUINONE AEROSOLS

Y. Sosedova (PSI & Univ. Bern), K. Stemmler (PSI), H.W. Gäggeler (PSI & Univ. Bern), M. Ammann (PSI)

The kinetics of NO_2 uptake on a basic aqueous aerosol containing hydroquinone was investigated using the short-lived radioactive tracer ^{13}N and denuder techniques. An uptake coefficient of $>10^{-3}$ was measured.

INTRODUCTION

Heterogeneous processes on aqueous aerosols can influence the budget of water soluble trace gases such as NO_2 in the atmosphere. Therefore it is important to understand the factors limiting the processing of these gases. The rate of uptake is usually described in terms of the uptake coefficient, γ_{net}, which is the probability that a gas kinetic collision actually results in its loss in the bulk aerosol phase. In the steady-state approximation, the resistance to overall uptake ($1/\gamma_{net}$) can be expressed as a superposition of the resistances to bulk accommodation ($1/\alpha$) and to bulk reaction ($1/\Gamma_b$). The mass accommodation coefficient α determines the maximum rate with which a trace gas can be processed by the aerosol surface, i.e. the maximum γ_{net}. Previous estimates for α for NO_2 on aqueous surfaces are relatively low ($10^{-4}\div10^{-3}$) [1]. In this study, we attempt to get an improved estimate for α by using a stronger solution phase sink for NO_2 than in previous studies. We used hydroquinone (1,4-dihydroxybenzene), which is present in the environment (as part of building blocks of humid acids, for instance) and shows a high reactivity toward NO_2 in its deprotonated form.

EXPERIMENTAL

The gas containing the short-lived radioactive isotope ^{13}N ($\tau_{1/2}$=10 min) was delivered to our laboratory in the form of ^{13}NO in a O_2/He mixture (for details see [2]), where it can be diluted with N_2 and mixed with non-labelled NO to cover the concentration range from 10 to 700 ppb. NO was oxidized to NO_2 over CrO_3. Traces of HONO were absorbed by the basic surface of a Na_2CO_3 coated tube prior to entering the reactor. The total gas flow of 1100 ml/min was injected into a jacketed glass flow reactor (1150 ml) through an injector. The aerosol flow (additional 1050 ml/min) entered the reactor upstream of the injector. The reaction time could be varied by changing the position of the injector (from 0.6 to 30 seconds).

The aerosol was produced by nebulizing a mixture of aqueous solutions of NaOH (2 M) and hydroquinone (1 M) in a flow of N_2, dried with a silica gel diffusion dryer, neutralized and than conditioned to the necessary relative humidity (20÷60%). This leads to a polydisperse particle distribution with a mode diameter of about 100 nm and a surface concentration of ~5×10^{10} nm^2/cm^3, which is known from the measurement with a scanning mobility particle sizer (SMPS).

To chemically separate NO_2 from the reaction mixture after the flow reactor, it was trapped in a denuder coated with a mixture of n-(1-naphtyl) diethylenediamine-dihydrochloride (NDA) and KOH. Aerosol particles were trapped using a glass fiber filter. This allowed distinguishing between the radioactive decays associated with gas phase NO_2 and that of its products on the aerosol particles.

RESULTS

A typical experimental profile is presented in Fig. 1. The counts per second resulting from the γ-decays of ^{13}N-labeled NO_2 and particulate products were recorded and inverted to the flux of these molecules to the NDA denuder or particle filter, respectively.

In absence of aerosol only the NO_2 signal on the NDA-denuder was observed, and no signal from the particle filter could be detected. In presence of aerosol, the particle signal increased steadily with increasing reaction time. An analysis of the data from this and similar experiments shows that the uptake coefficient, γ_{obs}, averaged within 30 s, was in the range of $10^{-2}\div10^{-3}$. This value was depending on the relative humidity, the hydroquinone bulk concentration and the aerosol surface area, but only to a small extent on the concentration of NO_2.

Thus γ_{net} values larger than 10^{-3} are obtained for the interaction of NO_2 with hydroquinone aerosol, which is already higher then earlier reported data, confirming that α is probably even larger than 10^{-2}.

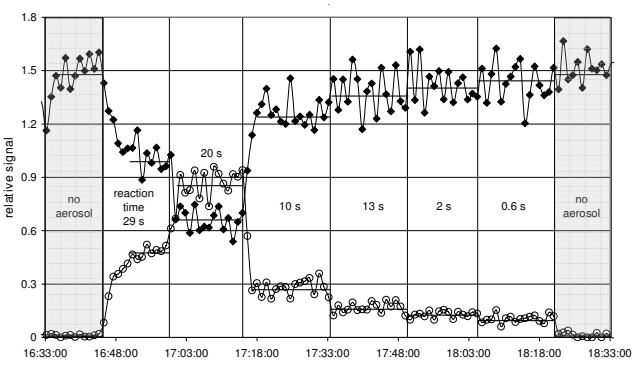

Fig. 1: Experimental profile of $^{13}NO_2$ interacting with hydrochinone sodium salt aerosol at 48% relative humidity. Plain symbols denote $^{13}NO_2$ and open symbols denote particulate ^{13}N activity. The numbers shown indicate the reaction time in presence of aerosol.

ACKNOWLEDGEMENT

The stable proton beams by the Accelerator Facilities at PSI and the service by IP-2 is highly appreciated. This project is also supported by the Swiss National Science Foundation.

REFERENCES

[1] S. Mertes, A.Wahner, J. Phys. Chem., 99, 38, 14000 (1993).

[2] M. Ammann, Radiochim. Acta, 89, 831 (2001).

PHOTOSENSITISED REDUCTION OF NITROGEN DIOXIDE ON HUMIC ACID AS A SOURCE OF NITROUS ACID

K. Stemmler, M. Ammann, M. Birrer (PSI), C. Donders (Univ. Bern), Y. Elshorbany, J. Kleffmann (Univ. Wuppertal), M. Ndour, C. George (Univ. Lyon), B. Bohn (Forschungszentrum Jülich)

The present study shows that natural surfaces containing soil or humic substances are photoreactive and react with nitrogen dioxide (NO_2) by efficiently converting it into nitrous acid (HONO). Under simulated solar irradiation the observed NO_2→HONO conversion on the surface of a soil sample is fast enough to explain the daytime HONO formation measured in the lower troposphere. The results of this study show for the first time that photochemistry on the Earth surface can significantly affect the core mechanism of atmospheric chemistry.

Nitrous acid has been measured for more than two decades in the polluted troposphere and it has been recognized as an important photolytic initiator of radical chain reactions occurring there. The sources of nitrous acid in the troposphere, however, are still poorly understood. Recent atmospheric measurements revealed a strongly enhanced formation of nitrous acid during daytime via unknown mechanisms. Humic substances represent the largest pool of organic compounds on the Earth surface. They stem from the degradation of biological materials.

Here we expose humic acids either in the form of films, as a component in natural soil, or in the form of aerosol to nitrogen dioxide in irradiated gas flow reactors and find that reduction of nitrogen dioxide on light-activated humic acid containing surfaces is a major source of gaseous nitrous acid. Fig. 1 shows a typical experimental result for the conversion of NO_2→HONO on a photo-activated 1 mg humic acid film and on 20 mg soil dust. During irradiation, we observed a substantial loss of NO_2 and a concurrent formation of HONO with a yield of about 80%, which is enhanced by a factor of 30 as compared to production in the dark.

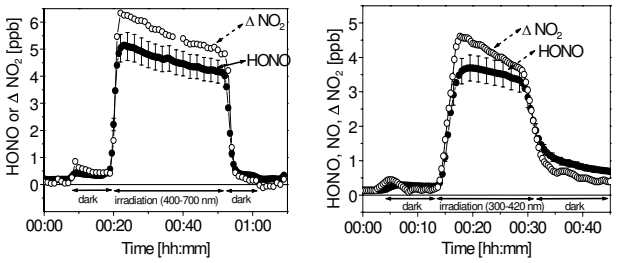

Fig. 1: Left panel: Conversion of NO_2→HONO on 1 mg films (8 μg cm^{-2}) of humic acids initiated by visible light (400-700 nm, $[NO_2]_0$=20 ppb, 20% rel. humidity, gas residence time in the reactor is 0.6 s). Right panel: Conversion of NO_2→HONO on irradiated on 20 ± 5 mg artificially acidified soil dust (pH 4.6, H_2SO_4) under UV-A irradiation (300-420 nm, $[NO_2]_0$=17 ppb, 30% rel. humidity). The filled circles represent the concentrations of HONO formed; the empty circles represent the amount of NO_2 removed during the experiment.

Fig. 2 further illustrates the photochemical nature of the heterogeneous HONO-formation. Humic acid aerosol is exposed to visible light at different intensities. No HONO formation could be detected in the dark, but an increasing HONO-formation was observed with higher light intensities.

Our findings indicate that soil and other humic acid containing surfaces exhibit a hitherto unaccounted organic surface photochemistry. In contrast to the gaseous photochemistry in the atmosphere, which is driven mainly by UV light, the photochemistry observed in this study is effectively driven by light over the entire UV and visible range of the solar irradiance spectrum.

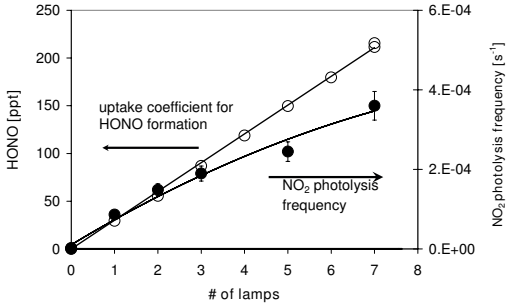

Fig. 2: HONO-formation on humic acid aerosol surfaces at different visible light intensities. The filled circles represent HONO-formation in the reactor. The empty cycles are experimentally determined NO_2→NO photolysis frequencies, indicating that the actinic flux in the reactor is proportional to the number of illuminated lamps. The measured actinic flux at full light intensity is 1.0×10^{17} photons cm^{-2} s^{-1} in the 400-750 nm range.

The observed rate of nitrous acid formation on an illuminated soil sample can explain the recently observed high daytime concentrations of nitrous acid in the boundary layer, the photolysis of which accounts for up to 60 per cent of the hydroxyl radical source strengths in the lowest part of the atmosphere. Therefore, we suggest that this photoinduced nitrous acid production on humic materials could have a significant impact on the chemistry of the lowermost troposphere. This generally most polluted part of the atmosphere is important for the oxidation of biogenic volatile organic compounds, which have a similar short atmospheric lifetime as HONO in the daytime atmosphere, and for the formation of secondary air pollutants and aerosols.

ACKNOWLEDGEMENT

This work was supported by the Swiss National Science Foundation and the European Science Foundation (project INTROP).

REFERENCE

[1] K. Stemmler et al. Nature 440, 195-198 (2006).

APPLICATION OF ^{1}H NMR TO HYGROSCOPICITY STUDIES OF ARACHIDONIC ACID PARTICLE OZONOLYSIS

O. Vesna (PSI & Univ. Bern), S. Sjogren (PSI ENE), H.W. Gäggeler (PSI & Univ. Bern), E. Weingartner (PSI ENE), V. Samburova, M. Kalberer (ETHZ), M. Ammann (PSI)

Aerosol particles consisting of the polyunsaturated organic compound arachidonic acid (AR) were reacted with ozone in a flow reactor. A correlation between the hygroscopicity of oxidized AR particles and the ratio of carboxylic acid to aliphatic groups has been observed.

INTRODUCTION

Hygroscopicity and CCN activity influence the direct and indirect aerosol effects on the Earth's radiation balance [1]. Oxidation of primary organic compounds is expected to have an effect on both. Arachidonic acid (AR), a polyunsaturated C20 fatty acid, has been used as a proxy to monitor such changes. Here we demonstrate that the hygroscopic changes can be related to a functional group analysis based on proton nuclear magnetic resonance (^{1}H NMR) without a detailed product analysis.

EXPERIMENTAL

Hygroscopicity of AR particles was measured using a Hygroscopicity Tandem Differential Mobility Analyzer (H-TDMA) [1]. The experimental set up has been fully described in the proceeding report [3], the only difference being that the sample was measured offline with ^{1}H-NMR. The AR particles were prepared in concentrations of 2×10^6 #/cm^3 by homogeneous nucleation in a condenser behind an evaporator held at 160±5 °C, respectively. The ozone concentration was varied from 0 to 1.85 ppm and the relative humidity (RH) from 0 to 83 % in the aerosol flow reactor. Particles were collected on a Teflon coated quartz fiber filter (TQFF). Extraction of the filter with deuterated dimethylsulfoxide (DMSO-d_6) and further details of sample preparation for ^{1}H NMR analysis will be given elsewhere.[4]

RESULTS

Figure 1a shows the effect of concentration on the hygroscopicity at high RH (75%) in the reactor for different ozone exposures: 0, 1.8×10^{-4}, 3.9×10^{-4}, 6.7×10^{-4} atm s. Hygroscopicity is expressed as the growth factor (GF), defined as the ratio of the particle diameter (D) at a given humidity in the H-TDMA to its diameter under dry conditions (D0). Figure 1b demonstrates the significant effect of humidity during the ozonolysis reaction at constant ozone exposure of 6.7×10^{-4} atm s on the hygroscopic growth of the processed AR particles. Thereby, the RH in the H-TDMA chamber was kept at 90% RH. The plot shows a gradual increase of hygroscopic growth from 1.01 under dry ozonolysis conditions in the reactor to 1.07 for ozonolysis at 88% RH in the reactor.

Figure 1b also includes the ratio of acid protons (-COOH) to aliphatic (-CH_n) protons in β- position and further away from the COOH groups as obtained from the corresponding peak intensities of ^{1}H NMR spectra from each sample. This ratio is characteristic for the change in the carboxylic acid group content and therefore the content of hydrophilic sites of the particles induced by ozone processing. The plot shows the gradual increase of the COOH/CH_n ratio in the aerosol with increasing RH in the flow reactor, in good correlation with measured hygroscopic GFs.

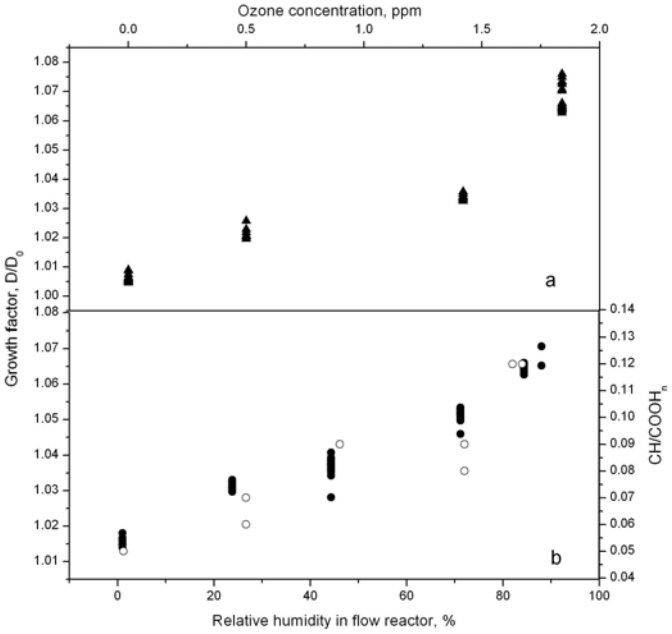

Fig. 1: [a] Hygroscopicity of oxidized AR particles as function of ozone concentration. [b] (○) COOH/CH_n ratio and (●) GF of oxidizedAR particles as function of RH in the aerosol flow reactor. The humidity in the H-TDMA measurements was 90 %. The initial ozone concentration was kept at 1.84 ppm during the experiment.

Therefore, the increased hygroscopicity is related to the increased concentration of carboxylic acids in the particles with increasing humidity during ozonolysis, which indicates that the chemical mechanism under humid conditions promotes the formation of acids more than under dry conditions.

ACKNOWLEDGEMENT

We thank T. Didenko (Laboratory of Physical Chemistry, ETH Zurich) for carrying out ^{1}H-NMR measurements.

REFERENCES

[1] V. Ramanathan et al., Science 294, 2119 (2001).
[2] O. Vesna et al., Ann. Rep. Labor Radio- & Umweltchemie, Univ. Bern & PSI (2006).
[3] E. Weingartner, Environ. Sci. Tech., 36, 55 (2002).
[4] V. Samburova, Atmos. Env., in preparation.

THE EFFECT OF BUTANOL ON THE SURFACE COMPOSITION OF DELIQUESCED POTASSIUM IODIDE: A HIGH-PRESSURE PHOTOELECTRON SPECTROSCOPY STUDY

M. J. Krisch, R. D'Auria, M.A. Brown, D.J. Tobias, J.C. Hemminger (UCI), H. Bluhm, D.E. Starr (LBNL), M. Ammann (UCI/PSI)

The depth profile of iodide on the surface of deliquesced potassium iodide in presence of butanol is investigated using high-pressure X-ray photoelectron spectroscopy. In the absence of butanol, iodide is significantly enhanced at the interface, the effect of a nearly complete monolayer of butanol is to flatten the iodide profile. Molecular dynamics simulations of butanol in an aqueous electrolyte solution observe the same effect.

INTRODUCTION

It has been suggested that enhanced anion concentrations at the liquid/vapor interface of airborne sea salt particles are important for the atmospheric chemistry of the marine boundary layer. Recent X-ray photoelectron spectroscopy (XPS) measurements taken at near ambient pressures at beamline 11.0.2 of the Advanced Light Source (ALS) at Lawrence Berkeley National Laboratory gave the first direct experimental evidence for the enhanced concentration of bromide and iodide at the surface of pure aqueous solutions [1]. The present experiments were performed on the surface of deliquesced potassium iodide in presence of 1-butanol. 1-Butanol is a model for surface active organics that are thought to be associated with marine aerosol [2]. Its behaviour in water and its surfactant properties are reasonably well established, while only little is known about its mixtures with halide solutions.

EXPERIMENTAL

The principle of the photoemission spectrometer allowing investigation of samples at pressures of up to 10 torr has been described in detail elsewhere [1,3]. The tunability of the X-ray source allows photoelectron spectra to be taken as a function of incident photon energy. As the photoelectron escape depth is a well established function of kinetic energy, the probing depth can be varied in this way, and depth profiles of individual elements can be obtained [1].

For the experiments presented here, a vacuum cleaved KI single crystal was transferred to the UHV chamber, which was first pumped to a pressure of about 10^{-11} Torr. Water vapor was admitted to the chamber through a leak valve to maintain a pressure around 2 Torr. The relative humidity over the sample was increased to the deliquescence point by lowering the sample temperature from room temperature to between -9 and -12°C. 1-Butanol was added into the chamber through a second leak valve, either together with the water vapor or after the sample surface was deliquesced. The vapor pressure of butanol was measured using a baratron and a quadrupole mass spectrometer attached to the chamber. It was adjusted to about 0.2 Torr, which is expected to lead to a butanol : water ratio of about 0.05 in the aqueous phase (assuming Henry's Law for a salt free solution). At these concentrations, a nearly complete monolayer of butanol is expected to form on the surface [4].

XPS spectra of O1s, C1s, I4d and K2p were taken at different photon energies to obtain measurements at kinetic energies between 150 eV and 800 eV. O1s and C1s spectra were deconvoluted to obtain separate contributions by gas phase water and butanol.

RESULTS

The addition of 1-butanol to an aqueous potassium iodide solution modifies the interfacial profile of ions at the liquid - vapor interface. Fig. 1 clearly shows that the surface enhancement of iodide anions, an effect observed in aqueous potassium iodide solutions, disappears in the presence of 1-butanol. The accumulation of butanol at the surface is in line with expectations from its surfactant properties.

These results are also in agreement with molecular dynamics simulations (not shown). They indicate that butanol is preferentially oriented with the OH head group into the aqueous interface and that it appears to interact with both the anion and the cation. Also the orientation of the water molecules at the interface seems to change in presence of butanol.

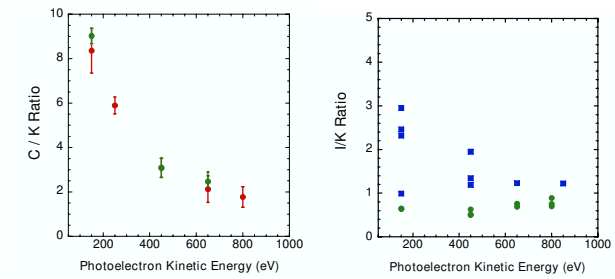

Fig. 1: C/K and I/K elemental ratios as a function of photoelectron kinetic energy (i.e., probing depth). The left plot shows the ratio of condensed phase butanol carbon to potassium in presence of gas phase butanol either added together with water (red symbols) or sequentially (green symbols). The right plot shows the iodide to potassium ratio in presence (green) or absence of butanol (blue).

ACKNOWLEDGEMENT

M. Ammann would like to thank the AirUCI institute and Prof. B.J. Finlayson-Pitts for generous support.

REFERENCES

[1] S. Ghosal et al., Science 307, 563 (2005).
[2] D.J. Donaldson and V. Vaida, Chem. Rev. 106, 1445, 2006.
3 H. Bluhm et al., J. El. Spectr. Rel. Phen. 150, 86, 2006.
[4] B.E. Wyslouzil, Phys. Chem. Chem. Phys. 8, 54, 2006.

A CLIMATE CELL FOR THE X-RAY MICROSCOPE AT THE POLLUX BEAMLINE

T. Huthwelker, M. Birrer (PSI), J. Raabe (PSI SLS), G. Tzvetkov (PSI SLS & Univ. Erlangen-Nürnberg), M. Ammann (PSI)

Using soft X-Ray microspectroscopy, the chemical environment of small samples can be studied with a spatial resolution as small as 40 nm. To study high vapour pressure condensed matter with this technique, a prototype for a climate cell was developed for the newly built scanning X-Ray microscope at the PolLux beamline. Samples can be studied under a controlled gas phase.

INTRODUCTION

Soft X-Ray radiation (ca. 100-1000 eV) can be used to characterize carbon and oxygen containing soft condensed matter [1]. High vapour pressure condensed matter, with vapour pressures up to a few Torr, is of interest in many fields. Examples include natural and artificial aerosols, which are mixtures of inorganic salts, aqueous solutions with organic compounds, biological cells, but also substances used in technical applications, such as lubricants. Typically, in an X-Ray microscope, samples are kept in vacuum or under a helium atmosphere to minimize the absorption of the X-Ray radiation in the gas phase. Hence, to study high vapour condensed matter under realistic conditions, a small cell for the sample with a defined gas phase is required.

EXPERIMENTAL

In X-Ray transmission microscopy, a well focussed beam of photons is used. Using a zone plate, the beam is focussed to about 35 nm spot size. The transmitted intensity is detected behind the sample. The sample is moved with a high precision sample mount perpendicular to the beam direction to produce scanned images of the sample. The whole setup is very small, as the distance between sample and zone plate, is on the order of 500 μm. Furthermore, a pinhole, the so-called order sorting aperture (OSA) must be brought between sample and zone plate. Also the detector must be positioned as close as possible behind the sample to avoid loss of intensity.

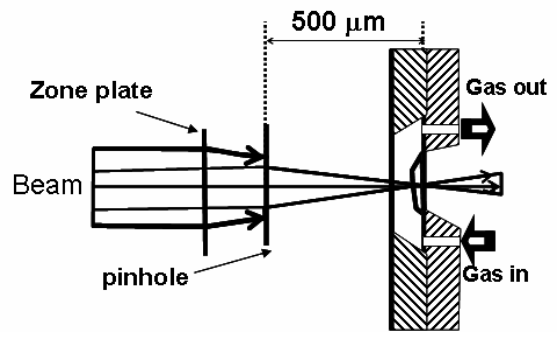

Fig. 1: Conceptual drawing of the climate cell.

Following concepts as described by Drake et al. [2], a cell was designed from a sandwich of two silicon wafers of 100μm thickness, as shown schematically in Fig. 1 and as a photograph in Fig. 2. Each of the wafers is covered with a 100 nm thick layer of silicon nitride, which serves as window for the X-Ray radiation. The cell is closed airtight by gluing it to a sample mount.

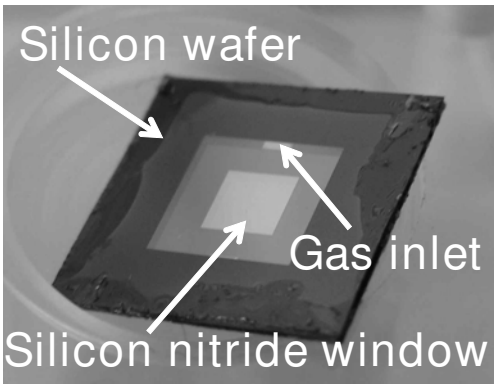

Fig. 2: Photograph of the climate cell. The two silicon nitride wafers are glued to each other.

RESULTS

A proof of concept experiment has been performed using thin films of an ammonium sulphate / adipic acid mixture. A droplet of an aqueous solution of both substances was carefully brought onto the silicon nitride window and dried. Fig. 3 shows the response of the film to changes in the gas phase humidity. The spectrum marked as 'dry' is taken with dry Helium flowing though the cell. The spectrum labelled as 'humid' is taken at a humidity high enough to deliquesce the salt film.

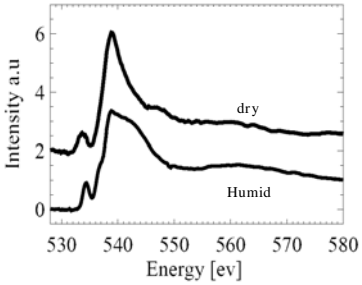

Fig. 3: Oxygen K-edge spectrum of an ammonium sulphate / adipic acid film kept under dry and humid conditions in the climate cell.

REFERENCES

[1] H. Ade et al., Europhys. Lett., 45, 529-532 (1999).

[2] I.J. Drake et al., Rev. Sci. Instr., 75, 10, 3243 (2004).

THE ADSORPTION OF ACETONE ON ICE STUDIED BY X-RAY PHOTOELECTRON SPECTROSCOPY

H. Bluhm, D.E. Starr (LBNL), M. Ammann (UCI/PSI)

The adsorption of acetone on ice is investigated using ambient pressure X-ray photoelectron spectroscopy. This is the first direct spectroscopic evidence for adsorption on ice under atmospherically relevant conditions. Observed coverages are in agreement with flow tube studies and with a simple Langmuir adsorption model.

INTRODUCTION

It has been well established that chemical processes on ice in snow and cirrus clouds are important for atmospheric chemistry, biogeochemical cycling of trace constituents and archiving of trace species in ice [1]. Acetone has been observed as a product of photochemical reactions above polar snowpacks, and its partitioning behaviour has also been suggested to affect the HOx budget in the upper troposphere. Driven by the importance of such processes, adsorption of acetone has been extensively studied recently using methods, where its partitioning to ice surfaces is measured indirectly by observing its depletion in the gas phase above the ice surface. Sofar, no direct spectroscopic evidence of an adsorbed species on ice under atmospherically relevant conditions is available, nor is information about the ice substrate and the influence of adsorbates on it. X-ray photoelectron spectroscopy (XPS), which probes core level electrons, is a well established tool for surface chemical analysis under UHV conditions. Experiments performed at beam line 11.0.2 at the Advanced Light Source (ALS) at Lawrence Berkeley National Laboratory have demonstrated that this well established surface sensitivity of XPS can be convincingly applied to the surfaces of high vapour pressure condensed matter [2]. In the present study, XPS experiments of acetone adsorption on ice are reported in the temperature range between 218 K and 243 K.

EXPERIMENTAL

The principle of the photoemission spectrometer allowing investigation of samples at pressures of up to 10 torr has been described in detail elsewhere [2]. The temperature-controlled sample holder was covered with a gold foil. An about 1mm thick ice film was grown on this substrate by deposition of water vapor (see Fig. 1). Acetone was then added to the chamber to reach pressures up to 0.1 torr. The acetone partial pressure was monitored using a differentially-pumped quadrupole mass spectrometer attached to the chamber. O1s and C1s spectra were taken while stepwise increasing the acetone pressure at a given temperature. Gas phase spectra of acetone were also taken for reference.

RESULTS

Figure 1 shows typical C1s spectra for adsorbed acetone, which are split in binding energy due to different oxidation states in the methyl and carbonyl groups. The peaks are broader than the gas phase reference spectra. The binding energy difference between the carbonyl and methyl C1s peaks is larger by 0.36 eV for adsorbed acetone than for gas phase acetone, indicating either adsorbate-adsorbate interactions or charge transfer from the carbonyl group to the ice substrate. Fig. 1 also shows that the C1s peak intensity monotonously increases with increasing acetone partial pressures. The data fit reasonably well to a simple Langmuir adsorption isotherm. A Van't Hoff plot of the Langmuir constant as a function of temperature yields an adsorption enthalpy of about 45 kJ/mol, which is well within the range reported in other studies [4]. Auger electron yield near edge X-ray absorption spectroscopy (NEXAFS) experiments (not shown) reveal that the O K-edge spectra, which are sensitive to the hydrogen bonding in ice [3], are not affected by the presence of acetone, indicating a weak acetone-ice interaction, in agreement with the relatively low adsorption enthalpy.

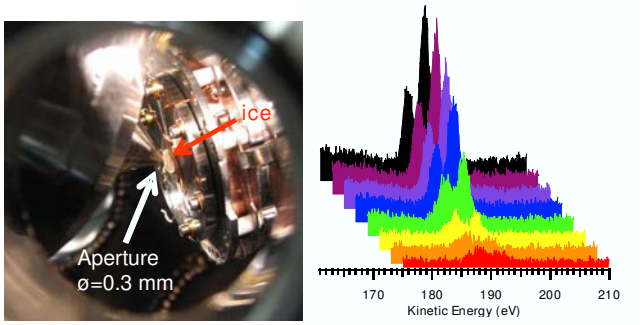

Fig. 1: Left: View of the sample holder with the ice film in the XPS chamber. The cone, through which photoelectrons are sampled into a differentially pumped lens system and the electron analyzer, is at about 0.5mm above the sample. Right: representative C1s photoelectron spectra of adsorbed acetone, with the colors coding increasing acetone partial pressure. The two peaks are due to methyl and carbonyl carbon of acetone, respectively.

ACKNOWLEDGEMENT

M. Ammann would like to thank the AirUCI institute at University of California, Irvine, and J.C. Hemminger and B.J. Finlayson-Pitts for generous support.

REFERENCES

[1] F. Domine, et al., Science 297, 1506, 2002.
[2] H. Bluhm et al., J. El. Spectr. Rel. Phen. 150, 86, 2006.
[3] H. Bluhm et al., J. Phys. Cond. Matter 14, L227, 2002.
[4] T. Bartels-Rausch et al., J. Phys. Chem. A 109, 4531, 2005.

CO-ADSORPTION OF HONO AND ACETIC ACID ON ICE

M. Kerbrat, T. Huthwelker (PSI), H.W. Gäggeler (PSI & Univ. Bern), B. Pinzer, M. Schneebeli (SLF), M. Ammann (PSI)

The uptake of gaseous nitrous acid (HONO) on ice was investigated in presence of acetic acid. It was found that the presence of an acidic co-adsorbate affects the uptake of HONO on ice.

INTRODUCTION

It has been shown that the snow pack can be a source of nitrous acid (HONO). Nonetheless, the mechanism of its production and release to the atmosphere is still not clear [1]. Here, we studied the influence of acetic acid (CH_3COOH) on the interactions of HONO with ice.

EXPERIMENTAL

The experiments were done using the PROTRAC facility [2], which provides radioactive nitrogen (^{13}N). The short-lived isotopes ($t_{1/2} \approx 10$ min) are continuously delivered in the form of nitrogen monoxide (^{13}NO). Radioactively labelled $HO^{13}NO$ is synthesized online from ^{13}NO before being injected into the packed ice column. Gaseous acetic acid was obtained by passing a small amount of nitrogen over pure acetic acid, which was kept far below its melting point. A schematic representation of the experimental set-up is show on Fig. 1.

The ice spheres were produced by spraying small droplets of ultra pure water (MilliQ) into liquid nitrogen and were subsequently annealed at -20°C.

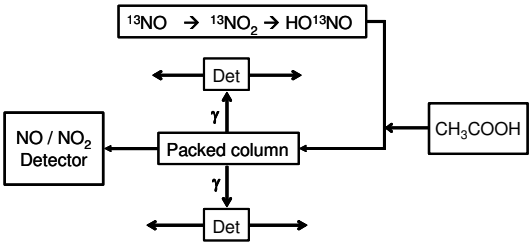

Fig. 1: Simplified experimental set up.

During an experiment, the ice column is continuously scanned by two gamma detectors. A profile of activity measured along the column is shown in Fig. 2. It represents the distribution of $HO^{13}NO$. The retention of HONO on the ice is calculated from such a profile. The migration velocity of a species through the column is given by

$$\frac{dx}{dt} = \frac{u}{1+k_i}, \qquad (1)$$

where u is the velocity of the carrier gas and $k_i = n_{ads} / n_{gas}$ is the partitioning coefficient. The rate of decay of ^{13}N is given by

$$\frac{dN}{dt} = -\lambda N, \qquad (2)$$

where λ is the decay constant of ^{13}N ($\lambda = 0.00116$ s $^{-1}$). Integration of the coupled equations (1) and (2) leads to

$$\ln N = -\frac{\lambda(k_i+1)}{u}x + \ln N_0 . \qquad (3)$$

Therefore plotting the natural logarithm of the count rate as a function of the distance along the column gives rise to a straight line and k_i can be calculated from the slope.

RESULTS

Fig. 2 shows the distribution of HONO for a concentration in the gas phase of 5.5 ppb, before and after adding the acetic acid. The partitioning coefficient varies from k_i = 6880 for pure ice to k_i = 3130 when a concentration of 60 ppb of acetic acid is added. This concentration corresponds to a coverage of 30% of a monolayer at this temperature [3]. Under these conditions, the amount of HONO on the ice is about 2.2 less than on pure ice.

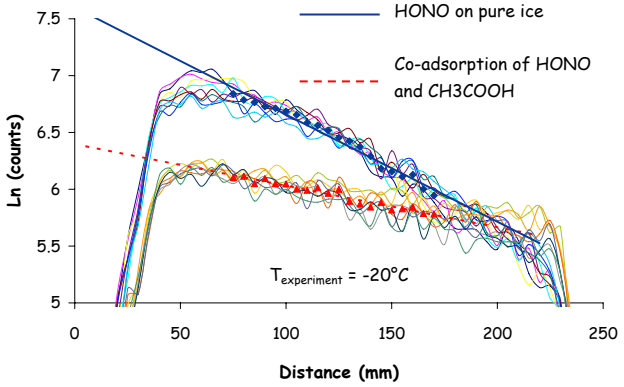

Fig. 2: Profiles of $HO^{13}NO$ in presence and absence of acetic acid.

There are two phenomena, which could explain the difference in HONO uptake. On the first hand, it can be explained by considering a competition for adsorption sites. On the other hand, if the adsorption process depends on surface pH, a competition for H^+ protons may have to be considered. Acetic Acid being a weaker acid (pK_a = 4.8) than HONO (pK_{a1} = 2.2, pK_{a2} = 3.3), this hypothesis will be investigated soon using a stronger acid as co-adsorbate.

Anyway, this study shows that the presence of acetic acid is likely to affect the release of gaseous HONO, and increases its concentration over a contaminated snow pack.

ACKNOWLEDGEMENT

This project is supported by the Swiss National Science Foundation. We appreciate the stable beams from the PSI accelerator facilities and the service by IP-2.

REFERENCES

[1] H.J. Beine et al, Atmos. Chem. Phys., 6, 2569 (2006).

[2] M. Ammann, Radiochim. Acta, 89, 831 (2001).

[3] S. Picaud et al, J. Chem. Phys., 122, (2005).

IS THE ICE SURFACE OF SNOW SMOOTH UNDER ALPINE CONDITIONS?

M. Kerbrat (PSI), B. Pinzer (SLF), T. Huthwelker, M. Birrer, M. Ammann (PSI),
H.W. Gäggeler (PSI & Univ. Bern), M. Schneebeli (SLF)

The presence of micro- or nanostructure on the ice surface of snow was investigated by measuring its specific surface area (SSA), which is a parameter depending on surface structures. Two methods allowing measuring SSA but having a different spatial resolution were used. The results were compared and no difference was found showing that the ice surface of snow is smooth up to a scale of 30 µm under alpine conditions.

INTRODUCTION

The structure of the ice surface of snow is related to its specific surface area (SSA), which is an important parameter when studying heterogeneous chemical reactions in snow and its metamorphism. Nonetheless, the presence or not of micro- or nanostructure on the ice surface of snow is still unclear. To shed some light on this question, the SSA of 5 different snow types from Davos, Switzerland, was measured using two methods whose spatial resolution is different. The adsorption method has a molecular resolution, whereas the X-Ray computer tomography (μCT) has a 30µm resolution.

EXPERIMENTAL

Three of the 5 types of investigated snow were prepared by sieving fresh snow after precipitation into boxes to ensure homogeneous samples. The boxes were stored at three different temperatures, allowing for equitemperature metamorphism at three different rates and were named: fresh snow (*fs*), metamorphosed I (*mI*), and metamorphosed II (*mII*). Two more snow types were collected in the field just before the measurements, denoted 'depth hoar' (*dh*), and 'wet snow' (*ws*).

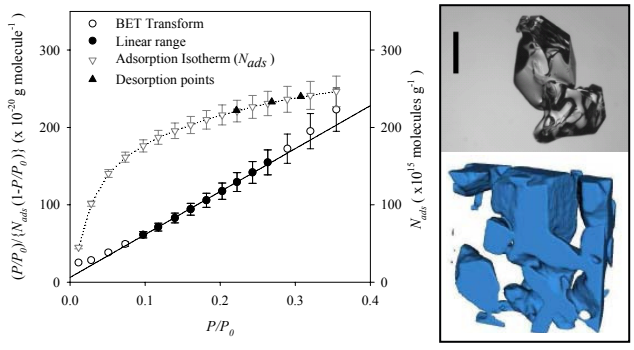

Fig. 1: Left panel: methane adsorption isotherm and its BET transform. Right panel: picture (upper part) of a depth hoar crystal together with its tomogram (lower part).

The adsorption method to determine the SSA of snow using methane has been described by Legagneux et al. [1]. In short, a small amount of gaseous methane is filled into a defined volume. Methane is then expanded into the evacuated sample holder kept at liquid nitrogen temperature, which contains the snow. The number of molecules, which has adsorbed on the snow surface, is assessed from the difference in the gas phase molar budget of methane before and after the expansion. An isotherm of adsorption is obtained by stepwise increasing the pressure of methane over snow, as shown in Fig. 1. Each isotherm obtained is subsequently processed applying the BET model [2].

For the second method, we used a modified Scanco µCT 80 desktop X-ray computer tomograph with a microfocus X-ray source to scan the snow samples. A 180° rotation of the sample was divided into 1000 steps. At each angular step, a 1024 x 128 CCD detector captured the absorption signal during an integration time of 250 ms, and averaged over two periods in order to reduce the noise. The apparatus resides in a cold room at -15 °C. A 3D image is reconstructed from the slices obtained during the scan. An example of such an image is shown in Fig. 1.

RESULTS

The results of the measurements are shown in Fig. 2. Although the two techniques used here are based on two different physical concepts, the correlation factor between both methods was found to be 1.03(±0.03), for SSA values ranging between 50 and 700 cm^2g^{-1}. The spatial resolution of the adsorption method is at the molecular level, while the effective resolution of the µCT is about 30 µm. Thus, the very good agreement between both measurements excludes the presence of micrometer or nanometer sized surface structures, which would remain undetected with the µCT. Consequently, our measurements prove that the ice surface in snow is smooth up to a scale of about 30 µm.

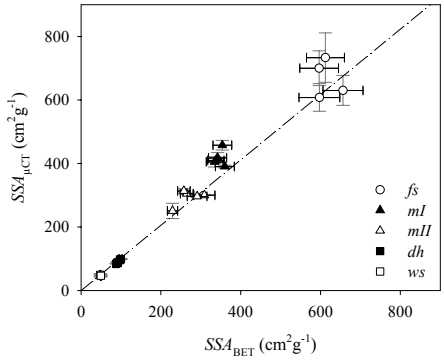

Fig. 2: Correlation between surface areas derived by methane adsorption (SSA_{BET}) and tomography ($SSA_{\mu CT}$).

ACKNOWLEDGEMENT

This work is supported by the Swiss National Science Foundation.

REFERENCES

[1] L. Legagneux et al., J. Geophys. Res., 107, 4335 (2002).
[2] S. Brunauer et al., J. Am. Chem. Soc., 60, 309 (1938).

DOMINANT IMPACT OF RESIDENTIAL WOOD BURNING ON PARTICULATE MATTER IN ALPINE VALLEYS DURING WINTER

S. Szidat (Univ. Bern & PSI), A.S.H. Prévôt, J. Sandradewi, M.R. Alfarra, U. Baltensperger (PSI LAC), H.-A. Synal (ETHZ & PSI), L. Wacker (ETHZ)

Within the project AEROWOOD (Aerosols from wood burning versus other sources), ^{14}C was used for source apportionment of carbonaceous aerosols at two Swiss Alpine valleys during winter. 88% and 65% of the carbonaceous matter originated from nonfossil sources inside and outside of the village, respectively, which is mainly attributed to wood burning.

1 INTRODUCTION

Carbonaceous aerosols as a major component of the total fine particulate matter (PM) burden comprise a huge variety of compounds [1]. Anthropogenic activities like fossil-fuel usage and biomass burning as well as natural processes like plant abrasion and secondary particle formation by atmospheric oxidation of biogenic precursors are identified as the major sources of the carbonaceous PM. Radiocarbon (^{14}C, $T_{1/2} = 5730$ a) measurements of the carbonaceous aerosol offer the opportunity of a direct distinction of fossil and nonfossil sources. Due to its age, ^{14}C has completely disintegrated in fossil substances, whereas modern plant material is on the contemporary radiocarbon level [2, 3].

2 METHODS

During January 2005, sampling was conducted in the center of the village of Roveredo in the Mesolcina Valley at a location close to the San Bernardino transit route. In February 2005, aerosol collection was carried out at a parking lot near the Gotthard transit route in the Reviera Valley, 800 m northeast of the small village of Moleno. Traffic emissions should be more important at this site due to the higher traffic density, whereas the influence from residential wood burning is assumed to be larger at Roveredo.

Fossil and nonfossil sources of organic carbon (OC) and elemental carbon (EC) were distinguished using ^{14}C determinations as described in detail elsewhere [2]. The organic mass (OM) and elemental carbon mass (ECM) was calculated from the carbonaceous particle fractions using these conversion factors [4]: 1.1 for all EC sources, 1.4 for fossil OC, and 2.25 for nonfossil OC.

3 RESULTS AND DISCUSSION

Figure 1 shows that $OM_{nonfossil}$ was the largest fraction independent of sampling site and daytime. Due to the lack of other sources of nonfossil OM, this fraction can be attributed to wood burning. This contribution is caused by the traditional usage of wood stoves for residential heating in this area and corroborated by strong inversion conditions in the narrow valleys. $OM_{nonfossil}$ contributions were higher during evening hours, when heating activities increased. On the other hand, OM_{fossil} showed higher percentages during the morning, whereas during evening hours, values decreased and even fell below the detection limit for Roveredo. As indicated by elevated fossil OM and ECM percentages, the traffic influence was generally higher at Moleno, which is consistent with the site characteristics.

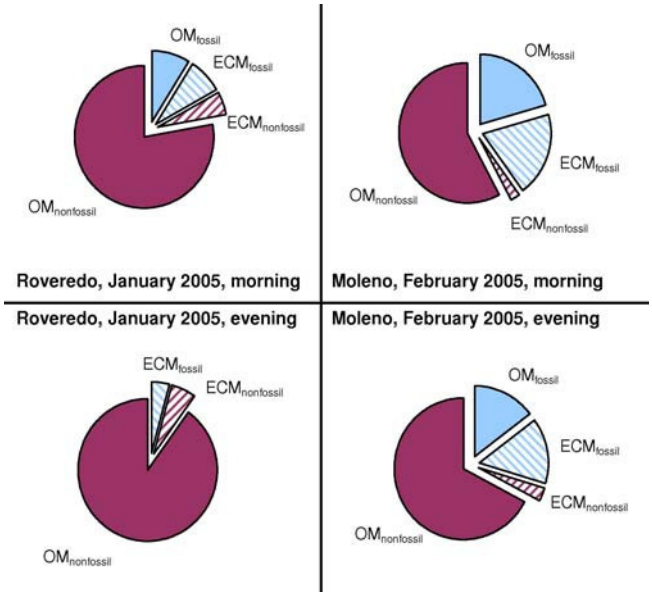

Fig. 1: Average ^{14}C-deduced contributions of fossil and nonfossil sources to the organic matter (OM) and the elemental carbon matter (ECM).

In conclusion, we observed an overwhelming impact of carbonaceous aerosols from residential wood burning on particulate matter in Alpine valleys during winter-time, which substantially surpassed traffic-related emissions even close to busy motorways. Especially at Roveredo, wood-burning emissions were dominant in spite of considerable transit traffic and aerosol sampling close to the transit route. Consequently, regulatory air quality measures are necessary for both PM sources, traffic and wood burning. However, only little attention was paid to the latter process for a long time, because the contribution of wood burning to the total energy consumption in industrialized European countries is only marginal.

REFERENCES

[1] M. Kanakidou et al., Atmos. Chem. Phys., 5, 1053 (2004).

[2] S. Szidat et al., J. Geophys. Res., 111, D07206, doi:10.1029/2005JD006590 (2006).

[3] S. Szidat et al., Radiocarbon, 46, 475 (2004).

[4] B.J. Turpin and H.-J. Lim, Aerosol Sci. Technol., 35, 602 (2001).

SOURCE APPORTIONMENT OF CARBONACEOUS AEROSOLS FOR THE WINTER SMOG EPISODE 2006 IN SWITZERLAND BASED ON RADIOCARBON (^{14}C) ANALYSIS

M. Wehrli (Univ. Bern), S. Szidat, H.W. Gäggeler, M. Ruff (Univ. Bern & PSI), L. Wacker (ETHZ), H.-A. Synal (ETHZ & PSI), J. Sandradewi, A.S.H. Prévôt, U. Baltensperger (PSI LAC)

The aerosol composition for three different sites in Switzerland was investigated for the winter smog episode in January and February 2006. Radiocarbon (^{14}C) was used as a tracer in order to identify different sources of biomass burning, fossil-fuel combustion and biogenic emissions.

INTRODUCTION

Major components of the ambient aerosol are carbonaceous particles, which originate from biogenic or anthropogenic sources. A large amount of anthropogenic emissions are caused by fossil-fuel combustion and biomass burning. In order to identify these different sources radiocarbon (^{14}C) is an important tracer. Since ^{14}C is already extinct in fossil fuels and biogenic sources emit aerosols on the present ^{14}C/^{12}C level, a direct determination of contemporary and fossil carbon in ambient aerosol is possible and enables, furthermore, an apportionment of biogenic and anthropogenic sources [1].

During the winter smog episode 2006, the daily maximum PM10 (particular matter with aerodynamic diameter <10 µm) concentration of 50 µg/m^3 according to the Swiss air quality standard was exceeded on several days. In this work we focus on the sources of carbonaceous aerosols during this episode in order to investigate the potential to reduce PM10 during similar events in the future.

METHODS

During the long-standing inversion weather conditions in January and February 2006, aerosol samples were collected on quartz fiber filters at an urban background site in Zurich, a heavily trafficked site in Reiden and a rural site at Sedel, both in the Canton Lucerne. Total carbon (TC) was subdivided into organic carbon (OC) and elemental carbon (EC) using a thermal method described in [2] and ^{14}C was then measured with accelerator mass spectrometry (AMS) at ETH Zurich.

RESULTS AND DISCUSSION

The aerosol composition for Reiden, Sedel and Zurich was very similar for the winter smog episode in Switzerland in January and February 2006. Carbonaceous particles contributed to ~40 % of PM10, whereof the contingents of OC and EC were 0.78 and 0.22, respectively (Fig. 1). On the average, EC consisted of 26 % biomass-burning and 74 % fossil material. On the other hand, OC was composed of 29 % fossil and 71 % nonfossil particles.

Time series indicated a maximum of >160 µg/m^3 PM10 on 31 January/1 February. The source apportionment with ^{14}C suggests an accumulation of local aerosols, due to the inversion weather conditions. There are indications that primary emissions from biomass-burning contributed only on a reduced scale to total particle mass on these days.

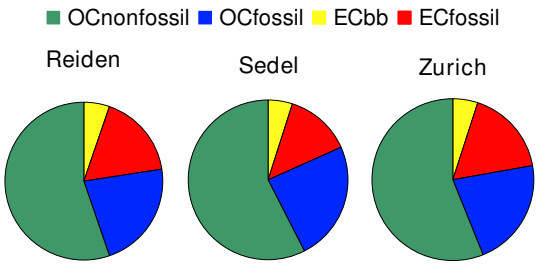

Fig. 1: Average percentage contributions of fossil and biomass-burning (bb) sources to EC and fossil and nonfossil sources to OC for Reiden, Sedel and Zurich in January and February 2006.

Biomass-burning EC was found to be mainly covered in PM1, whereas the EC in the coarse mode (particles with aerodynamic diameter between 1 and 10 µm) was predominantly fossil and originated possibly from tyre abrasion particles (Fig. 2).

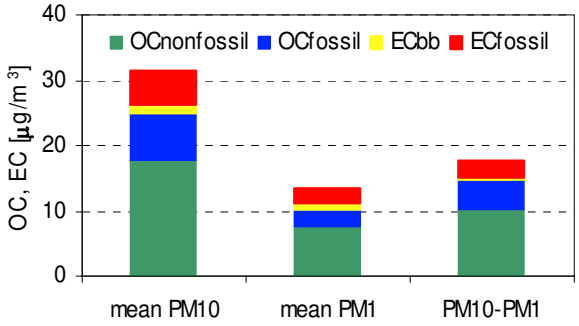

Fig. 2: Mean concentrations of nonfossil OC, fossil OC, biomass-burning EC and fossil EC for PM10 and PM1 filters collected at Zurich in January 2006.

ACKNOWLEDGEMENT

This work was supported by BAFU and Canton of Lucerne.

REFERENCES

[1] S. Szidat et al., Radiocarbon 46, 475 (2004).

[2] S. Szidat et al., Nucl. Instr. Meth. Phys. Res. B 223-224, 829 (2004).

[3] S. Szidat et al., J. Geophys. Res. 111, D07206 (2006).

AN INLET SYSTEM FOR SEMI-AUTOMATED GAS MEASUREMENTS OF RADIOCARBON

M. Ruff, S. Szidat, H.W. Gäggeler (Univ. Bern & PSI),
H.-A. Synal (ETHZ & PSI), L. Wacker, M. Suter (ETHZ)

A gas inlet system for the measurement of radiocarbon in gaseous samples was installed at the Mini Radiocarbon Dating System (MICADAS), the smallest accelerator of the PSI/ETH AMS group in Zürich. The system is constructed for semi-automated measurements of small and ultra-small samples containing 1-50 µg carbon.

MOTIVATION AND PROJECT GOAL

Radiocarbon measurements of small samples (<50 µg) with accelerator mass spectrometry (AMS) offer a great potential for environmental and biomedical samples. These measurements, however, are often challenging: Small amounts of organic material are difficult to handle, contaminations during the sample preparation are common and losses, especially during the graphitisation, are well described [1]. The use of a gas ion source is an option reducing these problems and making the analysis of ultra-small samples (1-10 µg) possible.

INSTRUMENTAL SETUP

An inlet system was constructed as shown in Figure 1. The flow into the ion source is defined by the pre-pressure of the gas mixture on the fused silica capillary leading into the source. The capillary is connected via a two position valve to a 1 ml gastight syringe, the central part of the system. At one hand, the syringe serves as a movable reservoir for the gas to keep a constant pre-pressure, at the other hand the total volume is adjustable to different sample sizes. This is important because the stability of the ion source depends on a constant ratio of carbon dioxide and helium.
The gaseous sample is sealed in a glass ampoule which is stored in the ampoule cracker under vacuum conditions. By opening the ampoule the carbon dioxide is released. As the gas volume of the cracker is similar to the volume of the syringe, about half of the sample diffuses into the syringe. The rest of the carbon dioxide is flushed with helium into the syringe in several steps. In this process we reach an efficiency of 70-90 %. The semi-automated system is controlled with by a LabView program.

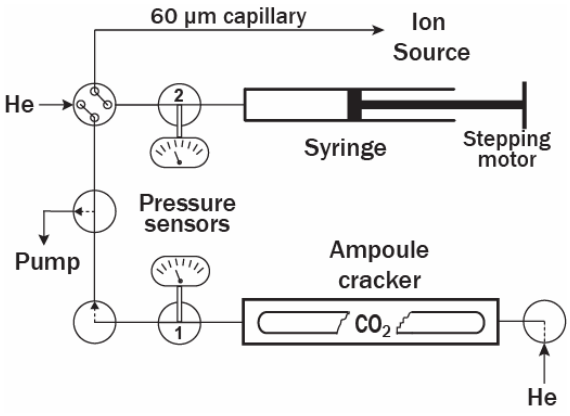

Fig. 1: Scheme of the gas inlet system [2].

RESULTS

The system is now running for a few months. During this time, two measurement cam-paigns with more than 70 small and ultra small samples could success-fully be measured. The currents we achieved for most measurements were in the range of 2.5 – 4.5 µA, with a total efficiency of 1 % of the carbon dioxide in the glass ampoule entering the detector. Figure 2 shows a typical variation of the standard samples (modern oxalid acid). 10 of 11 values are within 1 σ uncertainty, indepen-dent of the sample size (standards from 5.8 – 22.7 µg carbon). The blank values varied by a factor of 10 with an average $^{14}C/^{12}C$ ratio of 7 x 10^{-15} (older than 38.000 years). This level is a factor of 3-5 smaller compared to small samples measured as solid graphite. A further advantage is that the blank values seem to be less dependent on the sample sizes as observed for solid samples which makes data analysis much easier.

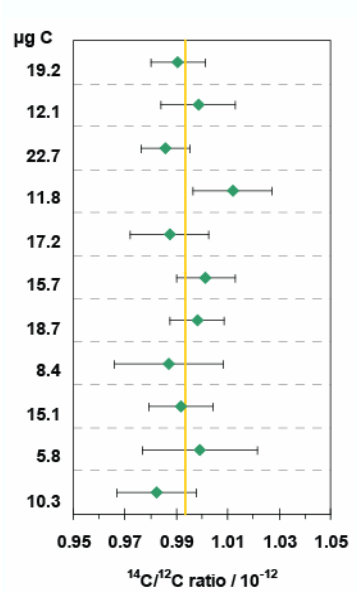

Fig. 2. Variation of the $^{14}C/^{12}C$ ratio of the OXA I standard during a measurement.

OUTLOOK

Next step is an automated combustion of sample materials by using an elemental analyser, which separates the combustion gases and isolates the carbon dioxide. This device shall directly be coupled with the gas inlet system in order to realise a fully automated system for combustion and on-line radiocarbon measurement of small organic samples.

REFERENCES

[1] T.M. Jenk et al., Nucl. Instr. Meth. Phys. Res. B, inpress.

[2] M. Ruff et al., submitted to Radiocarbon.

ICE CORE BASED RECONSTRUCTION OF HIGH-ALPINE TEMPERATURES

T.M. Jenk, H.W. Gäggeler (Univ. Bern & PSI), M. Leuenberger, P. Nyfeler (KUP),
A. Palmer (PSI, now at Univ. of Tasmania), S. Brütsch, M. Schwikowski (PSI)

In December 2002, an ice core was extracted from the Fiescherhorn-glacier. Two different approaches, the analysis of δD in the ice and the melt index were applied for the reconstruction of annual and seasonal (i.e. summer and winter) high-alpine temperatures from this natural climate archive.

Using isotope ratio mass spectrometry a continuous δD record was obtained for the ice core drilled in 2002 on the Fiescherhorn-glacier (FH, 46°33'3.2''N, 08°04'0.4''E; 3900 m asl.) [1]. The record covers the last ~320 years with a sub-seasonal resolution back to ~1800 AD. In the following, a first attempt using the δD record for the reconstruction of high-alpine annual (T_a, Fig. 1), summer (JJA, T_{JJA}) and winter (DJF, T_{DJF}) temperatures will be discussed. Additionally presented is the record of reconstructed T_{JJA} derived from a second approach which is based on the melt layer stratigraphy of the core (melt index) [2] (Fig. 2). Limited ice core quality (i.e. micro cracks in the core) did not allow the identification of ice layers in the lower part of the archive; therefore this record only reaches back to ~1850 AD.

To obtain the reconstruction of T_a (Fig. 1), the time period 1964-1969 AD - showing good correlation between reconstructed annual accumulation ($PP_{rec.}$) and instrumentally measured precipitation (PP_{annual}) - was used to establish a relationship between δD and T for the investigated area and archive. This relationship was obtained from the observed differences between maxima and minima of δD (FH) and T (instrumental data from Jungfraujoch (JFJ)), respectively. Accordingly, a change of 5.8±0.3‰ in δD represents a change of 1°C in temperature (≡0.71±0.4‰/°C for $\delta^{18}O/T$ (calculated)). This is in very good agreement with the observations at the nearby GNIP station (e.g. Grimsel: $\delta^{18}O/T$ = 0.71‰/°C). The finally derived reconstruction of T_a (Fig. 1) agrees fairly well with the available instrumental records from JFJ and Engelberg (1350 m asl.) (source Meteo-Schweiz) back to ~1910, indicating a 20th century warming of 2.0±0.2°C at this high-alpine site. Before 1910, a pronounced anomaly to higher temperatures is observed. The reconstructed T_{JJA} based on the melt index (Fig. 2) show good correlation with the instrumental data and a warming in summer temperatures of 2.6°C during the 20th century. For the time before 1910, this approach did not exhibit an anomaly to positive values, resulting in a better agreement with the instrumental data. This suggests that the δD signal observed for that time was not primarily influenced by temperature.

Possible reasons for the anomaly in the δD could be changes in air moisture origin or in the seasonality of precipitation. Back-trajectory calculations revealed that the moisture sources responsible for accumulated snow at FH were principally the Atlantic Ocean during winter and local (continental) sources during summer, at least in the investigated period September 1998 to August 1999 [3]. The reconstructed accumulation (average: 1.7 m weq yr^{-1}) was found to correlate highest with Engelberg summer PP (running 10-yr correlation back to 1910: r=0.48). This is reasonable, since PP_{JJA} is around a factor of two higher than PP_{DJF}, thus being the main season responsible for the accumulation at FH. However, no correlation was found for the period before 1910 for which lower precipitation rates and a positive shift in the summer to winter precipitation ratio is reflected in the instrumental data. This might be related to changes in the Northern Atlantic Oscillation (NAO) which affects the European continental climate [4]. The validity of the δD-T relationship (here established from a rather short calibration period of only 6 years) over long time-periods is thus questionable and further investigations for a final interpretation of the δD proxy have to be performed. A future d-excess record might thereby help to understand the factors influencing the stable isotope composition, as it is assumed to be a proxy of moisture sources (results of $\delta^{18}O$ and d-excess awaited by the end of Feb. 2007).

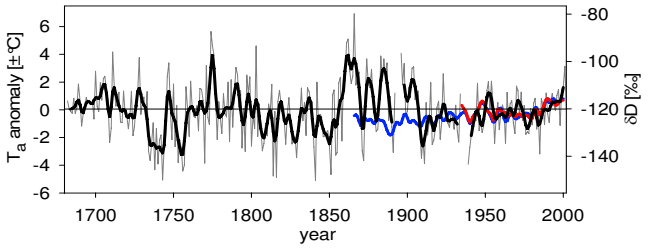

Fig. 1: Reconstructed annual temperatures (T_a) anomaly (thin line) compared with weighted running means (5 yr, thick lines) of T_a at JFJ (1933-2002, red) and Engelberg (1864-2002, blue). The right hand axis represents the corresponding δD scale and the zero line denotes the mean of the reference period 1960-2002.

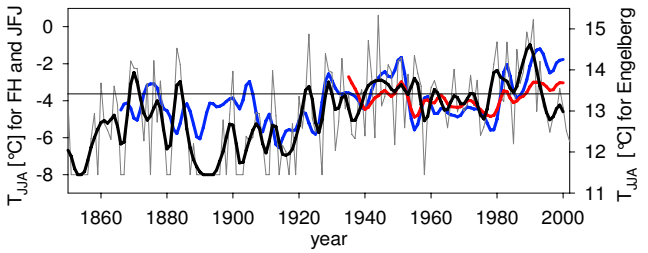

Fig. 2: Comparison of summer temperatures (T_{JJA}, weighted 5-yr running means) of at JFJ (red) and Engelberg (blue) with T_{JJA} reconstructed from the FH melt percent record (thin black line; the thick line denotes the weighted 5-yr running mean). Note the different scales. The horizontal line denotes the mean of the reference period 1960-2002.

ACKNOWLEDGEMENTS
The study was part of the NCCR Climate project VITA.

REFERENCES

[1] T.M. Jenk, PhD Thesis, Univ. Bern, 2006.
[2] K. Henderson et al., J. Geophys. Res. 111, 2006.
[3] B. Zubler, Semester Thesis, ETH Zürich, 2006.
[4] J. Luterbacher et al., Atmos. Sci. Lett. 2, 2002.

AIR POLLUTION RECORDS FROM THE FIESCHERHORN ICE CORE 2002

T.M. Jenk, H.W. Gäggeler (Univ. Bern & PSI), A. Palmer (PSI, now at Univ. of Tasmania), S. Brütsch, M. Schwikowski (PSI)

A 150 m long ice core extracted from the Fiescherhorn-glacier in 2002 revealed the history of air pollution in the Swiss alpine region. The record covers the last ~320 years (1680-2002).

In December 2002, an ice core was drilled on the Fiescherhorn-glacier (FH, 46°33'3.2''N, 08°04'0.4''E; 3900 m asl.) and analysed for concentrations of major ions (cations: Na^+, NH_4^+, K^+, Mg^{2+}, Ca^{2+}; anions: F^-, CH_3COO^-, $HCOO^-$, $CH_3SO_3^-$, Cl^-, NO_3^-, SO_4^{2-}, $C_2O_4^{2-}$) using ion chromatography (IC) [1]. The core, which reached bedrock at 150.5 m depth, was cut into 4317 samples resulting in an annually resolved record of Alpine air pollution history.

Due to the high resolution, dating of the archive could be performed using annual layer counting throughout the core, with the dating fixed by horizons such as Saharan dust layers originating from the events in 2000, 1977 and 1947 and the volcanic eruption of Katmai in 1912. By comparison with an earlier - but shorter - record from FH (1989), two additional fix-points of the chronology were derived by wiggle matching of distinctive peaks in the δD records [1, 2]. The matched peaks were attributed in the earlier core to the years of atomic nuclear tests in 1963 and 1956, based on tritium and ^{36}Cl analysis respectively [3]. The dating resulted in an age of 340±30 years at 150.5 m and which is in very good agreement with an independent dating using a physical ice flow model, considering ice-thinning and ice deformation at FH [4]. The records presented here (Fig. 1) cover only the last ~320 years (i.e. 1680-2002), since analysis of ionic species was not possible for the lowermost 40 cm of the core due to bad ice quality preventing preparation and decontamination of samples suitable for IC analysis.

Dislocation of ions to lower depths by percolating melt water was observed in the records for the time periods 1978-1998 and 1941-1946. However, as a comparison with the aerosol SO_4^{2-} concentrations from the nearby research station Jungfraujoch (JFJ) showed, these effects could be compensated by calculating 10-year averages.

Records of ions from mainly natural emission sources such as Ca^{2+}, Mg^{2+}, Na^+, Cl^- (mineral dust, sea-salt) and CH_3COO^-, $HCOO^-$, $CH_3SO_3^-$ (living biosphere, marine origin) are characterized by relatively low concentrations without trend. In contrary, the concentration records of NH_4^+, SO_4^{2-}, F^- and NO_3^- show a significant contribution from anthropogenic emission sources after the beginning of the industrialisation (~1850) (Fig. 1). The observed increase in i) NH_4^+ (~1850) concentrations is attributed to an extension in the agricultural production (fertilizers and animal manure), ii) SO_4^{2-} (~1860): the enhanced combustion of fossil fuels, iii) F^- (~1890): the aluminium production (starting 1890 in Switzerland) and more recently applications in the nuclear power plant technology and iv) NO_3^- (~1950): increasing traffic. Also in the Cl^- record, a contribution from anthropogenic emissions, i.e. from the combustion of hard coal and from the chemical industry, was detected after ~1850. The relatively low and constant concentrations before the observed increase in the above discussed ions reflect their emissions from natural sources. These are emissions from biomass burning and vegetation for NH_4^+ and NO_3^-, whereas mineral dust is a natural source for F^- (e.g. fluorspar) and SO_4^{2-} (e.g. gypsum) which also originates from sea-salt. The industrial maximum (1970-2000) to pre-industrial (1750-1850) mean concentration ratio is highest for F^- (14.0). This ratio is 4.2 for SO_4^{2-}, 3.4 for NO_3^- and 3.0 for NH_4^+. In the SO_4^{2-} and F^- records, decreasing concentrations after 1970 are attributed to air pollution control measures, aiming at reduction of emissions to the environment.

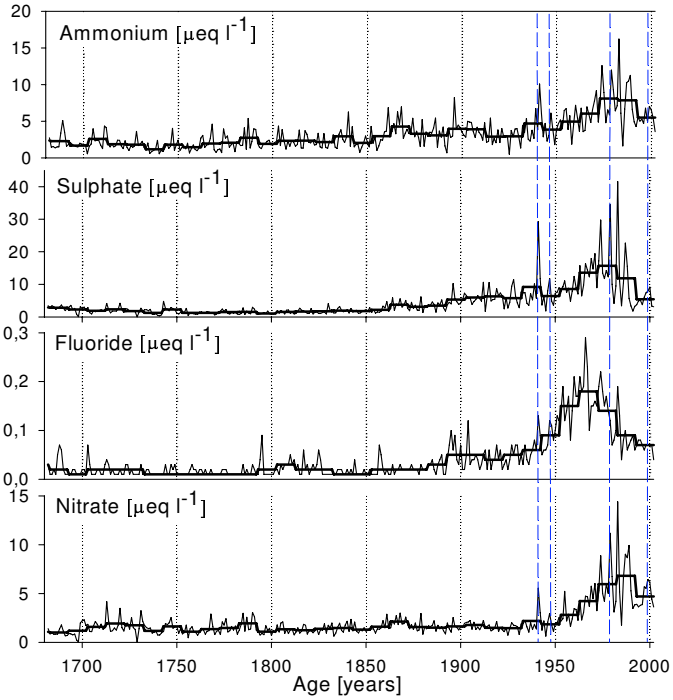

Fig. 1: Annual average concentrations (thin line) superimposed by the 10-year average (thick line) of NH_4^+, SO_4^{2-}, F^- and NO_3^-. The blue, dashed lines mark the sections influenced by percolating melt-water (see text).

ACKNOWLEDGEMENTS

The study was part of the NCCR Climate project VITA. Aerosol SO_4^{2-} concentrations from the Jungfraujoch are from the NABEL network of the BAFU.

REFERENCES

[1] T.M. Jenk, PhD Thesis, Univ. Bern , 2006.
[2] T.M Jenk et al., this issue p. 22.
[3] Schotterer et al., Proc. Int. Conf. Isotope Techniques, IAEA Vienna (1998).
[4] Schwerzmann et al., J. Geophys. Res. 111, (2006).

LONG-TERM TRENDS OF AIR POLLUTION RECORDED IN AN ICE CORE FROM COLLE GNIFETTI, SWISS ALPS

M. Sigl, T.M. Jenk, H.W. Gäggeler (PSI & Univ. Bern), C. Boutron (LGGE Grenoble), C. Barbante (Univ. Venice), D. Bolius, M. Schwikowski (PSI)

Based on studies of a high-alpine ice core from the Swiss Alps we show long-term trends of air pollution on a regional scale. Regression analysis allowed discriminating between different natural and anthropogenic sources of sulfate aerosols, which helps to answer questions associated with aerosol cooling effects on climate over time.

Air pollution in Europe has been regarded as a severe problem for decades. Not only it affects human health (e.g. smog, particulate matter) and terrestrial and aquatic ecosystems (e.g. acidification, eutrofication), but also it influences climate. In recent years it became obvious that the greenhouse gas forcing is partly compensated by several effects of aerosols in the atmosphere [1].

Ambient concentrations of aerosols and their precursors have widely been monitored in the recent past [2]. For longer timescales, emissions may be estimated by analysing past precipitation stored in glacial ice near the source regions [3].

Here we present a palaeochemistry record retrieved from a high-alpine ice core (Colle Gnifetti, 4450m a.s.l., Swiss Alps). We show deposition records of NO_3^-, NH_4^+ and SO_4^{2-} originating mostly from the emissions of NO_x, NH_3 and SO_2 and calculate the strengths of different sources of SO_4^{2-} over time.

The 82 m long ice core, drilled in 2003, contains a continuous record of past precipitation for at least the last Millennium. Ion concentrations were analysed by ion chromatography in overall 2900 subsamples.

Two time windows were chosen for this study:

- the 20th century (0-39 m; n=925)
- the time period from 1750-1870 (as a natural background level; 44-56 m; n=549).

The upper part of the ice core was dated by counting annual layers, using parameters with a high seasonal variability (e.g. NH_4^+, $\delta^{18}O$), with an accuracy of ±1-2 years. The age of the background period was derived from a glacier flow model that is fitted through well known reference horizons (e.g. Saharan dust events, 1977, 1947, 1936, 1901) and ^{14}C dating points within the lowermost part of the core [3]. For this time period the dating error is up to ±20 years.

To discriminate different sources of SO_4^{2-} we selected Na^+ as a sea-salt tracer and Ca^{2+} as a tracer for mineral dust. The sea-salt and mineral dust contributions to the SO_4^{2-} concentration were estimated by regression analysis of the background level data, taking a SO_4^{2-}/Na^+ molar ratio of 0.12 and a non-sea-salt SO_4^{2-} / non-sea-salt Ca^{2+} molar ratio of 0.194. Constant transport patterns and deposition processes over time can be assumed, as no long term concentration trend in Ca^{2+}, Mg^{2+}, Na^+ and K^+ exists.

The concentration records of SO_4^{2-}, NO_3^- and NH_4^+ all show a strong increase within the 20th century. SO_4^{2-} reached a maximum level in the early 70ies with concentrations being a factor of nine higher than the natural background. 77% of the total SO_4^{2-} depositions from 1900 on could be attributed to excess-SO_4^{2-} (total SO_4^{2-} corrected for mineral dust and sea salt contribution) originating from the emissions of SO_2 to the atmosphere. In the last 25 years the excess-SO_4^{2-} concentration decreased by a factor of two, reflecting the continuous reduction of anthropogenic emissions. The contribution of sea-salt to the SO_4^{2-} has been constant over time. In the pre-industrial period long-range transported mineral dust from the Saharan region was the dominant contributor, which accounted for 74% of the total SO_4^{2-}.

NO_3^- and NH_4^+ show both a continuously increasing long-term trend over the last 100 years with now a factor of 5 higher concentrations than the background level, underlining the drastic changes in the reactive parts of the N-cycle observed in the recent past [4]. The main sources are emissions through traffic and agriculture. Aerosol mass-wise the combined reactive nitrogen species have overtaken the sulphur species in recent years, which is remarkable and important, especially for estimating aerosol effects on climate.

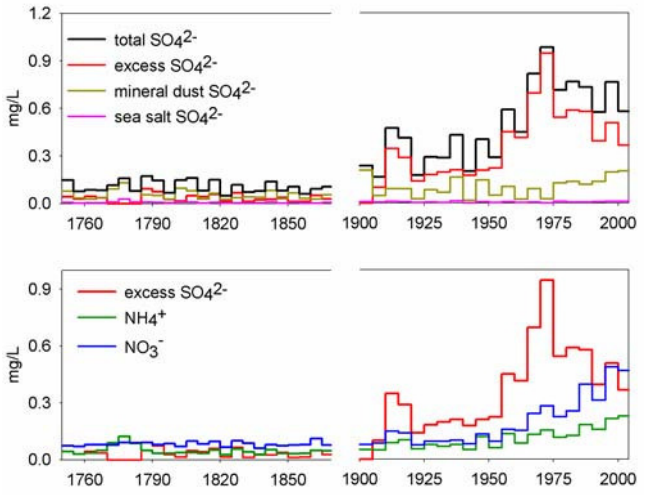

Fig. 1: (Top) concentration record of SO_4^{2-} and contribution from different sources; (bottom) concentration record of excess SO_4^{2-}, NO_3^- and NH_4^+.

ACKNOWLEDGEMENT

This study is part of the NCCR Climate project VIVALDI.

REFEERENCES

[1] M. Andreae et al., Nature, 435, 1187-1190 (2005).

[2] E. Berge et al., J. of Env. Man., 57, 31-50 (1999).

[3] M. Schwikowski et al., Tellus, 51B, 938-951 (1999).

[4] T.M. Jenk, PhD Thesis Univ. Bern (2006).

[5] J.N. Galloway et al., Biogeoch., 70, 153-226 (2004).

ARE OUTER ICE CORE PARTS USABLE FOR ANALYSES OF TRACE SPECIES?

A. Eichler, C. Roost (PSI), T. Papina (IWEP), M. Schwikowski (PSI)

An 11 m part of the ice core from Belukha glacier, Siberian Altai was analysed for concentrations of major ions to investigate contamination effects on outer core parts. Interestingly, records agree well between inner and unrinsed outer ice core parts, whereas rinsed outer samples reveal lower concentrations due to dilution effects.

The 140 m long ice core from Belukha glacier in the Siberian Altai was recovered in 2001. Glacio-chemical investigations of the upper 86 m showed that the atmospheric composition and climatic conditions are well preserved in this ice core section covering the time period 1815-2001 [1,2]. However, the deepest ice core parts between 110 and 140 m depth are of poor quality and consist mainly of small ice chips. Thus, for this 30 m part the conventional decontamination through cutting of an inner sample with a band saw is not possible.

An 11 m long part of the ice core (88-99 m depth) was used to investigate possible effects of contamination (e.g. from drilling and handling) on the concentration records of trace species. Concentrations of the main ionic species (Na^+, NH_4^+, K^+, Mg^{2+}, Ca^{2+}, $HCOO^-$, CH_3COO^-, $CH_3SO_3^-$, Cl^-, NO_3^-, SO_4^{2-}, $(COO)_2^{2-}$) were analysed comparatively in inner (decontaminated) and outer (not decontaminated) samples with a size of about 1.9x1.9x2.5 cm using ion chromatography (IC). In the lower 4.5 m outer samples were rinsed with ultra pure water prior to analyses (161 samples), whereas the upper 6.5 m (215 samples) were analysed without further treatment.

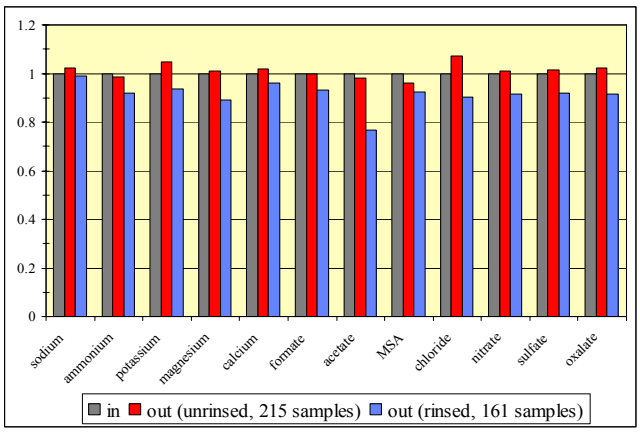

Fig. 1: Average normalized concentrations of trace species in inner and outer samples along the 88-99 m part.

Interestingly, concentrations in the unrinsed outer samples agree well with those of the inner samples (Fig. 1). So far, outer ice core parts have been assumed to be contaminated from drilling procedure and handling. Obviously, the contaminations located in a very thin layer on the surface of the ice core are diluted by the rest of the sample.

Concentrations in the rinsed outer samples are on average 9% lower than that of the respective inner samples indicating that the ultra pure water remaining on the ice samples leads to a dilution of the trace species.

Besides the absolute concentrations also the concentration records of the trace species are in good agreement for inner and outer samples (see e.g. formate, Fig. 2).

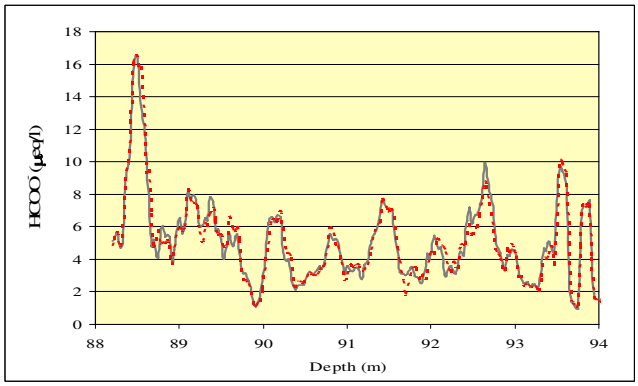

Fig. 2: Five-point moving average concentration record of formate along inner (grey) and outer parts (red).

To quantify the agreement between the inner and outer concentration records, logarithms of 5-point moving averages were compared (Fig. 3). The best correlation was found for NH_4^+, $HCOO^-$, Cl^-, NO_3^-, SO_4^{2-}, and $(COO)_2^{2-}$ (r^2>0.86). A slightly lower correlation for the concentrations of Mg^{2+}, Ca^{2+}, Na^+, and K^+ (0.8<r^2<0.83) is attributed to a larger inhomogeneity of the mainly dust originating species in the ice. The lowest correlation found for CH_3COO^- and $CH_3SO_3^-$ is due to separation problems from F^- during IC analyses and concentrations close to the detection limit, respectively.

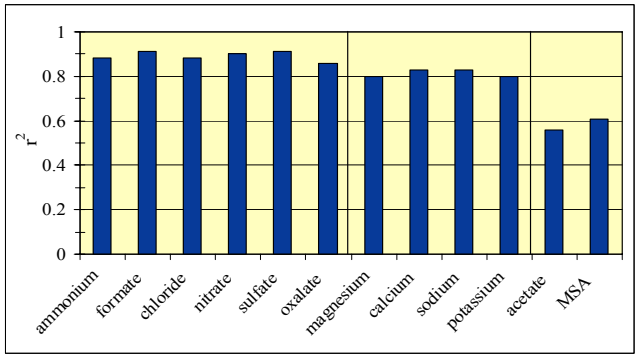

Fig. 3: Correlation (r^2) between concentration records of inner and outer samples (88-99 m depth).

To conclude, even from the analyses of ice core parts with poor quality, historical records of trace species for paleo atmospheric studies can be obtained.

ACKNOWLEDGEMENTS

This work is supported by the SNF, Marie Heim-Vögtlin program, Grant no. PMPD2-110174.

REFERENCES

[1] S. Olivier et al., J. Geophys. Res. 111, D05309, doi: 10.1029/2005JD005830 (2006).

[2] K. Henderson et al., J. Geophys. Res. 111, D03104, doi: 10.1029/2005JD005819 (2006).

THE SIGNAL OF THE "LITTLE ICE AGE" PRESERVED IN AN ICE CORE FROM THE SIBERIAN ALTAI

A. Eichler, A. Laube, S. Olivier, K. Henderson (PSI), T. Papina (IWEP), M. Schwikowski (PSI)

The upper 125 m of the ice core from Belukha glacier, Siberian Altai were used to reconstruct the climate and atmospheric composition during the period of the "Little Ice Age"(LIA) in Central Asia. Minima in the records of $\delta^{18}O$ values and NH_4^+ concentrations as well as a high volcanic activity were detected during the LIA.

The "Little Ice Age" (LIA) was a period of colder climate from the 15th to the mid of the 19th century. Causes for the cooling are suggested to be a decreased solar activity and increased volcanic activity, but are not fully understood yet. Ice core data can help to improve the understanding of the temporal and geographical occurrence of this climate fluctuation in the late Holocene.

An ice core from Belukha glacier in the Siberian Altai recovered in 2001 was used to reconstruct the climate and atmospheric composition during the LIA in Central Asia. Analyses of the main ionic species were completed for the entire 140 m long core, whereas $\delta^{18}O$ data are so far available for the upper 125 m only (results for the first 86 m see [1], [2]). Preliminary dating of the core using annual layer counting, a simple glaciological flow model, and volcanic eruptions reveals that the upper 125 m of the ice core cover the time period 1570(±10) – 2001.

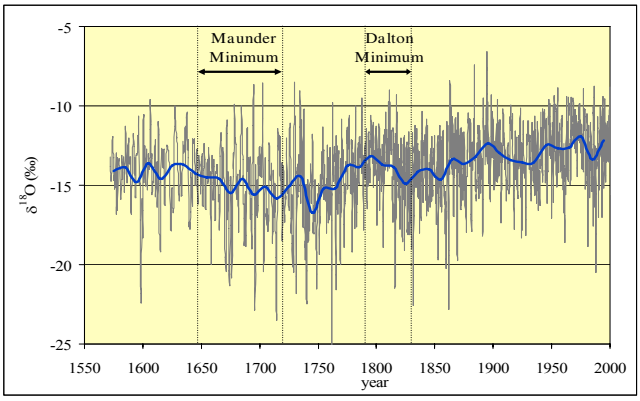

Fig. 1: Record of $\delta^{18}O$ (grey) together with a 10-year mean (blue) along the upper 125 m (period 1570-2001).

The $\delta^{18}O$ values are used as a proxy for the surface air temperature in the period March-November, the assumed main precipitation season at Belukha [2]. The record of the $\delta^{18}O$ values (Fig. 1) reveals two interesting features: a warming trend since the mid-19th century, discussed in [2], and two periods of colder climate (~1660-1750 and ~1810-1860), which are attributed to the LIA. The two minima in temperature agree well with reconstructed northern hemisphere temperatures [3]. Both periods of colder climate coincide with periods of low sunspot activity (see Fig. 1: Maunder and Dalton minimum).

In addition to the minimum in sun activity increased volcanic activity was observed during the LIA. Explosive volcanic eruptions were shown to produce different extents of Northern Hemisphere cooling (see e.g. [4]). In fact, various volcanic eruptions could be detected in the ice core $exSO_4^{2-}$ record in the period 1570-1860, that apperently caused a minimum in $\delta^{18}O$, indicating a cooling effect (see Fig. 2). For this study we used only volcanoes with a volcanic explosivity index (VEI) ≥5 (except Hekla, Iceland, 1766, VEI=4). However, the question remains still open, if those short-term cooling events cause the lower temperatures during the LIA.

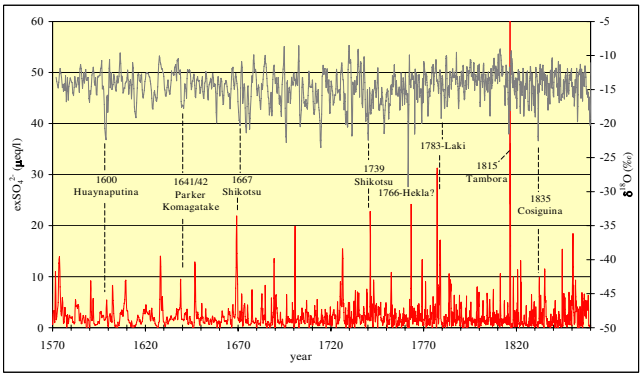

Fig. 2: Records of $\delta^{18}O$ (grey) and $exSO_4^{2-}$ (red) in the time period 1570-1860, indicated are documented volcanic eruptions causing a minimum in $\delta^{18}O$ and a maximum in $exSO_4^{2-}$ (non-dust sulfate).

Another indication for the low temperatures during the LIA are the low concentrations of NH_4^+ during the period 1640-1850. Generally, $\delta^{18}O$ values and NH_4^+ concentrations are well correlated (see Fig. 3, r=0.7). Thus, NH_3 emissions (mainly from biosphere and agriculture) were reduced during the colder period of the LIA.

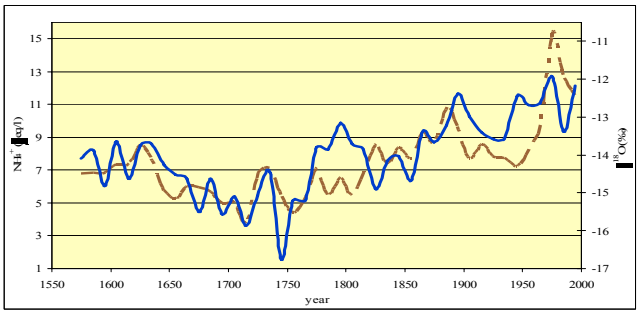

Fig. 3: 10-year means of $\delta^{18}O$ (blue) and NH_4^+ (brown) between 1570 and 2001.

Further work includes the interpretation of the ice core data of the remaining 15 m, after $\delta^{18}O$ analyses are completed.

ACKNOWLEDGEMENTS

This work is supported by the SNF, Marie Heim-Vögtlin program, Grant no. PMPD2-110174.

REFERENCES

[1] S. Olivier et al., J. Geophys. Res. 111, D05309, doi: 10.1029/2005JD005830 (2006).
[2] K. Henderson et al., J. Geophys. Res. 111, D03104, doi: 10.1029/2005JD005819 (2006).
[3] M.E. Mann et al., Nature 392, 779-787 (1998).
[4] K.R. Briffa et al., Nature 393, 450-454 (1998).

FIRST LEAD RECORD FROM THE ILLIMANI ICE CORE

T. Kellerhals, H.W. Gäggeler (PSI & Univ. Bern), S. Brütsch, L. Tobler, M. Schwikowski (PSI)

Concentrations of lead and a range of other elements were determined by Continuous Ice Melting (CIM) ICP-SFMS in an ice core from Nevado Illimani, Bolivia. The temporal evolution of the lead concentration shows a different pattern than in European glaciers and concentrations are lower by a factor of ten. In a method comparison, the records obtained with CIM ICP-SFMS and ion chromatography were in excellent agreement.

INTRODUCTON

For the glaciochemical dating of ice cores by annual layer counting and for the reconstruction of past atmospheric conditions and anthropogenic air pollution, highly resolved records of various chemical species are needed. To expand the range of elements beyond the species accessible by ion chromatography (IC), a method for the Continuous Ice Melting (CIM) analysis of trace elements in ice cores by Inductively Coupled Plasma Sector Field Mass Spectroscopy (ICP-SFMS) has been developed [1, 2] and further improved [3] to yield reliable and accurate high-resolution trace element records. Highly resolved (~1 cm) records are essential especially in the lower parts of ice cores from high-mountain glaciers, where strong layer thinning leads to annual ice layers only a few centimetres thick.

Here we present first preliminary records of lead and aluminium from the Illimani ice core (Eastern Bolivian Andes [4]). To show the accuracy of the CIM ICP-SFMS method, we compare two parallel records of sodium obtained by CIM ICP-SFMS and IC.

METHODS

For the CIM ICP-SFMS analysis, cuboid ice bars of about 70 cm length were placed on a heated melting head inside a freezer. The meltwater from the inner drain was acidified to ~0.3 M HNO_3 and introduced into the ICP-SFMS (Element1, Finnigan MAT) via an APEX sample introduction system [3].

For the ion chromatographic determination, the ice core was cut into samples of 2-3 cm length that were allowed to melt just before the IC analysis.

ILLIMANI LEAD RECORD

In contrast to a lead record from the Colle Gnifetti (Swiss Alps) where concentrations up to 3µg/L were measured [5], concentrations about 10 times lower are observed in the Illimani core (Fig. 1). Furthermore, the chronological trend of the record is surprising. Unlike in other lead records from the Northern Hemisphere, where a strong concentration increase was observed after 1940 due to the introduction of leaded gasoline, there is no increase visible from the 1940s onwards at least until the early 1960s, but a maximum around 1920 stands out. As the aluminium record (a tracer for dust) indicates, these elevated lead values did not originate from contributions of high dust loadings (which also contain some lead), but probably from anthropogenic emissions (smelting).

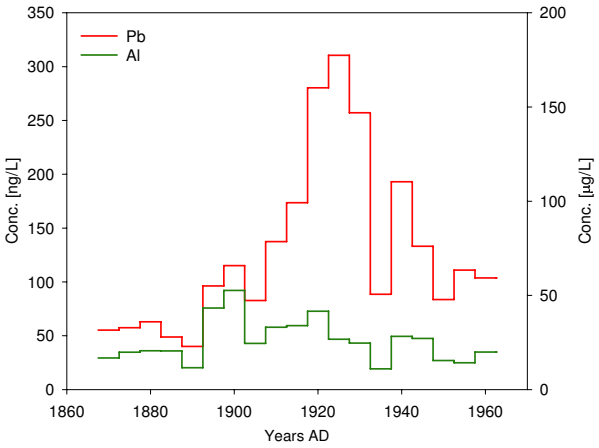

Fig. 1: 5-year averaged records for Pb (red, left axis) and Al (green, right axis) from the Illimani ice core.

METHOD INTERCOMPARISON

Two parallel sections of the Illimani ice core were analysed with IC as well as with CIM ICP-SFMS. The comparison of these independently obtained records resulted in an excellent agreement for all elements that were analysed with both methods. As an example, the corresponding records of sodium are shown in Fig. 2.

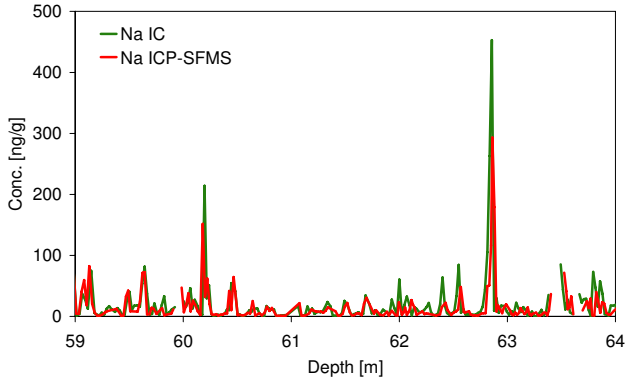

Fig. 2: Records of sodium for a section of the Illimani ice core, analysed with IC (green) and ICP-SFMS (red).

REFERENCES

[1] S. Knüsel et al., Environ. Sci. Techn. 37, 2267 (2003).
[2] S. Knüsel, PhD Thesis, Univ. Bern, (2003).
[3] T. Kellerhals et al., Ann. Rep. Lab. für Radio- und Umweltchemie (2005), p. 33.
[4] S. Knüsel et al., JGR, Vol. 108, No. D6, 4181, doi:10.1029/2001JD002028, (2003).
[5] M. Schwikowski et al., Environ. Sci. Techn. 38, 957 - 964, (2004).

FIRST RESULTS OF THE DEEP ICE CORE OF MERCEDARIO, ARGENTINA

A. Ciric, H. W. Gäggeler (PSI & Univ. Bern), E. Vogel (Univ. Bern), L. Tobler, M. Schwikowski (PSI)

The Mercedario ice core shows a well preserved fingerprint of the Pacific Ocean with high MSA concentrations and a chloride to sodium ratio of 1.05. The dating with the radionuclide ^{210}Pb gives an estimated annual accumulation of 0.3 m weq, which is much lower than accumulation obtained by counting of annual layers (0.45 m weg).

A major aim of the project *Paleo climate from Andean ice cores and lake sediments* is to find a suitable glacier archive in the South American Andes for paleo climate reconstruction in an area strongly influenced by the El Niño-Southern Oscillation. The La Ollada glacier on Cerro Mercedario (31°58‘S, 70°07‘W, 6100 m a.s.l.) in the Central Argentinean Andes is most promising and in February 2005 a 104 m long ice core was drilled. In this region the amount of winter precipitation is significantly correlated to the Southern Oscillation Index with higher values during El Niño years [1]. Shown here are results of the chemical analysis of the first 43 m water equivalent (weq.).

Since the major part of the humidity is expected to come from the Pacific, there should be a direct fingerprint of the ocean. The observed high MSA (methanesulfonic acid) concentrations (up to 59 μg l^{-1}) and also the chloride to sodium ratio, which is close to the seawater ratio (seawater: 1.16, here 1.05, Fig. 1), support this assumption. In ice cores the chloride to sodium ratio is normally smaller than in the ocean. This can have several reasons. Sodium might have an additional source, e.g. mineral dust and the two species might have different transport behaviour in the atmosphere or a different behaviour after deposition on a glacier, especially when melting occurs [2]. In this specific core the latter can be excluded, since no melt features were observed. A smooth density profile and low borehole temperatures (-16.7°C at 104 m depth to -18.5°C at 10 m below surface) support this.

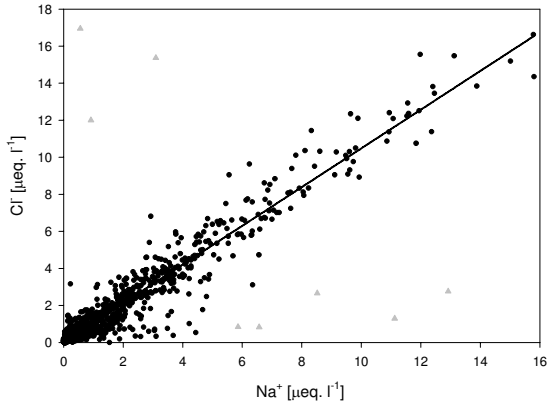

Fig. 1: Chloride against sodium in the Mercedario ice core with linear regression: slope 1.05, outliners marked with grey triangles (R^2 = 0.94, n = 1850).

For dating of the core several methods like the identification of annual layers (δ^{18}O and concentrations of ammonium), volcanic horizons as well as nuclear dating with ^{210}Pb were applied and they gave different results. The δ^{18}O signal and the ammonium concentrations showed strong fluctuations, which were attributed to seasonal variations (Fig. 2). Minima (maxima) in the δ^{18}O signal and low (high) ammonium concentrations were assumed to correspond to austral winter: June, July, and August (austral summer: December, January and February). Counting of these layers in the first 30 m weq. gives a time span of 66 years (1939-2005) yielding an average annual accumulation of 0.45 m weq.

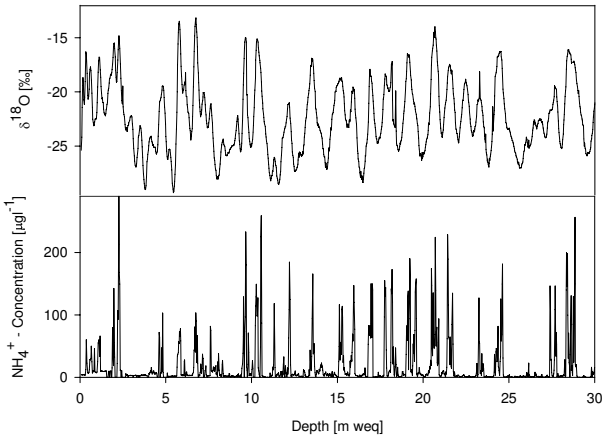

Fig. 2: Ammonium concentrations (below) and δ^{18}O (above) profile in the upper 30 m weq of the Mercedario ice core.

Dating with ^{210}Pb resulted in an average annual accumulation of 0.30 m weq. which is much lower compared to annual layer counting. Between 20 and 25 m weq. several peaks in the sulphate to calcium ratio along with high sulphate concentrations were identified, most probably originating from volcanic eruptions. They can be attributed to the volcano Quizapu in Chile (35°S), which had several eruptions between 1916 and 1932. This is in agreement with ^{210}Pb dating and results in an age of 115 years for the first 30 m weq. Analysis of tritium for finding the nuclear weapon tests horizon of 1963 is ongoing.

It has to be assumed that there is a loss of snow due to wind erosion or an inconsistent precipitation pattern. The appearance of small stones (up to 0.9 g) and dust in the core might support this. The transport of such stones from the surrounding rocks over the glacier surface to the drilling side (approximately one km distance) needs strong winds.

REFERENCES

[1] P. Aceituno, Mon. Weather Rev., 116, 505-524 (1988).

[2] A. Eichler, M. Schwikowski, H.W. Gäggeler, Tellus, 53B, 192 (2001).

MERCURY IN SNOW FROM JUNGFRAUJOCH AND FIRN- AND ICE FROM LA OLLADA-GLACIER, ARGENTINA

M. Schläppi (Univ. Bern), M. Schwikowski, L. Tobler (PSI), A. Ciric, H.W. Gäggeler (Univ. Bern & PSI)

Atomic fluorescence spectrometry was used to determine total mercury concentrations in snow-, firn- and ice samples from Jungfraujoch and La Ollada-Glacier, Cerro Mercedario (Argentina).

INTRODUCTION

Mercury (Hg) is the only metal, whose elemental form has a natural cycle. Due to its high vapour pressure it is extremely toxic. However, there are still large uncertainties about atmospheric Hg-fluxes and Hg-concentrations. Also the chemical behaviour of mercury after deposition is not well known [1]. To improve the understanding, reconstructions of Hg-concentrations from natural archives like glacier ice might contribute [2]. In this studies Hg-concentrations in snow samples from Jungfraujoch and firn- and ice samples from La Ollada-Glacier on Cerro Mercedario, Argentina were investigated [3].

EXPERIMENTAL

About 25 g of snow, firn or ice was transferred into a PFA container and BrCl-solution was added to oxidize all forms of Hg to Hg^{II} oxidation state. After about 14 hours the sample was neutralised by adding NH_2OH*HCl solution to eliminate all free halogens [4, 5].

The samples were directly injected into the cold vapour atomic fluorescence spectrometer (Mercur, Analytik Jena) and mixed in the reactor with $SnCl_2$-solution to reduce Hg^{II} to Hg^0 oxidation state. Then Hg^0 was separated from the liquid phase in the gas-liquid separator, and was transported with argon gas to the gold trap where Hg^0 was accumulated. After releasing Hg^0 by heating the gold trap, it was transported with argon gas to the fluorescence vessel where detection took place [5].

RESULTS AND DISCUSSION

Snow samples were collected on Jungfraujoch from a 63 cm and a 35 cm deep snow pit on 11 May and 12 May 2006, respectively (Fig. 1.). The upper 35 cm consisted of homogenous low-density snow, whereas the deeper layer from 35-63 cm was more compact but still homogenous.

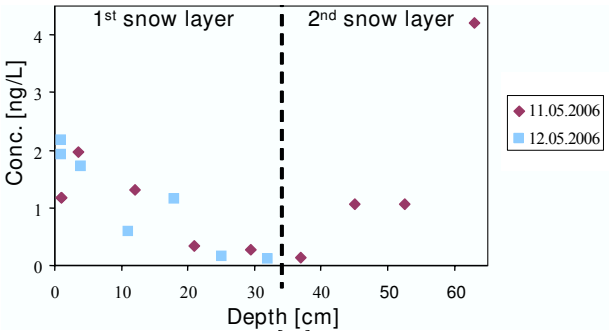

Fig. 1: Mercury concentrations against depth in the two snow pits from Jungfraujoch.

In the first snow layer Hg concentrations decreased from 2 ng/L to just above detection limit of about 0.14 ng/L. The agreement between the samples from the two consecutive days is good. There is no indication of a loss of Hg by evaporation. Interesting is also the second snow layer: An increase of Hg-concentrations with depth was detected, suggesting highly variable deposition conditions or concentrations in the atmosphere. However, the experiment was too short to fully understand mercury deposition and conservation in snow and a more detailed study is needed.

Hg concentrations in firn and ice samples from la Ollada-Glacier are shown in figure 2a and b. Hg concentrations ranged from detection limit (0.14 ng/L) to 400.4 ng/L with a average of 1.96 ng/L (maximum value of 400.4 ng/l not included). 18% of the samples contained dust particles (indicated in Fig. 2). These samples also showed the highest Hg concentrations, identifying mineral dust as main source of mercury. This was confirmed by the significant correlation of concentrations of Hg with Mg^{2+} (r=0.36) and Ca^{2+} (r=0.35). After mineral dust correction there remain at least four Hg peaks at 5.8 m weq, 33.2 m weq, 36.3 m weq and 40.9 m weq., which could indicate volcanic events.

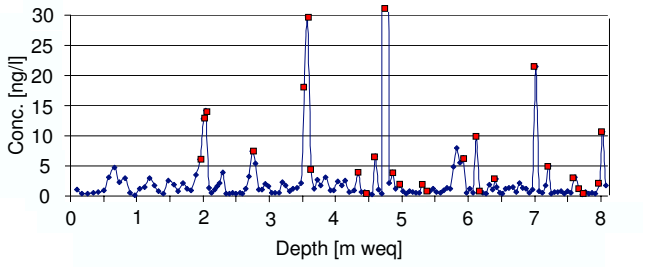

Fig. 2a: Hg concentration record of the upper 8 m weq of the ice core from La Ollada-Glacier. Red points mark visually observed dust in samples.

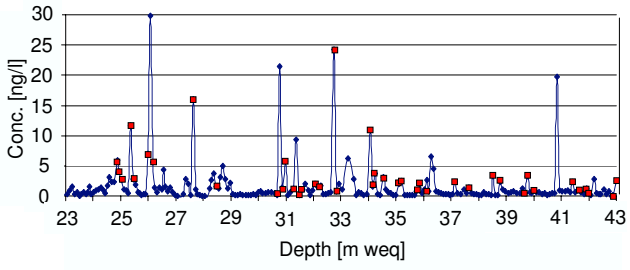

Fig. 2b: Same as Fig. 2a, but for 23-43 m weq. depth.

REFERENCES

[1] M.B. Parsons & J.B. Percival, Mineralogical Association of Canada (2005).

[2] P.F. Schuster et al., Env. Sci. Tech. 36, 2303 (2002).

[3] A. Ciric et al., this issue p. 28.

[4] S. Eyrikh et al., in preparation.

[5] United States Environmental Protection Agency (EPA), Method 1631 (2001).

A NEW 50 M LONG ICE CORE FROM THE SOUTHERN PATAGONIAN ICEFIELD

M. Schwikowski, T. Jenk, B. Rufibach (PSI), G. Casassa, A. Rivera, M. Rodriguez, J. Wendt (CECS)

In August 2006 an ice core was recovered from a glacier flowing to the northwest from the summit of Cordón Mariano Moreno, reaching a depth of 50 m which is a new record for ice core drilling in Patagonia. The core is assumed to contain information about paleo climatic and environmental conditions for at least several decades.

The Patagonian Icefields constitute a unique location in the Southern Hemisphere for obtaining non-polar paleo records from ice cores south of 45°S. Nevertheless, no ice core record with meaningful paleoclimate information has yet been obtained from Patagonia. This deficiency is on the one hand due to extremely harsh field conditions, and on the other hand to the fact that the main plateaus of both the Northern and Southern Patagonian Icefield are strongly affected by melt water percolation. Nevertheless, a recent study showed that there is good potential for well-preserved paleo-records within glaciers in the Patagonian icefields located higher than 2300 m such as on Cerro Mariano Moreno and San Valentín [1].

A reconnaissance flight was conducted on 14 April 2006 in order to select the drilling site and to explore a possible escape route accessible with skies when bad weather conditions might prevent the use of a helicopter. Based on glacier topography, the northern plateau of Cerro Mariano Moreno was selected for deep ice coring (Fig. 1). A new drilling tent was constructed by FS INVENTOR AG (http://www.icedrill.ch/eb_start.html) with a particularly rigid frame and canvas cover to resist the strong winds in Patagonia (Fig. 2). The tent was tested on the Jungfraujoch in June 2006.

During the drilling expedition the stay in Chile extended from 7 August to 11 September 2006. Weather conditions allowed establishing of the drilling camp on Cerro Mariano Moreno on 19 August. A radar survey with a 6 MHz system indicated glacier thicknesses between 70 and more than 300 m in the area, and a drilling site with a thickness of 170 m was selected (49°16'S, 73°21'W, 2600 m a.s.l.). After two days of drilling a depth of 50.64 m was reached. At this depth warm and wet ice was encountered and drilling had to be stopped. However, due to heavy snow storms and high wind speeds we had to wait until 2 September before we could evacuate. During these bad weather conditions the drilling tent proved to be sufficiently stable, which was essential for maintaining the camp. A network of 9 stakes was set up around the drilling site, where detailed surface topography was measured with a dual-frequency GPS receiver, as well as accumulation rates during a 10-day period. Continuous GPS measurements were performed in one stake for determination of short-term ice velocities.

Temperatures measured in the borehole were just slightly below 0°C, indicating temperate ice (Fig. 3). This is surprising, since an annual mean temperature in the range of -6°C to -9°C was estimated for this area and elevation, assuming an altitudinal lapse rate of 0.6°C/100 m [2]. Chemical analysis of the core will start in January 2007.

ACKNOWLEDGEMENTS

National Geographic (Grant No. 7587-04); FONDECYT (Grant No. 1061269); CECS.

REFERENCES

[1] M. Schwikowski et al., Annals Glaciol. 43, 8-13 (2006).

[2] A. Rivera, PhD thesis, University of Bristol (2004).

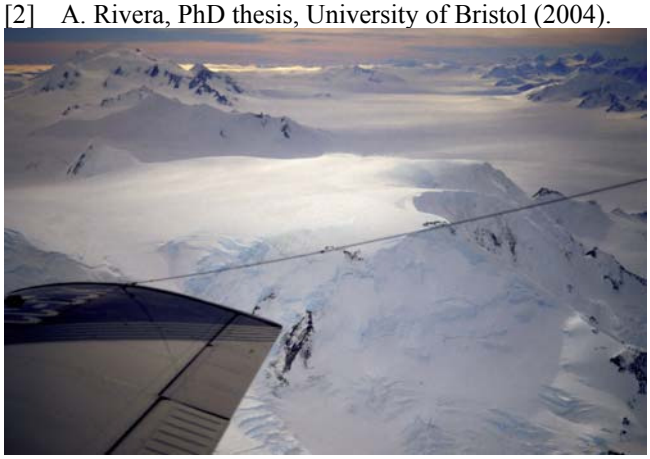

Fig. 1: Photo of the northern plateau of Cerro Mariano Moreno taken during the reconnaissance flight.

Fig. 2: Setting-up of the new drilling tent on Mariano Moreno in August 2006.

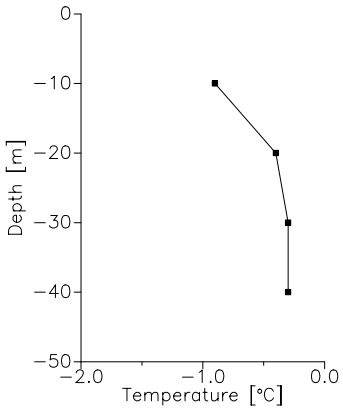

Fig. 3: Temperature profile in the borehole.

TRACE ELEMENT ANALYSIS WITH CRI-ICP-MS

Ch. Stenger, H.W. Gäggeler (Univ. Bern & PSI), K. Li (Uni. Bern), M. Schwikowski (PSI)

Trace element analysis with inductively coupled plasma mass spectrometry (ICP-MS) has several problems with interferences, especially when a quadrupole mass analyser is used. Such an ICP-MS can not separate molecular interferences, i.e. oxides and other polyatomic interferences, from an element with nearly the same mass, because of the insufficient resolution of the mass analyser. The collision-reaction interface (CRI) is a newly developed tool to eliminate such interferences, and its performance was tested.

INTRODUCTION

ICP-MS is a widely used method to analyse trace elements in solid, liquid or even gaseous samples. The principle of ICP-MS is to ionize atoms in a high temperature Argon plasma (5'000-10'000 K). The ions are focused in the ion optic part and separated with a mass analyser, e.g. a quadrupole or sector field (SF) [1]. The ion optic and mass analyser part are under vacuum, around $1.5x10^{-2}$ torr and $9x10^{-5}$ torr, respectively (Fig. 1).

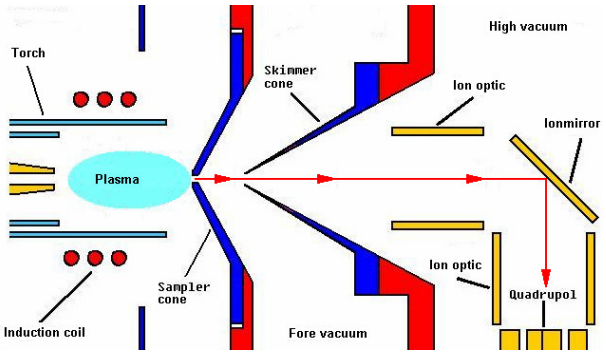

Fig. 1: Schematic view of an ICP-MS ion source and ion optic (adapted from www.icp-ms.de).

In the plasma ions or atoms can react with each other. For example, ^{40}Ar can react with ^{16}O to the molecular ion $^{40}Ar^{16}O^{+}$ (39.962u + 15.995u = 55.957u) which interferes with the mass of ^{56}Fe (55.935u) [1]. A quadrupole mass analyser can not separate such interference (Δm=0.022u). Other mass analysers, like a SF instrument, have the potential to separate the interferences in most of the cases. To overcome this problem the collision-reaction interface (CRI) was developed. The core of the CRI is the double layer sampler and skimmer cone where gases such as H_2 and/or He can be injected. Thus, the collision-reaction gas enters the ion beam directly at the orifices of the cones where the temperature and plasma density is relatively high.

EXPERIMENTAL AND RESULTS

For comparison the analysis of 1 ppb Arsenic in 0.1% to 2% HCl solution was performed without and with CRI gas flow with our ICP-MS (VARIAN 820). Normally, determination of ^{75}As in a solution that contains ^{35}Cl is difficult, because of the reaction of ^{40}Ar with ^{35}Cl to the mass 75 [1]. Fig. 2 shows the intensities of the ^{35}Cl and the ^{75}As, signal for various HCl concentrations obtained in normal ICP-MS mode. With increasing HCl concentration the ^{75}As and ^{35}Cl intensities increase proportionally, indicating that only the interference molecular ion is detected. When using the CRI (80ml/min H_2 at the skimmer cone) the ^{75}As signal is not affected .

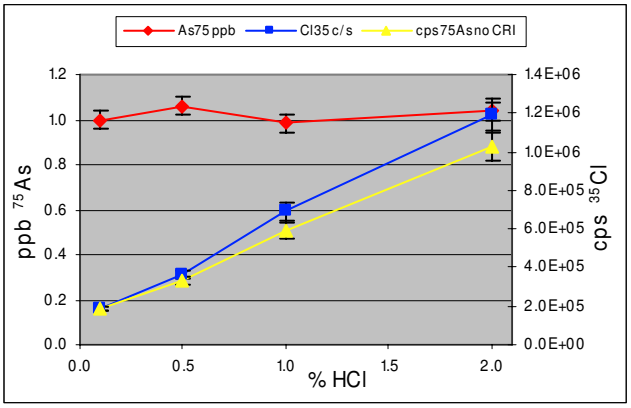

Fig. 2: Signal intensity of 1ppb As solutions depending on HCl concentrations, with and without CRI.

The CRI system allowed analysis of a range of elements in different matrixes with less than 6% error.

Detection limits (DL) obtained with the new CRI-ICP-MS and with a SF-ICP-MS (Element 1, Thermo Finnigan MAT) in low resolution (R=300) and medium resolution (R=3000) mode were comparable (Tab. 2).

Tab. 2: Detection limits for some elements (LR=low resolution, MR=medium resolution).

Isotopes	CRI-ICP-QMS	SF-ICP-MS [2]	
	[ppt]	[ppt] LR	[ppt] MR
^{23}Na	72.5	170	
^{27}Al	15.5	53	11.9
^{75}As	38.5		
^{146}Nd	1.7	0.38	
^{238}U	1.6	0.16	
^{51}V	1.6		1.4
^{56}Fe	165		187

REFERENCES

[1] R. Thomas, Spec. Tutorial, part I-XIV, 16(4)-18(2), (2001-2003).

[2] L. Tobler, Laboratory of Radiochemistry and Environmental Chemistry, personal communication.

AN APPROACH TO DETERMINE THE PROVENANCE OF DUST IN DIFFERENT ICE CORES BY PRINCIPAL COMPONENT ANALYSIS OF RARE EARTH ELEMENTS

L. Tobler (PSI), T. Kellerhals (PSI & Univ. Bern), M. Schwikowski (PSI)

Rare earth elements (REE) were analysed by inductively coupled plasma sector field mass spectrometry in ice cores from different sites. These elements are used as tracers for aeolian dust deposited in the ice cores. A principal component analysis was applied as statistical tool in order to compare these results with literature data of REE concentrations in ice cores and possible source areas.

Mineral dust in ice cores is of purely aeolian origin and is a tracer for atmospheric transport and circulation. Lanthanoides, also called rare earth elements, comprise a group of 15 elements from La to Lu, of which Pm does not occur naturally in the earth's crust, while all others are found in all types of rocks. REE have been widely adopted as proxies for different geochemical processes. REE contents might help to investigate the composition and to determine the provenance of the dust, because REE are mostly transported in the atmosphere in the particulate phase.

The aim of this study is to obtain an improved understanding of the origin of aeolian dust and its atmospheric pathways to different ice core sites by comparison of the REE concentrations in the ice cores to that of possible source area samples [1, 2]. Furthermore, literature data of REE concentrations in ice cores from Greenland [1], Antarctica [3], and the Inilchek glacier (Tien Shan; Kyrgyzstan), [4] were included in the evaluation of the data.

The concentrations of La, Ce, Pr, Nd, Sm, Eu, and Yb were determined by inductively coupled plasma sector field mass spectrometry (ICP-SF-MS, Element1, Thermo Finnigan) in ice cores from the Belukha (Siberian Altai, 49°48'N, 86°34'E), the Colle Gnifetti (Swiss Alps, 45°56'N, 7°53'E) and the Illimani (Bolivian Andes, 16°39'S, 67°47'W). Only the soluble dust fraction (in 0.2 n HNO_3) was analysed.

Principal component analysis (PCA), a statistical tool to investigate and interpret multidimensional datasets, was applied. PCA linearly transforms the data to a new reference frame such that the greatest variance by any projection of the data comes to lie on the first coordinate (the first principal component), the second greatest variance on the second coordinate, and so on. By plotting the samples in the new reference frame it should be possible to identify samples characterized by a similar behavior. In order to eliminate the influence of the absolute REE concentration levels and to compare the shape of the REE pattern, the concentrations for each sample were normalized to the Ce concentration before PCA was applied. The PCA was performed by using the statistical toolbox of the commercial software MATLAB®.

Fig. 1 shows all the samples projected onto the first two principal components. The first principal component explains 56.2 % and the second component 39.3%, together about 95% of the total variability. The pattern of this plot shows, that in general samples from the same site cluster more or less together. The Belukha samples are centered close to the origin of the frame. The only possible source area sample showing a similar position is from the Gobi desert in Mongolia. However, the other Mongolian desert sample is located outside of the Belukha cluster, indicating the inhomogeneity of the source. This sample shows the same characteristics as the samples from the Ilnichek glacier. As expected, for the Central Asian ice cores the mineral dust source seems to be the Gobi desert. Interestingly, samples from Colle Gnifetti and Illimani group together below the Beluka samples in direction of negative second principle component, although both glaciers are assumed to receive dust from different sources, i.e. the Sahara and the arid regions in the Andes. The source area samples from the Sahara (Mauretania) are opposite to the Colle Gnifetti and Illimani cluster, where no potential soure area sample appears. Thus, for mineral dust in Colle Gnifetti and Illimani ice samples no conclusive provenance determination could be made at this stage. Greenland ice core samples fall within the region of Chinese loess samples, whereof, among other indications, Svensson et al. suggested an Asian provenance of the dust in this core [1].

It has to be taken into account that samples used in this study have been differently prepared and analysed. Furthermore, the age of the samples is very different, covering a time span from 150ky BP over the last glacial maximum to modern times. These factors might influence the REE tracer characteristics and therefore be a limiting factor for this provenance determination of ice core dust.

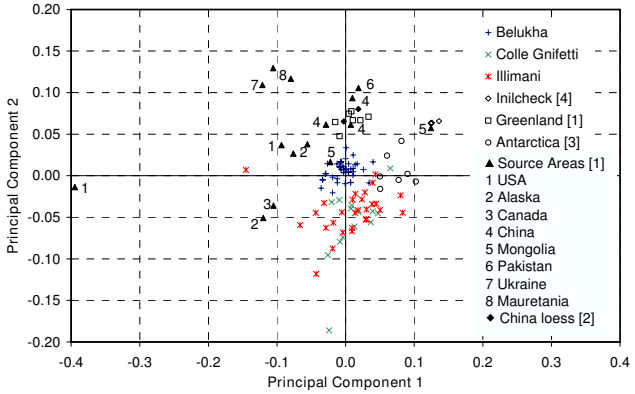

Fig. 1: PCA of the first two primary components for the REE concentrations normalized to Ce.

ACKNOWLEDGEMENT

We thank A. Svensson, University of Copenhagen, for providing the REE concentration data from [1].

REFERENCES

[1] A. Svensson et al., J Geophys Res, 105, 4637-4656 (2000).
[2] C-Q. Liu et al., Chem Geol, 106, 359-374 (1993).
[3] P. Gabrielli et al., Anal Chem, 78, 1883-1889 (2006).
[4] K.J. Kreutz, E.R. Sholkovitz, Geochem Geophy Geosy, 1 (2000).

BIOGENIC SILICA: A POWERFUL TOOL FOR QUANTITATIVE CLIMATE RECONSTRUCTIONS FROM LAKE SEDIMENTS

M. Grosjean (Univ. Bern & NCCR Climate), A. Blass (Univ. Bern & EAWAG), S. Köchli, M. Schwikowski (PSI), E. Vogel (Univ. Bern), M. Sturm (EAWAG)

Current research in annually laminated Lake Silvaplana, Engadine (NCCR Climate VIVALDI project), and in high-elevation lakes of the Central Andes shows that biogenic silica (BSi) has a great potential as a climate proxy in remote lakes and for time periods, when anthropogenic eutrophication played a minor role.

High-resolution, quantitative long-term climate reconstructions are essential to place the recent, probably anomalous climate changes into a longer perspective. One particular quality of lake sediments is (i) the potential for very long records, and (ii) the presence of multiple biological (e.g., pollen, diatoms, etc.), physical and bio-geochemical proxies (e.g. magnetic susceptibility, grain size distribution, mineralogy, stable isotopes, alkenones, Tex86, and many others) within the same paleoenvironmental archive.

A particular challenge in current paleolimnology is calibration and quantification of the proxy data. A major obstacle with biological proxies is that taxa identification and preparation of the data set is very time-consuming and expensive. This makes the search for rapid physical and bio-geochemical methods in lake sediments a very active field of investigation. The disadvantage here is that many of these proxies are controlled by the site-specific lake basin and lake catchment configuration (climatic zone, vegetation, geology, topography, etc.), which requires genuine calibration between a proxy and related environmental variables at every new site. This phenomenon is partly also known from ice cores.

BSi is present in lake sediments as diatom opal, phytoliths and Chrysophyte cysts, among others. Following the method by Mortlock and Froehlich, BSi is leached from the lake sediments with 1 M NaOH for 3 hrs at 90°C. In order to account for Si leached from inorganic alumino-silicates, BSi concentrations are corrected using the Al concentration in the leachate [1]. This method has been validated by absolute diatom valve counts on standardized samples. The Al correction is the reason why ICP-OES is the preferred analytical technique.

Figure 1 shows the results for Lake Silvaplana. An annually laminated (varved) freeze-core of Lake Silvaplana was dated using varve counting, ^{137}Cs, ^{210}Pb and event stratigraphy. Annual laminae were sampled year by year back to AD 1580. Annual biogenic silica flux to the sediments calibrated against instrumental autumn (September – November) temperatures (AD 1864 – 1949) revealed a very high and significant correlation ($r = 0.7$, $p < 0.01$; Figure 1). This correlation is stable in time. Comparison with (i) early instrumental data back to 1760 AD, and (ii) two fully independent temperature reconstructions for the same area (based on dendro- and documentary data) back to 1580 AD is consistent [2, 3].

BSi based quantitative reconstructions in lakes of the arid Central Andes (L. Pululos, 4500 m, NW Argentina) are under investigation (Fig. 2). BSi concentrations compare favourably with annual precipitation 1950-1998, precipitation-sensitive tree ring chronologies, documentary data from the Spanish, and ice accumulation in the Sajama ice core (Bolivia) suggesting that, in this case, BSi is an excellent high-resolution proxy for effective moisture when nutrient transport to the lake is enhanced.

For the first time, evidence is presented for a distinct humid period during the Inka conquest in the 15th century.

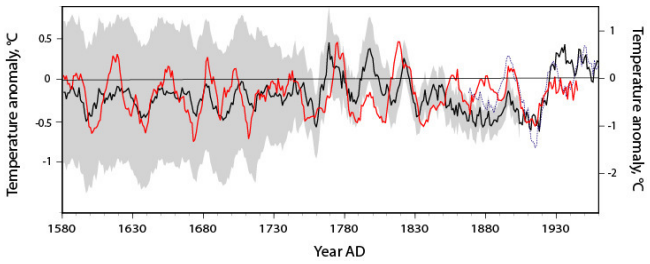

Fig. 1: Reconstructed decadal-scale SON temperature anomalies (wrt 20th century mean) based on annual BSi flux data calibrated with instrumental data of Sils Maria from AD 1864-1949 (gray line, shaded envelope 2σ). The 150-yrs low pass filtered reconstruction is compared with the European autumn temperature reconstruction (Xoplaki et al. 2005, GRL, black). Note that the scale of the Engadine reconstruction (right) is twice the scale of the European reconstruction (left) where local departures are smoothed out. The negative excursion between 1790-1810 AD coincides with a strongly positive anomaly of the NAO index (Luterbacher et al. 2002, Atm Sc Lett); from [2].

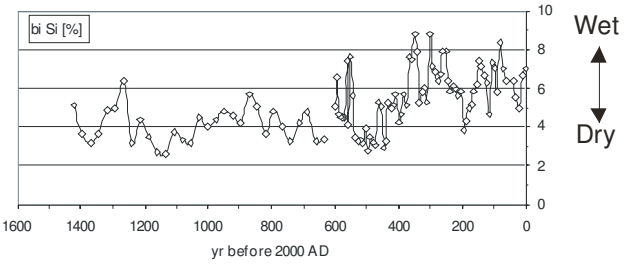

Fig. 2: BSi in the sediment of Laguna Pululos, Argentina.

REFERENCES

[1] C. Ohlendorf & M. Sturm, J. Paleolim. (in press).

[2] A. Blass et al., submitted to Quat. Res.

[3] A. Blass, PhD thesis Univ. Bern (2006).

^{210}Pb-DATING OF SNOW SAMPLES FROM JUNGFRAUJOCH, SWITZERLAND AND FEDCHENKO GLACIER, TAJIKISTAN

L. Tobler, M. Schwikowski (PSI), S. Kaspari (University of Maine), V. Aizen (University of Idaho); H.W. Gäggeler (Univ. Bern & PSI), B. Muther, E. Vogel (Univ. Bern)

The radioactive decay of ^{210}Pb with a half-life of 22.8 years is often used for dating of environmental archives like ice cores. ^{210}Pb activity is normally measured with α-spectroscopy through its granddaughter ^{210}Po, which has to be in radioactive equilibrium with ^{210}Pb. In this work the new approach was tested to apply this method for dating of snow/firn samples presumably younger than two years in which the two nuclides are not in equilibrium yet.

^{222}Rn, a member of the ^{238}U decay series, emanates from the earth's crust into the atmosphere. There it decays through a series of shorter-lived products into ^{210}Pb which attaches to aerosol particles. After a residence time of several days, aerosol particles carrying ^{210}Pb are deposited as wet or dry fallout onto the earth's surface. Under favourable conditions, i.e. constant input over time and no exchange with the surrounding environment, ^{210}Pb (half-life 22.3 years) can be used to date ice cores [1]. The ^{210}Pb activity is measured with α-spectroscopy of its grand-daughter nuclide ^{210}Po (half-life of 138.9 days) which is separated from the samples. The in-growth of ^{210}Po is described (neglecting the daughter activity ^{210}Bi) by:

$A_{^{210}Po}(t) = A_{^{210}Po}(\infty)\cdot(1-e^{-\lambda\cdot t})$ (1) with

$A_{^{210}Po}(\infty) = A_{^{210}Pb}$, $\lambda = \ln(2)/T_{1/2}$ decay constant of ^{210}Po;

and t = time between deposition and separation.

In order to obtain the ^{210}Pb activity from the ^{210}Po measurement, ^{210}Po has to be in radioactive equilibrium with ^{210}Pb, which is the case only after about 2 years.

The aim of the present work is to evaluate the possibility of the age determination in younger snow samples without waiting for the radioactive equilibrium. This might be an attractive alternative method to determine snow accumulation rates from shallow snow sampling.

Samples from the Alpine site Jungfraujoch (3500 m asl.) (Switzerland) were collected by drilling a 6.8 m long shallow core on 11 May 2006, whereas samples from the Fedchenko glacier (5365 m asl.) in the Pamir mountains (Tajikistan) originated from a 2 m deep snow pit taken on 29 July 2005. From the snow cores two aliquots per 20 cm long sections were prepared for the ^{210}Po α-spectroscopic measurements. Separation of ^{210}Po in the first aliquot was conducted between 5 and 28 days after sampling, following the procedure described in [2]. Separation of the second aliquot took place 150 days resp. 180 days after sampling. From the two measurements the following ratio was calculated:

$A_{^{210}Po}(t_1)/A_{^{210}Po}(t_2) = (1-e^{-\lambda t_1})/(1-e^{-\lambda t_2})$ (2)

The time t_i corresponds to the sum of the unknown time interval Δt_x between deposition date and sampling date and the time t_i between sampling date and separation date i, i.e. $t_i = \Delta t_x + \Delta t_i$ i=1,2

Inserting this into equation 2 and transforming it, gives the sample age:

$$\Delta t_x = \frac{1}{\lambda}\ln\left[\frac{A_{^{210}Po}(t_2)e^{-\lambda\Delta t_1} - A_{^{210}Po}(t_1)e^{-\lambda\Delta t_2}}{A_{^{210}Po}(t_2) - A_{^{210}Po}(t_1)}\right]$$

Fig. 1 shows the ^{210}Po activities of the two measurements and the calculated sample age for the two investigated sites. For the Jungfraujoch samples, a steady increase in age was observed until 400 cm depth, when the snow from the last autumn was reached (age about 200 days). Below that depth, ^{210}Po activities and ages show higher variability, which might be the effect of melting at this temperate glacier. Nevertheless, the resulting accumulation of 400 cm of snow for seven month seems reasonable for this site.

The Fedchenko samples show a steady increase in age throughout, with an age of about 300 days for the sample at 200 cm depth. Thus, the annual accumulation is assumed to be larger than 200 cm of snow, which is in agreement with results derived by layer counting of the δ^{18}O signal in a firn core. Thus, the new method seems suitable for dating of snow samples younger than one year if the samples are not affected by melting.

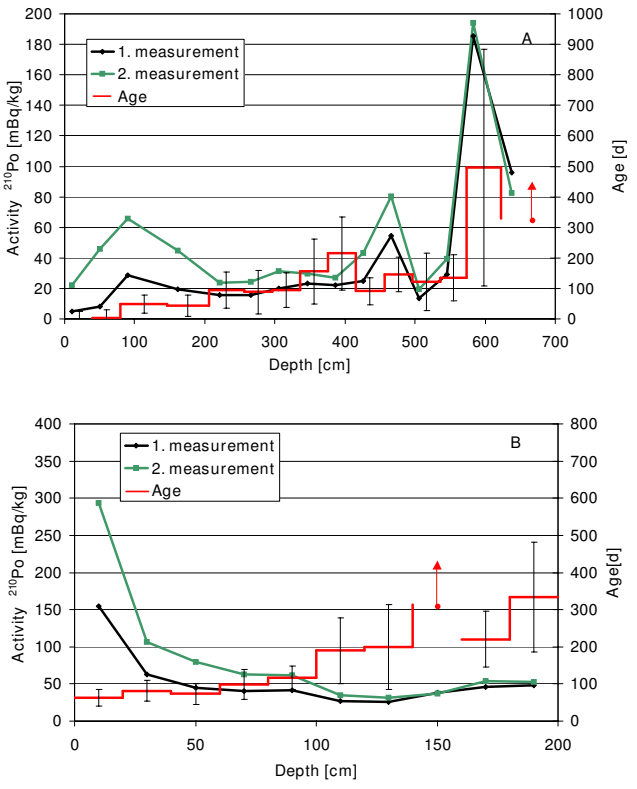

Fig. 1: Dating of the Jungfraujoch shallow core (A) and the Fedchenko glacier snow pit (B).

REFERENCES

[1] A. Eichler et al., J. Glaciol. 46, 507 (2000).
[2] H. Gäggeler et al., J. Glaciol. 29, 165 (1983).

PRECISION MEASUREMENT OF THE DECAY RATE OF ^{7}Be IN HOST MATERIALS

Y. Nir-El, G. Haquin, Z. Yungreiss (Radiation Safety Division, Soreq Nuclear Research Centre, Yavne, Israel), M. Hass, G. Goldring, S.K. Chamoli, B.S. Nara Singh, S. Lakshmi (Department of Particle Physics, Weizmann Institute of Science, Rehovot, Israel), U. Köster (ISOLDE, CERN, Geneva, Switzerland, Science Division, Institut Laue Langevin, Grenoble, France), N. Champault, A. Dorsival, V.N Fedoseye (ISOLDE, CERN), G. Georgiev (ISOLDE, CERN, CSNSM, CNRS/IN2P3; Univ Paris-Sud, ORSAY-Campus, France), B.A. Marsh (Physics Department, University of Manchester, Manchester, UK), D. Schumann, S. Teichmann, G. Heidenreich (PSI Villigen, Switzerland) and the ISOLDE Collaboration

A controlled and precise determination of the cross-sections of the fusion reactions $^{7}Be(p,\gamma)^{8}B$ and $^{3}He(^{4}He,\gamma)^{7}Be$, which play an important role in determining the solar neutrino flux, necessitates the knowledge of a precise value of the electron-capture half-life of ^{7}Be. This half-life may depend on the material hosting the ^{7}Be atoms via small modifications of the electron density around the ^{7}Be nucleus. In this brief communication we report on the measurement of 7Be implanted in four materials: copper, aluminium, sapphire and PVC. The four results are consistent with a null host dependence within two standard deviations and their weighted average of 53.236(39)d agrees very well with the adopted value in the literature, 53.22(6)d. The present results may exhibit a slight (0.22%) increase of the half-life at room temperature for metals compared to insulators that requires further studies.

1 INTRODUCTION

The decay rate of radioactive nuclei that undergo orbital electron capture (EC) depends on the properties of the atomic electron cloud around the nucleus. Hence, EC may exhibit varying decay rates if the nucleus is implanted into host materials with different properties of their corresponding electron clouds. The first suggestion of this effect in ^{7}Be, which is the lightest nucleus that decays by EC, and reports of experiments trying to investigate this phenomenon, have been presented in [1-3]. This effect has been qualitatively attributed in the past to the influence of the electron affinities of neighboring host atoms [4]. Recently, the life-time modification has been suggested to stem from differences of the Coulomb screening potential [5] between conductors and insulators (see below).

The present work has been undertaken in order to probe this phenomenon yet again in an experimental approach that takes full advantage of the experience gained in measuring implanted ^{7}Be activity in a controlled and precise manner for cross section determinations of the solar fusion reactions mentioned above [6,7]. The same setup has also been used for determining the ^{7}Be activity ensuing from the $^{3}He(^{4}He,\gamma)^{7}Be$ reaction [7].

2 EXPERIMENTAL

We report the measurement of the half-life of ^{7}Be implanted in four host materials: copper, aluminum, aluminum oxide (sapphire - Al_2O_3) and PVC (polyvinyl chloride -$[C_2H_3Cl]_n$). The primary source of ^{7}Be for implantation was a graphite target, from the Paul Scherrer Institute (PSI), used routinely for the production of π mesons [8]. Graphite material from the PSI meson production target was placed in an ion-source canister and was brought to ISOLDE (CERN); ^{7}Be was extracted at ISOLDE by selective ionization using a resonance laser ion source. Direct implantation of ^{7}Be at 60 keV in the host material was subsequently followed. A detailed description of the extraction and implantation of ^{7}Be at ISOLDE is provided in detail in [9,10].

3 RESULTS

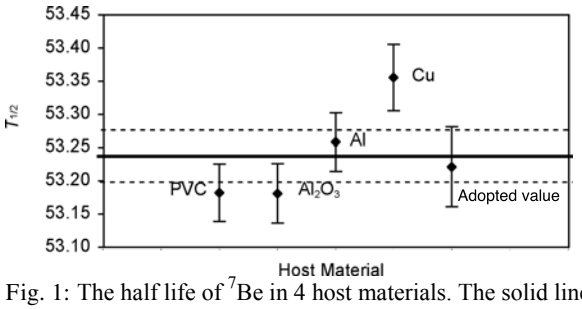

Fig. 1: The half life of ^{7}Be in 4 host materials. The solid line represents the weighted average; the broken lines correspond to a 1-σ interval. Also shown is the adopted value in the literature [11].

Even though the statistical test of the present data (Fig.1) supports a null effect within 1 σ, the average life times for the two insulators (PVC and Al_2O_3) and the two metals (Cu and Al) are 53.180(31) d and 53.299(33) d, respectively, a difference of 0.22%. A possible interpretation of the half-life results follows a recent observation by Wang et al. [12] of an approximately 1% increase in the lifetime of ^{7}Be in metallic vs. insulator environments at low temperature. This change is consistent with the Debye screening model [5] that has been successfully used to explain the screening potential for nuclear reactions at very low beam energies. A further investigation of such a small trend and its detailed temperature dependence is clearly called for.

REFERENCES

[1] E. Segre, Phys. Rev. 71, 274 (1947).
[2] E. Segre and C.E. Wiegand, Phys. Rev. 75, 39 (1949).
[3] R.F. Leininger, et al., Phys. Rev. 76, 897 (1949).
[4] P. Das and A. Ray, Phys. Rev. C 71, 025801 (2005).
[5] K.U. Kettner et al., J. Phys. G 32, 489 (2006).
[6] L. T.Baby et al., Phys. Rev. Lett. 90, 022501 (2003).
[7] B.S. Nara Singh et al., Rev. Lett. 93, 262503 (2004).
[8] G. Heidenreich, Proc. AIP 642, 122 (2002).
[9] L.T. Baby et al :, Phys. Rev. C 67, 065805 (2003).
[10] U. Koester et al., Nuc. Inst. Meth. B 204, 343 (2003).
[11] J.K. Tuli, Nuclear Wallet Cards, 7th ed., (2005), www.nndc.bnl.gov
[12] B. Wang et al., Eur. Phys. J. A 28, 375-377 (2006).

SEPARATION OF ^{10}Be FROM PROTON-IRRADIATED GRAPHITE TARGETS

D. Schuman, S. Horn, J. Neuhausen, P. Kubik, I. Günther-Leopold (PSI)

High-concentration samples of carrier-free ^{10}Be were separated from proton-irradiated graphite targets and analysed both with accelerator mass spectrometry and ICP-MS. The analytical results of both methods differ by less than 6%. The ^{10}Be-samples are foreseen for scientific experiments in basic nuclear research and nuclear astrophysics.

1 INTRODUCTION

Be-isotopes are of high interest in several nuclear physics and astrophysics research areas, such as the study of halo nuclei of light elements [1,2]. Access to exotic long-lived radionuclides would allow to study nuclear potentials, charge-symmetry properties, and spectroscopy of light and cluster nuclei.

Proton-irradiated graphite targets contain considerable amounts of ^{10}Be. These carbon targets are used at PSI for myon production in the target E station of the 590 MeV ring cyclotron complex. Several irradiated targets are available and had been analysed concerning their ^{10}Be content. The ^{10}Be-richest sample is foreseen for application in several scientific experiments.

2 EXPERIMENTAL

Usual exposure times of the graphite targets are 1 to 3 years. The beam doses vary from 4 to 11 Ah (590 MeV proton beam). The main activation products are ^{3}He, ^{14}C and ^{10}Be (after a cooling time of several years waiting for the decay of ^{7}Be).

Analytical determinations were carried out using two different methods, the Inductively Coupled Plasma Mass Spectrometry (ICP-MS) and Accelerator Mass Spectrometry (AMS). Both methods require the addition of a stable carrier isotope (^{9}Be) in known amounts, because the measurements are based on the determination of isotope ratios.

Separation procedure for analytical samples (AMS)
About 20-30 mg of carbon were dissolved in a $HNO_3/HCl/HClO_4$ mixture by stirring under heating for several hours. 2 mg of ^{9}Be were added to each sample. After complete dissolution, $Be(OH)_2$ was precipitated with diluted ammonia solution. The samples were purified by ion exchange on a DOWEX 50 column as described in [3]. Due to the relative high expected content of ^{10}Be, they were diluted with stable Be in a ratio of 1:1000. After a second precipitating step, the hydroxides were glowed to the oxide at 900°C.

Separation procedure for carrier free samples
5-14 g of carbon were pulverized with a ball mill and then treated with a mixture of $HNO_3/HClO_4/H_2SO_4$ in a three-neck vessel under stirring and heating for several hours. ^{7}Be was added to monitor the chemical yield. The outgoing gas flows through a $Ba(OH)_2$ solution in order to adsorb the carbon dioxide. The remaining solution containing the beryllium and tritium was filtered. Fe^{3+} was added and beryllium hydroxide was co-precipitated together with iron hydroxide by use of ammonia solution. The $Fe(OH)_3$ was dissolved in 7 M HCl and the iron separated by use of an anion exchange column. Purification from boron (^{10}B is an interfering isobar in ^{10}Be analysis) can be reached by adsorption onto a cationic column from diluted nitric acid solution and following elution with 4 M HCl. Aliquots from these final solutions were mixed with carrier solution and the content of ^{10}Be was determined by ICP-MS.

3 RESULTS

Tab. 1 shows the analysis results for the determination of ^{10}Be in 4 graphite target samples. Measurements were done by AMS and ICP-MS.

Tab. 1: Analytical results from several carbon targets and available amounts of ^{10}Be for scientific experiments - columns 4 and 5 indicating the total amount of ^{10}Be separated from the respective sample (a - outer part of the target wheel - beam entrance; i- inner part of the target wheel - no direct beam contact)

Sample	^{10}Be [Bq/g] ICP-MS	^{10}Be [Bq/g] AMS	Total amount of atoms	Total amount in μg
1a	220		$6.7\cdot10^{16}$	1.1
1i		95		
2a	291	316	$8.4\cdot10^{16}$	1.4
2i		7		
3a	506	495	$6.5\cdot10^{16}$	1.1
4a	2049		$1.0\cdot10^{18}$	16.7

The ^{10}Be content for the inner parts was too low for ICP-MS measurement, but the outer parts could be measured with a sufficient precision (3%). Two of the outer part samples could be measured by both methods showing a very good agreement (<6%).

Aliquots of sample 4 are being provided for two experiments:

- Spectroscopy of ^{10}Be on the search for the beryllium halo nuclei charge radii (collaboration with GSI Darmstadt and Uni Mainz)
  Production and the acceleration of a new ^{10}Be beam at the CRC/UCL facility (Louvain-la-Neuve Belgium).

REFERENCES

[1] I. Tanihata et al., Physical Review Letters. 55, 2676-2679 (1985).

[2] I. Tanihata, Journal of Physics G. 22, 157-198 (1996).

[3] D. Schumann et. al. ND 2004, AIP Vo.769, p. 1517.

THE EXCITATION FUNCTION FOR THE PRODUCTION OF ^{108m}Ag VIA THE REACTION ^{209}Bi(p,xpyn)^{A}Z

D. Schumann, J. Neuhausen (PSI), R. Michel (ZSR Hannover)

A chemical separation procedure was developed which allows isolating silver from bismuth targets irradiated with protons in an energy range up to 2.6 GeV. The cross sections in dependence on the proton energy were determined; the excitation function is shown. The studies are aimed to complete the data sets on calculation codes for predictions of the nuclide inventory of an Accelerator Driven System (ADS) based on a Lead-Bismuth-Target.

1 INTRODUCTION

In previous works [1-2] we reported on the development of chemical separation procedures for the determination of residue nuclides produced in proton-induced nuclear reactions with the target element lead. However, one of the foreseen target materials in a possible ADS system is Lead-Bismuth-Eutectic (LBE), very recently tested in the MEGAPIE test experiment (MEGA-Watt-Pilot-Experiment) at PSI with extraordinary success. Besides the demonstration, that a 1MW power liquid target station can be operated with high reliability, it was also shown that the neutron yield is about 80% higher as with a solid lead target [3]. Therefore, LBE seems to be a serious alternative for a new target design based on liquid metal technology and the knowledge of the residue nuclide production is essential for estimation and validation of the target handling after operation, including also options for intermediate or final disposal. Long-lived radionuclides with half-lives of more then 10 years are of special interest in this context. Therefore, a similar, but extended separation program was developed as for the target element lead, which includes besides the "standard radionuclides" ^{36}Cl, ^{129}I, ^{26}Al and ^{10}Be also several Polonium isotopes ($^{208\text{-}210}$Po) as well as the long-lived ^{108m}Ag with a half-live of 418 years. While the determination of the other isotopes is still ongoing, the present work reports on the results of the silver determination.

2 EXPERIMENTAL

The targets consist of ultra-pure Bi-foils with a thickness of 0.25 mm and a typical weight between 400 and 600 mg. They were irradiated in the years 1994-1996 at The Svedberg Laboratorium (TSL) in Uppsala/Sweden (proton energies > 180 MeV) and at Laboratoire National Saturn (LNS) in Saclay/France (proton energies above 180MeV) using a stack technology described in detail in [4].

The proton-irradiated Bi-targets were dissolved in half-concentrated HNO_3, and chlorine and iodine were separated similar to the separation scheme described for the lead targets [1]. After distillation to dryness, the residue of $Bi(NO_3)_3$ was dissolved in 7 M HNO_3 and 2 drops of $AgNO_3$ solution were added. The mixture was stirred and 2 drops of conc. HCl were added leading to a white precipitation of AgCl. The over-standing solution was decanted and the precipitate was dissolved in diluted ammonia solution in order to dissolve all traces of ^{108m}Ag. AgCl was re-precipitated by freshly acidifying the solution. The precipitate was filtered on filter paper. After drying, the sample is ready for γ-measurement. The chemical yield of the silver separation was determined by carrying out analogous experiments with non-irradiated Bi and carrier-free ^{111}Ag which was produced by neutron activation of Pd. An average yield of about 58±10% was reached.

3 RESULTS

In Fig.1, a representative γ-spectrum of the Ag-fraction is shown. All 3 main γ-lines of ^{108m}Ag are detected.

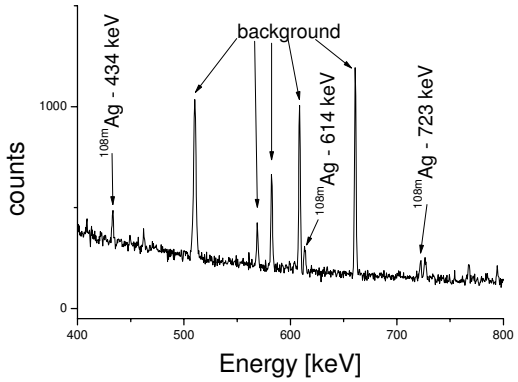

Fig.1: γ-spectrum of the silver fraction.

In Fig.2, the determined cross sections for the production of ^{108m}Ag in dependence on the proton energy are shown.

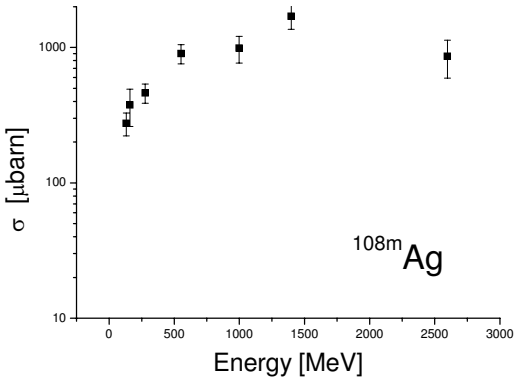

Fig.2: Excitation function for the production of ^{108m}Ag in the reaction ^{209}Bi(p,xpyn)^{A}Z.

The results are in good agreement with other cross section data of the same nuclear reaction for isotopes in similar mass segments like $^{105/106/110m}$Ag [4].

REFERENCES

[1] D. Schumann et.al. NIM A 562 (2006) 1057.
[2] D. Schumann et.al. AIP Conf. Proc. Vo.769, p. 1517.
[3] K. Clausen, private communication.
[4] M. Gloris PhD thesis Univ. Hannover 1998.

A COPPER BEAM DUMP AS SOURCE FOR EXOTIC RADIONUCLIDES PART I: SAMPLE DESCRIPTION AND CHEMICAL ANALYTICS

D. Schumann, J. Neuhausen, S. Horn, P. Kubik, H.-A. Syna1, S. Köchli (PSI), G. Korschinek (TUM Garching)

The copper beam dump of the BMA station at PSI is a source for several exotic radionuclides to be used in a number of nuclear physics related studies. First step for a successful exploitation of this valuable material is the complete analytical characterisation of the nuclide inventory. First results are presented.

The BMA station was operated from 1980 till 1992 to produce pions for cancer treatment. The copper beam dump of the facility received a total beam dose of approximately 0.16 Ah (590 MeV protons) and was dismounted in 1993. It was cut into 7 pieces as shown in Fig.1 and Fig.2. Samples were taken from the center (X.1) and peripheral region (X.2). For the piece No. 3, 5 samples were taken in equal distances of 10 mm, starting from the central position (X.1 - X.5).

After the above described sample taking for analytics, the central regions of the pieces 2 - 5 were drilled out with a diameter of 20 mm - see Fig. 1. With this procedure 500 grams of highly-active copper chips were obtained which can be used for the separation of exotic radio-isotopes (see the report on the ERAWAST research program [1]) .

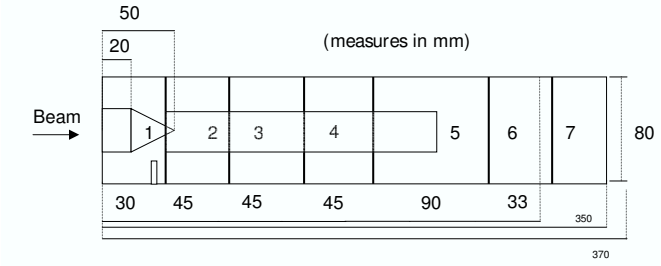

Fig.1: Schematic view of the copper beam dump. The selected area in the pieces 2-5 marks the drilling region

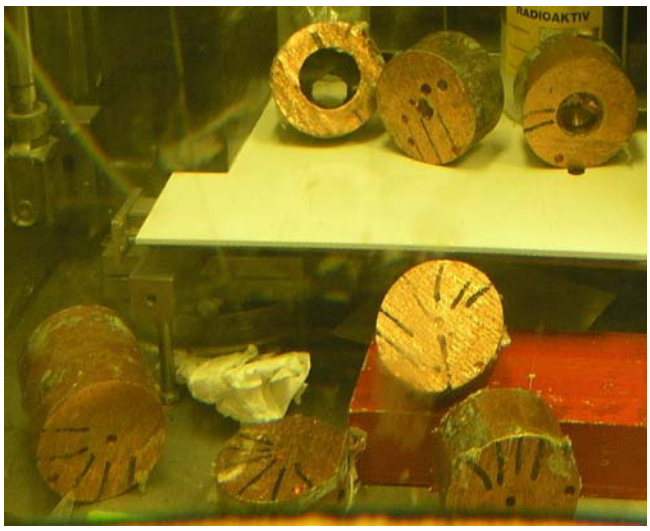

Fig.2: Photo of the beam dump pieces after sample taking and before drilling. The piece number is marked with black lines; the piece 3 with the 5 with the sample taking positions can be seen in the upper part of the picture.

The amounts of radionuclides listed in Tab.1 were determined by use of γ-spectroscopy, AMS and LSC, mainly after chemical separation. The procedures for the chemical separations are described elsewhere [2,3].

Tab. 1: Specific activities of selected samples of the copper beam dump, measured by γ-spectrometry (^{44}Ti, $^{110/108m}$Ag, ^{60}Co), LSC (^{63}Ni, ^{55}Fe), AMS (^{36}Cl, ^{26}Al, ^{53}Mn); bold: Values from the central sample positions used to estimate the total amount of available material.

Sample (X.Y)	^{44}Ti [kBq/g]	^{36}Cl [Bq/g]	^{63}Ni [kBq/g]	^{55}Fe [kBq/g]	^{26}Al [Bq/g]	^{110m}Ag [Bq/g]	^{108m}Ag [Bq/g]	^{53}Mn [Bq/g]	^{60}Co [kBq/g]
1.1	4.8	4.06	220.3	233.6	0.154	1.21	1.77		224.0
1.2	0.54	0.49	133.7	37.3	0.016	1.98	2.52		85.7
2.1	1616.0		34151.1	42450.3	140	3.89	62.58	6900	49957.1
2.2	0.2	0.30	217.7	108.6		2.48	1.35	0.6	111.6
3.1	740.8		36566.7	44136.3	56	2.3	37.27	4310	37969.6
3.2	18.6		2006.0	2562.0	1.1	0.453	9.19	112	2691.8
3.3	1.5		1109.7	1552.4	0.2	1.32	9.22	17.6	1239.4
3.4	0.6		1841.6	257.0	0.03	0.92	1.69	5.6	663.2
3.5	0.4	0.35	706.2	154.7	0.01	0.56	1.06	4.3	438.8
4.1	778.1		16776.3	26590.4	41	1.64	27.70	3600	47256.0
4.2		0.24	799.1	132.5		0.09	1.27	2.1	505.5
5.1	95.0		5764.1	11520.4	3	11.70	13.64	998	10091.9
5.2		0.27	545.6	157.8		0.59	1.80	2.0	415.0
6.1	-	0.13	1005.7	287.6	0.012	3.75	3.93		459.0
6.2	-	0.08	233.2	127.8	0.0019	0.49	0.94		169.8
7.1	-	0.08	170.2	350.7		1.4	1.34		148.6
7.2	-	0.04	118.8	233.6	0.0013	1.85	0.86		91.1

Using these analytical results, a first estimate shows that about 100 MBq ^{44}Ti, 500 Bq (10^{17} atoms) ^{53}Mn and 7 kBq (10^{17} atoms) ^{26}Al can be expected to be available for scientific use from the 500 g drilled chips. The determination of ^{60}Fe and ^{59}Ni is ongoing. Due to the high content of ^{60}Co, an automatic separation technique in a hotcell will be necessary for the chemical separation.

REFERENCES

[1] D. Schumann et.al., this report p. 40.

[2] D. Schumann et.al., , AIP Conference Proceedings 769, Melville, New York, 2005, p. 1517.

[3] D. Schumann et.al. NIM A 562 1057 (2006).

A COPPER BEAM DUMP AS SOURCE FOR EXOTIC RADIONUCLIDES PART II: THEORETICAL CALCULATIONS

D. Schumann, J. Neuhausen, M. Wohlmuther (PSI)

Theoretical predictions by use of Monte Carlo simulations are an essential tool for the estimation of the radionuclide inventory of activated materials. The copper beam-dump of the former BMA-station at PSI, which is foreseen for chemical separation of long-lived exotic isotopes, has to be characterized using MCNPX and a modified version of FISPACT. First results are presented..

1 INTRODUCTION

All particles that are accelerated in an accelerator facility will be lost - intended or not. They will then interact with surrounding matter, initiate particle cascades and activate the material hit. Some of the secondary particles produced in these cascades have sufficient energy to initiate a new particle cascade and will therefore as well activate the material.

The copper beam dump of the BMA facility represents an intended beam loss point, as all protons hitting the beam dump are stopped. The primary protons and secondary particle species such as neutrons and pions have activated the beam dump during its life time. After dismantling, the beam dump was cut into pieces and samples were taken at different radii - see [1]. The irradiation was simulated using the particle transport code MCNPX [2] together with a modified version of the build-up and decay code FISPACT [3].

2 THE METHOD

Monte-Carlo methods coupled to build-up and decay codes are used at PSI to model components at or near to major loss points. It is essential to benchmark the theoretical predictions to get an estimate for the performance of the particle transport codes. At PSI the particle transport code MCNPX is used to simulate the interaction of particles with matter.

The BMA beam dump was activated in a mixed radiation field of primary protons, secondary high energy spallation neutrons (E > 20 MeV), secondary protons, pions as well as low energy neutrons (E ≤ 20 MeV). MCNPX is used to determine the nuclide inventory produced by the primary protons as well as by the high energy (E > 20 MeV) secondary particles created in spallation reactions. Moreover, low energy neutron spectra (E < 20 MeV) are calculated for part of the BMA beam dump. These neutron spectra are folded within FISPACT with cross sections of the EAF libraries. Combining the nuclide inventory produced by low energy neutrons (E < 20 MeV) with the nuclide production rates calculated with MCNPX in the physics model region (E > 20 MeV) a full description of the residual nuclei is obtained.

3 RESULTS

Theoretical predictions for the production of the residue nuclides like ^{36}Cl, ^{44}Ti, ^{26}Al, ^{53}Mn, ^{55}Fe and others (see tab.1 in [1]) were obtained. In Fig. 1, the radial distribution of ^{44}Ti in the third piece of the beam dump is shown as an example.

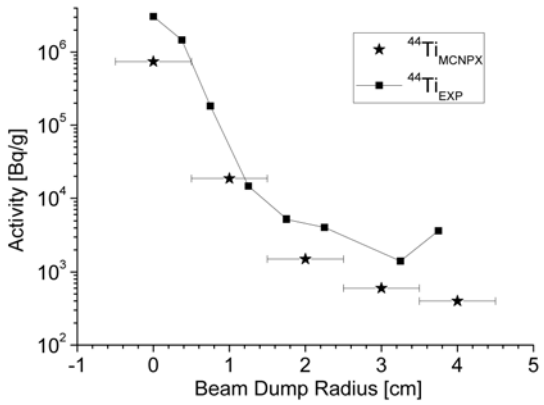

Fig. 1: Radial distribution of the specific activity of ^{44}Ti in the third piece of BMA copper beam dump.

A steep fall-off of the Ti production is seen in the theoretical predictions as well as in the experimental data. This behavior is explained by the fact that all reactions leading to the above mentioned end products have high thresholds and therefore production rates will be high in the presence of high energy particle fluxes. The highest high energy particle fluxes are located in the region around the primary proton beam. In general a good agreement between measurement and theoretical prediction is found.

REFERENCES

[1] D. Schumann et.al., this report p. 38.
[2] D. Pelowitz, *MCNPX™ User's Manual*, LA-CP-05-0369, Los Alamos National Laboratory 2005.
[3] R. A. Forrest, FISPACT-2003: User manual, UKAEA Fus 485, Culham Science Center 2002.

EXOTIC RADIONUCLIDES FROM ACCELERATOR WASTE FOR SCIENCE AND TECHNOLOGY

D. Schumann, J. Neuhausen (PSI), F. Käppeler (FZ Karlsruhe), G. Korschinek (TUM Garching), F. Rösch (Univ. Mainz), Z. Fülöp (ATOMKI Debrecen)

An ESF exploratory workshop aimed to establish a network on the exploitation of exotic radionuclides was held at Villigen from 15th till 17th November 2006.In total, 33 Participant from 12 countries presented experimental and theoretical contributions covering topics from astrophysics, basic nuclear physics, radiochemical and pharmaceutical chemistry, accelerator mass spectrometry, and relates research fields.

Exotic radionuclides, such as for instance ^{44}Ti, ^{60}Fe, ^{26}Al, ^{10}Be and many others, are of great interest in several research domains like astrophysics, nuclear medicine, geophysics, fundamental nuclear physics or radioactive beam facilities.

The production of all these nuclides in sufficient amounts is very time consuming and extremely expensive. Conventional techniques in commercial radioisotope production - restricted mainly on reactor-based or accelerator-driven production routes – are approaching their limitations. Consequently, alternative production possibilities and ways of cooperation in large basic-physics facilities are discussed. One of these possibilities is the exploitation of accelerator waste.

In the past, activated parts from accelerators played a minor role the nuclear waste management due to the small amounts of expected material. This situation changed drastically with the advent of new large accelerator facilities. The construction of powerful accelerators, spallation neutron sources, radioactive-beam-facilities as described in the EURISOL project [1] as well as new innovative energy concepts like accelerator driven systems (ADS) – a concept given high priority by the EC by supporting projects like EUROTRANS [2] - require also detailed and reliable analysis of the radionuclide inventory including activated materials.

The spallation neutron source SINQ at the PSI, is one of the most powerful facilities of its kind in Europe. Already some years ago, investigations were started to study the main (γ-) activity content of targets, shieldings, and beam dumps. Usually, the interest in nuclear waste was limited to an evaluation of the related hazards and to investigate possibilities of waste disposal at low risks and with low costs. However, some special kind of accelerator waste might be a source of valuable exotic nuclides, which are difficult to produce by other methods. Therefore, special analyses of some selected rare isotopes were carried out, and we found ^{60}Fe, ^{26}Al, and ^{10}Be in considerable amounts.. Because these materials contain also many other important isotopes, the idea to use this potential received great interest and was supported by the European Science Foundation.

The first ESF-sponsored Exploratory Workshop on this topic was held in Villigen in November 2006 with the aim to search for potential collaboration partners and to establish an international network for the exploitation of accelerator waste materials with regard to the use of exotic radionuclides in basic science and for technological and medical applications. In total, 30 participants from 12 countries decided to create an international collaboration expressed by the following program:

1. *Existing accelerator waste material*
   From a copper beam dump, which was irradiated at the 590-MeV proton beam station at PSI and was dismounted about 10 years ago, nuclides like ^{26}Al, ^{59}Ni, ^{53}Mn, ^{60}Fe, or ^{44}Ti can be separated. Also other irradiated materials, i.e. carbon (source for ^{10}Be), stainless steel, or concrete are available.

2. *Target material from the SINQ facility*
   Two irradiated lead targets from the spallation source are available as well, which can be used to extract heavier isotopes, such as ^{182}Hf or several rare earth nuclides (^{146}Sm and several Dy isotopes). In principle, lead targets from the SINQ will be available every second year.

3. *Nuclide extraction from Hg rods*
   Similar to lead, mercury can also serve as a spallation target for neutron production. In the frame of the EURISOL program, studies for isotope separation from such targets are foreseen. Two already irradiated Hg rods are available for preparing small samples of interesting isotopes. An extension of this possibility is expected with a working EURISOL facility.

4. *Special irradiations*
   The SINQ facility offers the possibility to irradiate materials with 590 MeV protons at special positions. So, tended experiments for isotope production can be offered.

Exotic radionuclides shall be provided from PSI site for experiments in basic nuclear research, nuclear astrophysics, nuclear medicine, AMS, and other related areas. A 4-year Scientific Network Programme for financial support of fellowships, workshops, exchange visits and conferences was launched according to the corresponding ESF call.

REFERENCES

[1] EURISOL (EUROpean Isotope Separation On-Line Radioactive Ion beam Facility) 6th framework of the EC EURATOM programme.

[2] EUROTRANS (EUROpean Research Programme for the TRANSmutation of High level Nuclear Waste in an Accelerator Driven System) 6th framework of the EC EURATOM programme.

DESIGN OF A ^{44}Ti/^{44}Sc GENERATOR SYSTEM

D. Schumann, S. Horn , J. Neuhausen (PSI)

A generator system for the production of carrier-free ^{44}Sc ($T_{1/2}$ =3.9 h) from the mother nuclide ^{44}Ti ($T_{1/2}$=63y), based on ion exchange technique, was designed. The generator can be used once a day with an yield of 86% of the totally possible activity.

1 INTRODUCTION

Scandium counts, like Yttrium, as a "semi-lanthanide". However, while Y represents mainly similar chemical properties compared to that of lanthanides, Sc shows surprising behaviour in some cases, especially if carrier-free radionuclides are studied. One of the chemical systems, where such an unexpected behaviour was observed, is HF containing aqueous solution [1]. For example, lanthanides form insoluble fluoride compounds, precipitating if weighable amounts are applied. Sc on the other hand forms soluble anionic fluoride complexes, similar to group IV elements. Carrie-free Sc-radioisotopes are, therefore, desired for detailed investigations of their chemical behaviour. ^{44}Sc, as the daughter nuclide of ^{44}Ti, represents an ideal isotope for such studies, because it is sufficient short-lived (3.9h) for easy laboratory handling and the mother nuclide ^{44}Ti is long-lived enough (63y) to provide the activity practically unlimited. So, a generator system, consisting of a solid matrix where the Ti is fixed and a mobile phase carrying the Sc, was developed.

2 EXPERIMENTAL

^{44}Ti containing solution (1 M HNO_3, separation and preparation as described in [2]) was evaporated to dryness, fumed several times with HF solution and dissolved in 1 M HF. The solution was passed through an anion exchange column (DOWEX1x8; 200-400 mesh, 2ml column volume). Titanium is adsorbed under these conditions. The elution of ^{44}Sc can be performed with mixed HCl/HF solution.

3 RESULTS

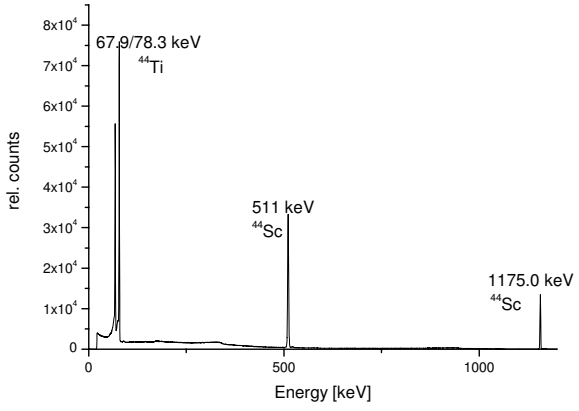

Fig. 1: γ-spectrum of ^{44}Ti-HF solution in equilibrium with the daughter nuclide ^{44}Sc.

In Fig. 1 the -spectrum of the starting solution of ^{44}Ti (1 M HF) is shown. This solution was passed through the anion exchange column and 44Sc was eluted with a mixture of 0.06 M HNO_3/0.4 M HF. As can be seen from Fig.2, ^{44}Ti is completely adsorbed onto the anion exchanger. The eluate is free from ^{44}Ti and other contaminations.

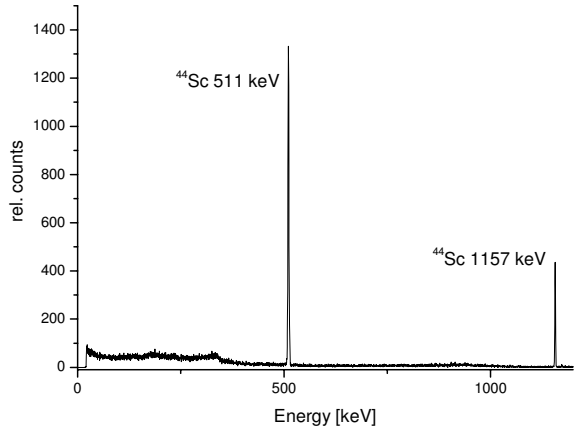

Fig. 2: γ-spectrum of the eluate (0.06 M HNO_3/0.4 M HF).

In Fig.3 the elution profile of the column is shown. About 90% of the ^{44}Sc activity can be eluted within 2-3 ml of eluent.

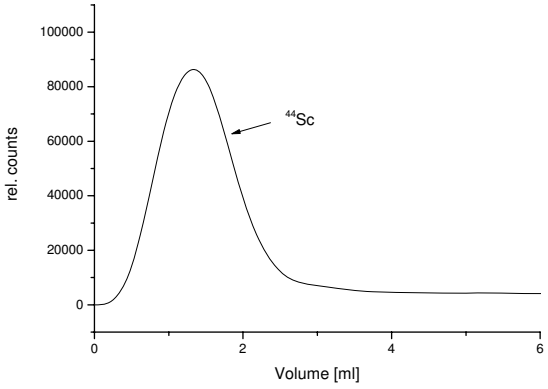

Fig. 3: Elution of ^{44}Sc from a ^{44}Ti/^{44}Sc generator column (DOWEX1x8) using (0.06 M HNO_3/0.4 M HF solution.

The present generator contains about 50 kBq ^{44}Ti being sufficient for many experiments in laboratory scale. Since the mother activity is used in carrier-free form, the total activity which is possible to be adsorbed. can be increased to several MBq. The generator can be eluted once a day.

REFERENCES

[1] D. Schumann et.al., Radiochim. Acta 93 (2005) 727.

[2] D. Schumann et.al., Annual Report Labor Radio- & Umweltchemie 05, p. 40.

ASSESSMENT OF THE MEGAPIE REFERENCE ACCIDENT CASE

F. Groeschel, J. Neuhausen, A. Fuchs, A. Janett (PSI)

Different scenarios for the reference accident case postulated for the MEGAPIE experiment are evaluated. The maximum possible release for the most relevant volatile elements is estimated based on data for vapour pressure and evaporation rate as well as the calculated cooling behaviour of the target. Measures to reduce the radioactivity release are discussed.

INTRODUCTION

In 2006 MEGAPIE (Megawatt Pilot Experiment) was started at PSI. In this experiment, the standard solid SINQ target is replaced by a liquid metal target employing liquid eutectic lead-bismuth alloy (LBE) target material. The experiment aims to demonstrate the feasibility of liquid metal spallation targets for application in science (e.g. spallation neutron sources or radioactive beam facilities) and technology (e.g. accelerator driven systems for the transmutation of long-lived nuclear waste). Furthermore, an increase of neutron flux in SINQ is expected from this new type of target.

A large amount of radioactive nuclides is produced inside the target by various nuclear reactions. In the standard solid target these radionuclides are bound in the solid matrix. In a liquid target however, the possibility of a spill of the target material has to be considered, accompanied by a release of radioactivity. Therefore, the swiss licensing authority, BAG, postulated a reference accident case. For the licensing of MEGAPIE, PSI had to demonstrate that the maximum dose to the public that can result from this worst case scenario is below 1 mSv. In this report we give an outline on the assessment of radionuclide release resulting from this reference accident case.

THE SCENARIO

The main ingredient of the reference accident case postulated by BAG is a spill of the target material due to a leak in the target. Furthermore, an interaction of the hot spilled target material with cooling water or water from the moderator tank as well as with the organic cooling fluid of the secondary cooling loop comes into play. This leads to a pressure increase resulting from evaporating water. Additionally, the possibility of ignition of the organic fluid has to be considered. Finally, the target enclosure is damaged in such a way that gases and vapours can escape from the target complex.

THE SOURCE TERMS

The evaluation of doses within the licensing procedure was based on the nuclide inventory calculated by Monte-Carlo simulations of a 200d irradiation with 1.4 mA/575 MeV protons [1]. From these calculations and an assessment of the volatility of the different elements, mercury and polonium were considered the most relevant for an accident study, apart from the noble gases. The radioactive inventories of the window cooling loop and the moderator tank have also been considered.

Noble gases are assumed to be completely released from the LBE to the expansion volume and vented into a decay tank every 30 days, limiting the maximum release to a 30 day production. Mercury and polonium are only partly released from the liquid metal. For dose calculations, three sources have to be considered: a) the expansion volume containing amounts of volatiles limited by their equilibrium vapour pressure, b) spilled LBE and c) an LBE film adhering to the hot target walls. For the latter two cases, the evaporation of Hg and Po were estimated based on their evaporation rate [2, 3] and the cooling behaviour calculated for the different surfaces. Finally, calculations were performed to estimate the amount of gas that escapes from the target complex to the public for different scenarios. The activity carried by that gas is fed into standard software to calculate maximum doses that can be expected for the public.

MEASURES TO REDUCE DOSE

The results of the evaluations described above led to the conclusion that some additional measures have to be taken to ensure the safety of the public in a worst case scenario:

The possibility of fire in the room where the interaction of LBE and organic coolant could take place is limited by reduction of the oxygen content.

The ventilation system in SINQ is upgraded with an autonomous, earth quake resistant exhaust device equipped with filters.

A mobile exhaust unit equipped with filters is provided as a back-up solution, and its operation e.g. in case of an earthquake is warranted.

REFERENCES

[1] E. Pitcher: Summary Report on Neutronics Work in Support of MEGAPIE; AAA Quarterly Report; September 2002.

[2] G.A. Greene, C.C. Finfrock: Brookhaven National Laboratory; Contract DE-AC02-98CH10996.

[3] J. Neuhausen: PSI TM MPR-3-NJ18-001/0; 2005.

SEGREGATION OF ^{210}Po IN EUTECTIC LEAD-BISMUTH ALLOY. ANALYTICS AND SAMPLE HOMOGENISATION

J. Neuhausen, F. von Rohr, S. Horn, D. Schumann (PSI)

A segregation of ^{210}Po was observed in samples of eutectic lead-bismuth alloy that were neutron irradiated in SINQ in summer 2003. The distribution of ^{210}Po in these samples was investigated by stepwise dissolution of the sample and analysis of the Polonium content of the different fractions by LSC. A method has been devised to homogenize the samples to facilitate their use for Po-release experiments.

INTRODUCTION

Liquid eutectic lead-bismuth alloy (LBE) is planned to be used as target material in future high power spallation targets for neutron production. In 2006, PSI performed the first test experiment to demonstrate the feasibility of such a target system in the MW range, MEGAPIE. One of the most significant problems when using LBE as target material is the production of significant amounts of the highly radiotoxic ^{210}Po by neutron capture on ^{209}Bi. According to Monte-Carlo simulations ^{210}Po is expected to be produced in gram amounts within the MEGAPIE project [1]. A thorough knowledge of its behaviour within the target system is a prerequisite for the safe operation of the target system and its disposal. Previous studies performed in our laboratory dealt with the evaporation of polonium from molten LBE [2].

The behaviour of polonium in solidified LBE may be of interest in the context of target handling after irradiation and final disposal. Literature indicates that the distribution of polonium in irradiated LBE samples becomes inhomogeneous after some time [3]. In this work, we study the distribution of ^{210}Po in LBE samples irradiated in SINQ using the NAA rabbit system.

EXPERIMENTAL

Polonium containing LBE samples were produced by irradiation of pieces of LBE in SINQ using the NAA rabbit system. Typical samples had a mass of ≈ 8 g and were irradiated for 1h without Cd-shielding. The samples investigated here were previously used to investigate the thermal release of Hg and Tl nuclides and afterwards stored in the laboratory for about 3 years at ambient temperature in closed PE-bags. Those samples that were not heated above 600 °C still contained enough ^{210}Po to yield acceptable count rates in α-spectroscopy. Therefore, they were considered to be useful to study the thermal release behaviour of Po from LBE under vacuum. However, for release experiments, it had to be ensured that Po is homogeneously distributed within the samples. Therefore, the distribution of ^{210}Po within these samples was studied.

The distribution of ^{210}Po in the samples was determined by successively etching-off a certain amount of the sample surface and analysing its ^{210}Po content. For this purpose, a sample of typically ≈ 1 g LBE containing carrier-free amounts of ^{210}Po was immersed in 7M HNO_3 for a certain time. Afterwards, the weight loss was measured and the ^{210}Po concentration of the dissolved LBE was analysed using LSC using the following procedure: The leaching solution was evaporated to dryness and dissolved in 5 ml 1M HNO_3. 1.25ml of this solution was mixed with 14 ml Aquasafe 300 and measured in the LSC-spectrometer (Packard Tri-Carb 2200CA) for 5h. Standard solutions containing varying known amounts of ^{210}Po and LBE-matrix was used for calibration.

RESULTS

Fig. 1 shows the variation of the ^{210}Po concentration in a typical sample as a function of mass remaining in the successive dissolution process. The diagram clearly shows that ^{210}Po is enriched in the surface region, while in the inner part of the sample its concentration remains more or less constant. The thickness of the enriched layer is estimated to be roughly in the order of 20 μm, based on the weight loss. The driving force for the segregation and its kinetics are a topic of further studies.

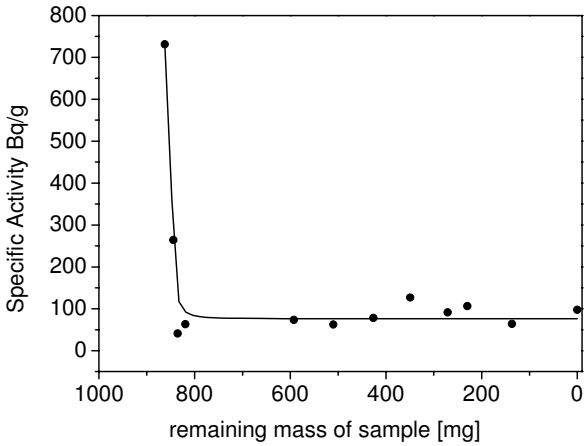

Fig. 1: Specific Activity of LBE-fractions successively dissolved from a ^{210}Po-containing LBE sample as a function of mass.

For the use of these samples for Po-release studies a method for homogenization of the Po distribution was devised. Homogeneity can be achieved by heating the samples at 500 °C in a H_2-atmosphere under mild agitation. Samples treated in this manner do not show a surface enrichment of ^{210}Po anymore immediately after solidification.

REFERENCES

[1] L. Zanini: Summary Report for MEGAPIE R&D Task Group X9: Neutronic and Nuclear Assessment, PSI Report Nr. 05-12, Paul Scherrer Institut, Switzerland, 2005.

[2] J. Neuhausen et al.: Radiochim. Acta 2004, 92, 917.

[3] T. Miura et al.: Appl. Radiat. Isot. 2004, 61, 1307.

THERMAL RELEASE OF ^{210}Po FROM LIQUID EUTECTIC LEAD-BISMUTH ALLOY UNDER VACUUM CONDITIONS

J. Neuhausen, F. von Rohr, S. Horn, D. Schumann (PSI)

For industrial scale Accelerator Driven Systems the use of windowless liquid metal spallation targets operating under vacuum is discussed. Under these conditions the release of volatiles will be strongly enhanced. To provide a basis to evaluate the volatility of ^{210}Po under these conditions, we started to study its thermal release from liquid eutectic lead bismuth alloy under vacuum conditions.

INTRODUCTION

High power spallation targets will be an important component of Accelerator Driven Systems (ADS) for the transmutation of long-lived nuclear waste. Because the current window materials cannot withstand the high energy deposition, windowless target designs are considered. In such a system, the liquid target material will be exposed to the vacuum of the proton beam line. Vacuum conditions will have a drastic influence on the evaporation behaviour of volatile radionuclides. However, investigations on the release behaviour of volatiles from liquid metals under vacuum are scarce. In case of a liquid eutectic lead-bismuth alloy (LBE) target, as considered e.g. within the EUROTRANS project, ^{210}Po is the most relevant nuclide due to its high radiotoxicity. There are a few literature data on Po release under vacuum [1], but for a reliable assessment of Po-release in such a system, more detailed studies are necessary.

EXPERIMENTAL

Polonium containing LBE samples were produced by neutron irradiation in SINQ as described in the preceding report. The experiments described before indicate that Po will be distributed rather homogenously in an agitated LBE melt, whereas in solid samples a surface enrichment is observed. For meaningful release experiments, it has to be ensured that the Po-distribution is similar to that within a spallation target system under operation. Therefore, the samples were homogenized as described previously.

Release experiments were performed in the apparatus depicted in Fig. 1. Before the experiment, a small part of the sample was cut off. The remaining part was put in a quartz boat lined with a quartz fleece, which was placed inside the quartz reaction tube. Additionally, a gold foil was placed in the tube to absorb the evaporated Po. The tube was evacuated using a turbo molecular pump. Typical pressures achieved were in the order of 1×10^{-5} mbar. A furnace was heated to the desired temperature. The reaction tube was then inserted in the furnace and kept there for 1 h. Afterwards, the tube was removed from the furnace, cooled to room temperature and vented. A small part of the LBE sample was cut-off. The parts that were cut off from the sample before and after heating were analysed by LSC to determine the release of Po.

RESULTS

Fig. 2 shows a comparison of the first results of release experiments performed in vacuum and those obtained in an

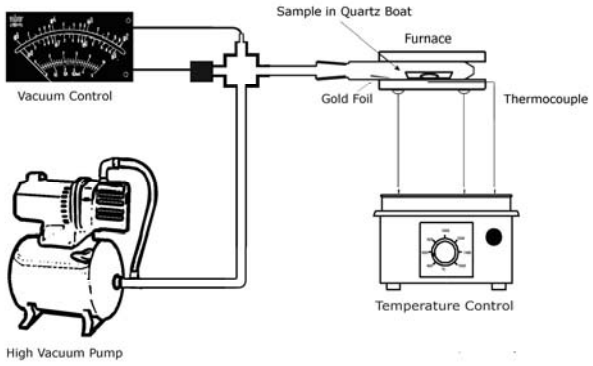

Fig. 1: Setup for release experiments in vacuum.

Ar/7%-H_2 atmosphere under ambient pressure [2]. The fractional release of Po is plotted as a function of temperature. It is evident that the evaporation of Po is significantly enhanced under vacuum, as expected. Apart from the missing points in temperature, further release experiments are planned, including long-term studies at temperatures close to the onset of Po release and investigations under different pressures, with the final goal of quantification of Po release rate. Already from the first results it can be concluded that in a windowless spallation target suitable measures have to be taken to catch the highly radiotoxic polonium isotopes.

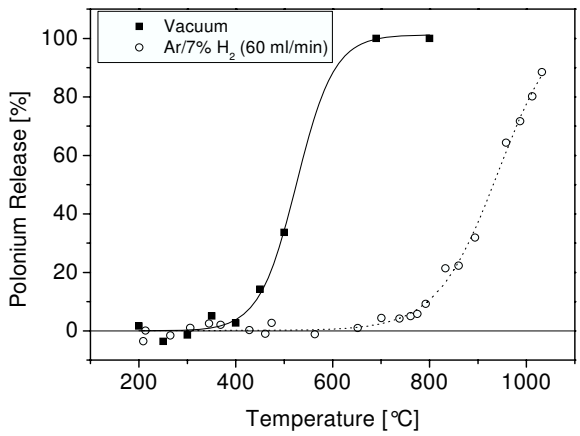

Fig. 2: Fractional release of Po from LBE under vacuum ($\approx1\times10^{-5}$ mbar) and Ar/7%-H_2 (ambient pressure).

REFERENCES

[1] R. B. Tupper et al.: Proc. Int. Conf. on fast reactors and related fuel cycles, Kyoto, Japan, 1991.

[2] J. Neuhausen et al.: Radiochim. Acta, 92, 917 (2004).

BEHAVIOUR OF NUCLEAR REACTION PRODUCTS IN LIQUID EUTECTIC LEAD BISMUTH ALLOY: SEMI-EMPIRICAL EVALUATION OF THE STABILITY OF BINARY CHEMICAL REACTION PRODUCTS

J. Neuhausen (PSI), N. Aksenov (JINR), D. Schumann (PSI), R. Eichler (PSI & Univ. Bern)

In contrast to a standard solid state spallation target where the mobility of nuclear reaction products is limited, in a liquid metal target chemical reactions are expected to run much more efficient because the liquid metal can act as a solvent. For an assessment of the stability of possible binary reaction products we employ a semi-empirical method.

INTRODUCTION

In a spallation target, substantial amounts of impurity elements are produced by nuclear reactions. Elements are produced in a range from atomic number 1 to Z+1, where Z is the atomic number of the target material. A typical distribution of nuclear reaction products calculated by Monte-Carlo simulations for the MEGAPIE target is shown in Fig. 1. Since liquid lead bismuth alloy is used in this experiment, the heaviest element produced in significant quantities is polonium. In general, the highest concentrations will occur for elements close to the atomic mass of the target material and around half of this mass. Additionally, rather large quantities of hydrogen and helium will be produced.

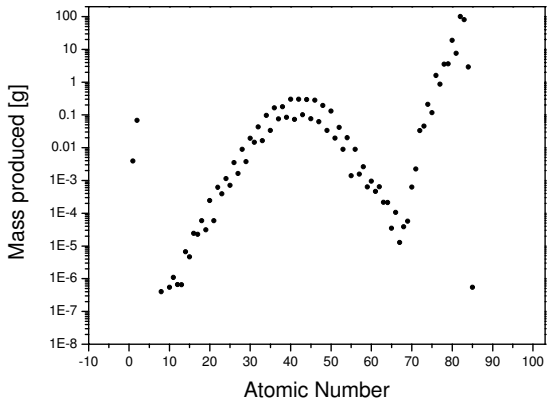

Fig.1: Calculated mass of spallation and fission products for the MEGAPIE target for 200 d irradiation with a 1.4 mA beam of 575 MeV protons.

From the chemical point of view, the target system is a highly complex multi-component system. Whereas in a standard solid target the nuclear reaction products are imbedded in a solid matrix, in a liquid metal target the target material can act as a solvent. This leads to an increased mobility of the impurities, resulting in an enhanced chemical reactivity. Convection of the liquid metal and temperature gradients still increase the complexity of the target system.

Possible chemical reactions include formation of intermetallic phases, corrosion processes and formation of oxides with the oxygen contained in the liquid alloy and in oxide surfaces of the construction materials. These products, when transported within the target system, may form precipitates that can influence the system behaviour. For example, suspended particles may cause abrasive effects on construction materials, or plating can lead to changes in heat transfer. Therefore, a basic understanding of the chemistry in liquid LBE is important. A prerequisite for the prediction of the chemical behaviour of impurity elements in the target is the knowledge of thermodynamical data. In a system as complex as a liquid metal spallation target, a large variety of complex chemical compounds could be formed. For many of these, thermodynamic data are not available. Even the formation of hitherto unknown phases is possible.

SEMI-EMPIRICAL CALCULATIONS

As a first step to understand the behaviour of different elements in a spallation target system we examine the heats of formation for binary compounds. These can be calculated for combinations of the elements of groups 1 to 16 of the periodic table using the Miedema model [1]. A map of heats of formation for compounds of composition $A_{0.5}B_{0.5}$ obtained in this way is shown in Fig. 2. The periodicity of the stability of the compounds is clearly visible, e.g. chalcogenides being particularly stable.

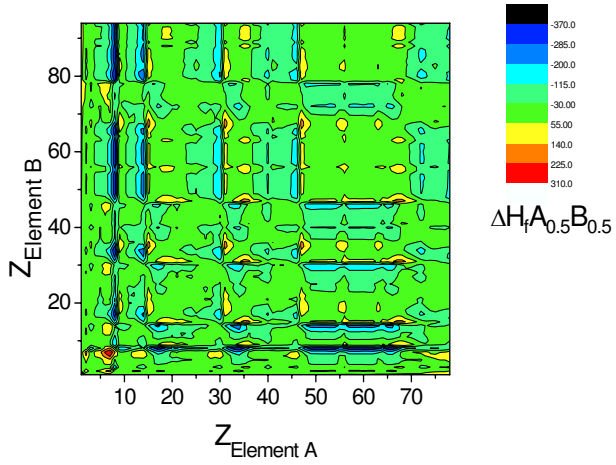

Fig. 2: Heats of formation for binary compounds of composition $A_{0.5}B_{0.5}$ calculated using the MIEDEMA model.

While the limitation to binary phases is clearly an oversimplification, it may as a first step give an indication on the specific behaviour of different elements. The results could be used to predict the chemical state of the elements within a target system, based on the abundance of the elements within the target system and the stability of typical compounds. Within the Post Irradiation Examination (PIE) program for the MEGAPIE experiment, the validity of such predictions could be verified.

REFERENCE

[1] F. R. de Boer et al.: Cohesion in Metals, Transition Metal Alloys, North-Holland, Amsterdam 1988.

RADIONUCLIDE PRODUCTION AND DISTRIBUTION IN PROTON IRRADIATED MERCURY SAMPLES

J. Neuhausen, S. Horn, D. Schumann (PSI), M. Eller, T. Stora (CERN)

Within the project EURISOL-DS, a spallation target in the MW range using mercury as target material is planned. For mercury purification, chemical separation procedures have to be developed to remove radionuclides from the target material. For this purpose, Hg samples have been proton irradiated at CERN. These samples are studied by γ-spectrometry to determine their radionuclide inventory and its distribution.

INTRODUCTION

EURISOL-DS is a design study investigating the construction of a next-generation radioactive beam facility (RIB) [1]. Within this study, a liquid metal spallation target with a power of several MW is designed to provide neutrons for a fission target, where neutron rich radionuclides will be produced. For the spallation target, mercury is planned to be used as target material. A large amount of radionuclides ranging from atomic number Z=1 to 81 will be produced in the liquid metal during long term irradiation. It is planned to remove those radionuclides by chemical or physicochemical methods to reduce its radioactivity. For the development of a purification procedure, knowledge about the chemical state of the different elements present in the mixture is required. Therefore, we started to investigate the behaviour of radionuclides in mercury. In this work, we study the production of radionuclides by proton irradiation and their distribution in mercury.

EXPERIMENTAL

Two 1 ml samples of Hg were filled in stainless steel capsules. These capsules were irradiated at CERN with a proton beam of 1.5×10^{15} protons of 1.4 GeV. After some weeks of cooling the samples were transferred to PSI, were they were measured on an HPGe-detector equipped with standard electronics. One sample (Sample 1) was opened in a Plexiglas glove box, which was filled with Ar. The Oxygen content of the system measured using an yttria-doped ZrO_2 solid electrolyte cell was in the range of 0.1 – 1 %. After opening, the Hg was removed from the steel capsule and poured into a glass vessel. γ-spectra of the steel capsule and the Hg sample were taken. Additionally, a part of the Hg was separated using a syringe, and a γ-spectrum of the removed fraction of Hg was measured. The main part of the Hg sample was filled into a second glass vessel and the first vessel checked for contamination. The second sample (Sample 2) of Hg remained in the original irradiation capsule. γ-spectra were taken repeatedly to facilitate nuclide identification based on decay properties.

RESULTS AND DISCUSSION

Fig. 1 shows a small section γ-spectrum of Sample 1 approximately 6 weeks after irradiation, clarifying the complexity of the spectrum. With the aid of spectra taken in the following months, various nuclides of the elements Ba,Ce, Gd, Eu, Lu, Hf, Re, Os, Ir, Pt, Au, Hg and Tl have been surely identified. For some isotopes of Se, Rb, Y, Zr, Nb, Mo, Ru, Sn and Yb the identification is less certain.

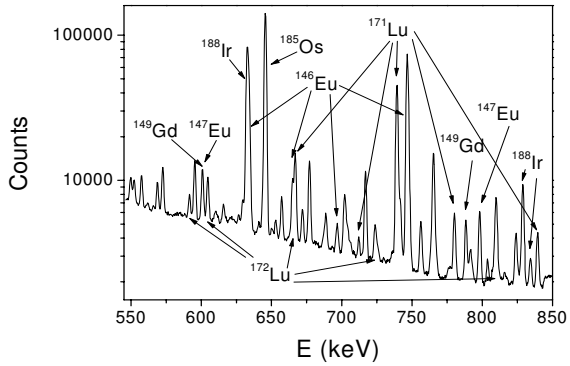

Fig. 1: Section of the γ-spectrum of sample 1 taken approximately 6 weeks after irradiation.

The γ-spectrum of the fraction of Hg separated using a syringe showed much less activity than expected. In fact, only gold isotopes could be identified in this sample. Since this sample was taken from the bulk, it is concluded that the remaining radionuclides are attached to the surface of the Hg droplet. The reason for this behaviour and the chemical state of the radionuclides located at the surfaces is not yet understood. Several reasons may lead to this behaviour. Some metals may simply segregate to the surface. Another reason for the separation may be oxide formation due to reactions with oxygen or oxide layers present in the capsule during irradiation. Finally, the radionuclides could also be bound to a very thin oxide layer present on the surface of the mercury. Such a layer will always be present, unless mercury is handled in an ultra-pure environment. Even a very small amount of oxide would be sufficient to adsorb the carrier-free amounts of radionuclides in the sample. In addition to the separation effect, a substantial fraction of the radionuclides tend to stick to the walls of the vessel when pouring the liquid metal from one container into another. For a liquid metal spallation target, several consequences of this effect have to be considered. For example, shielding calculations are performed assuming a homogeneous distribution of radionuclides in the target. A deposition of radionuclides on the walls of the loop could lead to higher than expected dose rates. Additionally, the radioactivity is not carried away with the liquid metal but partially remains in the loop after emptying the loop for maintenance operations. Furthermore, the deposition effect would influence the techniques that can be used for purification. First results from SNS at ORNL seem to indicate that these effects actually occur in a spallation target system [2].

REFERENCES

[1] http://www.eurisol.org

[2] F. X. Gallmeier, SNS/ORNL, personal communication.

SEPARATION OF LUTHETIUM AND HAFNIUM NUCLIDES FROM PROTON IRRADIATED MERCURY

J. Neuhausen, S. Horn, D. Schumann (PSI), T. Stora (CERN)

For the mercury spallation target designed within EURISOL-DS a separation of radionuclides from mercury is planned. The chemical procedures used to achieve this purification still have to be developed. We investigated the removal of luthetium and hafnium nuclides sticking on the surface of a proton irradiated mercury sample.

INTRODUCTION

Mercury purification is planned for the 4 MW liquid metal spallation target designed within EURISOL-DS [1]. This purification procedure will facilitate the re-use of the target material for long periods. Furthermore, the radioactive inventory is reduced for a final disposal. The possibility to use the separated radionuclides for medical or technical applications is also discussed [2]. To achieve a separation, knowledge about the chemical state of the different elements within a spallation target system is required. In general, some basic predictions can be made from general chemical principles: Noble gases will not undergo chemical reactions and will evaporate from the target. The majority of the elements however will either remain dissolved in Hg or precipitate as elements or insoluble compounds. Precipitated material can float on the Hg surface or form platings on the surfaces of the loop. Furthermore, sediments can be formed and dispersed particles can be carried with the flowing liquid metal. Different techniques have to be used to separate these materials from Hg. To evaluate the feasibility of different separation methods, we investigated the purification of proton irradiated mercury samples on a laboratory scale.

EXPERIMENTAL AND RESULTS

A sample of approximately 2 g Hg was proton irradiated at CERN. After cooling for several years under ambient conditions in contact with air, the sample was sent to PSI. γ-spectroscopy showed that the main activity remaining in the sample stems from long-lived isotopes such as ^{173}Lu, ^{172}Hf and its daughter ^{172}Lu as well as ^{194}Au as a daughter of ^{194}Hg. Visually, the sample did not show the bright metallic lustre displayed by pure mercury. Its surface had a rather dull grey appearance, indicating the presence of a thin oxide layer. A part of the mercury was separated from the bulk sample using a syringe in such a way that only material from the inner part of the Hg droplet was separated. The γ-spectrum of this fraction of Hg showed only the peaks of ^{194}Au, indicating that the Lu and Hf nuclides are attached to the surface of the sample rather than dissolved in Hg. Presumably, they are oxidised, since they are metals that are rather sensitive to oxidation. In principle, this behaviour is analogous to that observed in freshly irradiated samples described in the preceding report. Since a spallation target system is not an ultra-pure environment, oxidation processes can be expected to occur in such a system as well. Therefore, the formation of oxide material may occur in a target system, and methods to remove these can be an efficient way to remove a part of the radionuclides formed by nuclear reactions. The removal of this material should also help to prevent the deposition of solid materials at unwanted places, e.g. plugging of thin pipes.

To separate the surface layer from the liquid metal, the mercury droplet was brought into contact with oxidic materials having a rather rough surface. For the first experiments, the Hg droplet was moved in boats made of chinaware and sintered corundum. For the final experiment, the sample was poured over molecular sieve. Fig. 1 shows the γ-spectra of the sample before and after pouring over the molecular sieve. The Lu and Hf nuclides are almost quantitatively removed from the mercury, whereas the gold remains in solution. The Hg sample also showed bright metallic lustre after the cleaning procedure.

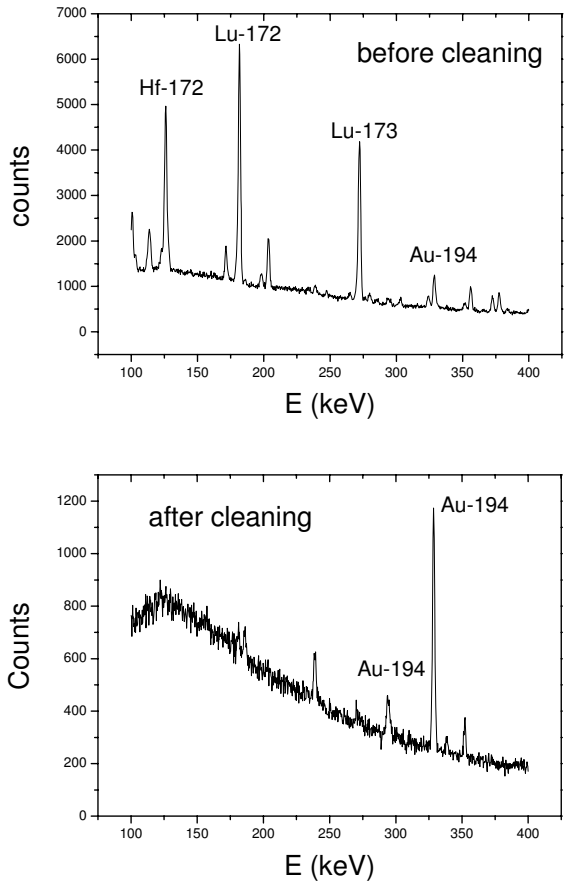

Fig. 1: γ-spectra of the Hg sample before and after pouring over molecular sieve.

REFERENCES

[1] http://www.eurisol.org

[2] H. L. Ravn et al., Feasibility Study For A European Isotope-Separator On-Line Radioactive Ion Beam Facility, European Commission Contract No. HPRI-CT-1999-500001, Appendix C.

SEPARATION OF GOLD FROM PROTON IRRADIATED MERCURY

J. Neuhausen, S. Horn, D. Schumann (PSI), T. Stora (CERN)

For the mercury spallation target designed within EURISOL-DS a separation of radionuclides from mercury is planned. The chemical procedures used to achieve this purification still have to be developed. We investigated the removal of dissolved gold from a proton irradiated mercury sample using metal absorbers.

INTRODUCTION

General aspects of the mercury purification planned for the 4 MW liquid metal spallation target of EURISOL [1] were discussed in the preceding report, together with the separation of solid oxidic material. For removal of dissolved radionuclides from mercury, one needs a material that shows a higher chemical affinity to the dissolved radionuclide than mercury. Furthermore the chemical affinity of the absorber material for mercury and its solubility in mercury should be low. In principle, for the removal of dissolved metallic species metal surfaces should be suitable candidates. The strength of intermetallic interactions can be deduced from thermodynamic data. In this way, suitable materials can be selected. We investigated different metals as candidates for an absorber that removes dissolved gold from mercury.

EXPERIMENTAL AND RESULTS

For our experiments, the Hg sample remaining from the Lu /Hf-separation experiments was used. It contains ^{194}Au as the major radioactive component detectable by γ-spectroscopy. From an evaluation of intermetallic interactions based on semi-empirical calculations, metals of Group 4 and 5 of the periodic table should have a higher affinity to gold than mercury. Furthermore, these metals are hardly soluble in mercury. Therefore, they should be suitable candidates for absorbers. In the first experiments, Ta and Zr foils were brought into contact with mercury, but no wetting of the metal surface could be achieved. Several methods of surface treatment have been examined to facilitate wetting of the metal surfaces, e.g. mechanical scratching, etching and treatment with complexing agents. Since none of them was successful, other candidates for metal absorbers had to be found. Copper seemed attractive since it is well known to form compounds with gold, and its solubility in mercury is fairly low. Furthermore, copper can be amalgamated fairly easily. Therefore, wetting of copper with mercury should be possible. In practice, wetting of copper is slow and incomplete when dipping a mechanically cleaned copper plate into mercury. The wetting can be enhanced by amalgamation of the copper plate. For this purpose, the copper plate is dipped in a saturated aqueous $HgCl_2$-solution for several hours. After this procedure, a Cu-amalgam layer has formed at the surface of the plate. After removal of precipitated CuCl the surface shows a silvery metallic lustre.

The amalgamated Cu-plate was placed in the gold-containing mercury sample for three days under ambient conditions. γ-spectra of the mercury sample were taken before and after the experiment. The Cu-plate was measured on the γ-detector after the experiment.

The results of γ-spectrometry are shown in Fig. 1. After the treatment Au is almost quantitatively removed from Hg and

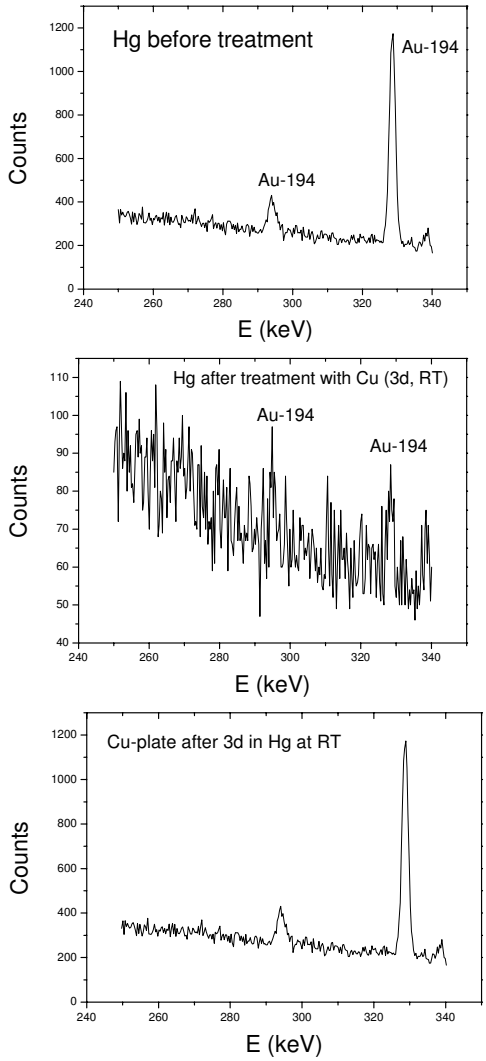

Fig. 1: γ-spectra of the Hg sample before and the Hg sample and Cu-plate after the adsorption experiment.

attached to the Cu-Plate. The Kinetics of the process is now under study. First results indicate that the process is quite fast, i.e. about 50 % of the gold adsorbed within 15 min.

The results obtained suggest that metal absorbers could indeed be used to remove dissolved nuclear reaction products from a spallation target system. However, in such a system concentrations of dissolved components will be much higher. Therefore, the capacity of such a metal absorber has to be determined. Other candidates that could be removed from Hg using a Cu-absorber would be e.g. Zn and Sn. These metals are soluble in Hg, and are known to form stable phases with Cu.

REFERENCE

[1] http://www.eurisol.org

AQUEOUS CHEMISTRY OF POLONIUM
PART IV: HALF-LIVES OF ^{206}Po AND ^{210}Po

R. Dressler, D. Schumann (PSI), U. Köster (CERN)

The α-half-lives of ^{206}Po and ^{210}Po were measured to be 8.838 d ± 0.024 d and 142 d ± 1 d respectively.

1 INTRODUCTION

In a previous report the determination of the EC/β^+-branching ratio of ^{210}Fr was determined [1]. The main uncertainty of this result grew up from the inaccuracies of the half-life of ^{206}Po and the EC/β^+-branching ratio of ^{210}Rn (see e.g. [2]). The ^{206}Po sample described in [1] was used for a long term measurement to increase the accuracy of the half-life determination of this isotope.

2 EXPERIMENTAL DETAILS

The sample was placed 20 mm in front of a 450 mm^2 surface barrier detector and measured using a standard α-spectroscopic counting system during about 400 d. In a first part (100 d) 20 measurements were performed in series. The last three measurements were nearly equally distributed over the remaining 300 d. Each measurement used an accumulation period of 5 d.

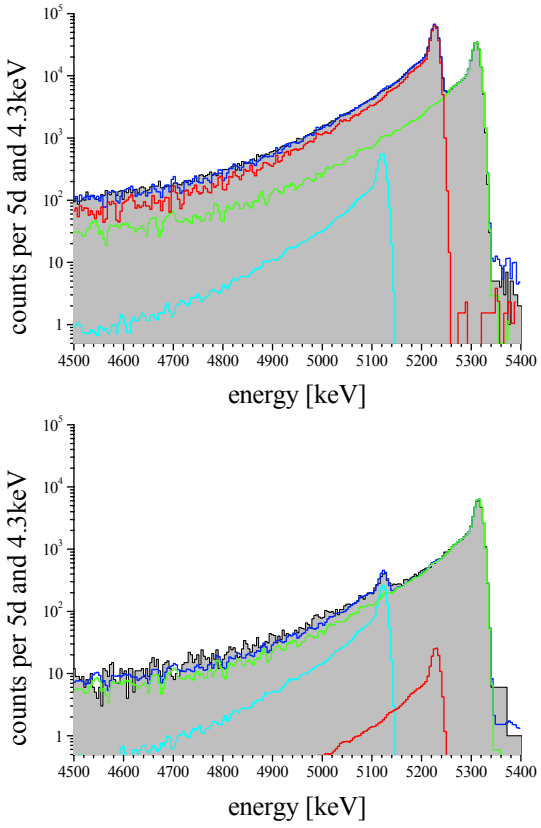

Fig. 1: Deconvolution of the first (top) and last (bottom) measurement, experimental data (gray shaded), ^{210}Po fit (green), ^{206}Po fit (red), ^{208}Po fit (cyan), sum of all fits with background (blue).

The determination of the peak area could not be performed using a standard procedure due to imperfection of the source preparation (pronounced low energy tailing) and electronically drifts of the spectroscopic system. Therefore, a histogram fitting method using an experimental determined peak form and a rebinning procedure to compensate small peak drifts was developed. The experimental peak form was deduced from the last measurements. As weight function of the nonlinear square fit (NLSF) the 95% error of the Poisson counting statistics was taken into account.

With this method all spectra could be reconstructed over a range of 900 keV using three independent peaks (^{210}Po, ^{206}Po, and ^{208}Po) and a constant background component. The spectra of the first and last measurement are given in Fig. 1, respectively, together with the peak deconvolutions. ^{210}Po is present in all spectra, whereas ^{206}Po only in the first measurements occurs. Surprisingly, from the 8th measurement ^{208}Po is clearly visible, i.e. obviously during the implantation of ^{210}Fr about 5% of ^{208}Fr or/and ^{210}Fr are transferred through the ISOLDE (CERN) separator.

3 RESULTS

Fig. 3 shows the obtained decay curves of ^{206}Po and ^{210}Po together with the results of NLSF of both time series. From these fits the half-lives of ^{206}Po and ^{210}Po were determined to be 8.838 d ± 0.024 d and 142.0 d± 1.1 d respectively. The established values given in [2] are 8.8 d ± 0.1 d and 138.376 d ± 0.002 d. The high uncertainty of the value of ^{210}Po rises due to the short measurement period of less than tree half-lives.

The uncertainty of the published ratio of α to EC/β^+-branch of ^{210}Fr taken from [1] was recalculated to be 2.00 ± (0.74+0.03+0.04), where the first uncertainty arise from the error in the ^{210}Rn EC/β^+-branch, the second from the error of the ^{206}Po half-life, and the last number collected all other uncertainties and statistical errors. The EC/β^+-branch of ^{210}Fr is now deduced to be 33% ± 13%.

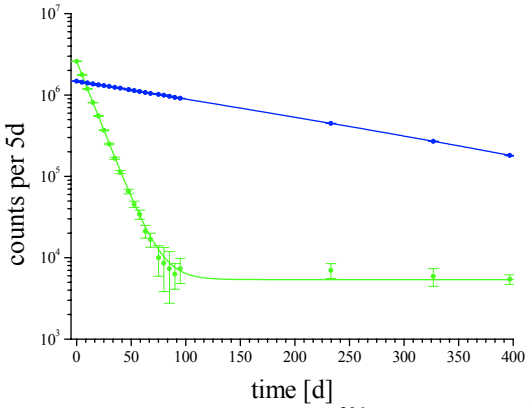

Fig. 2: Decay curves and NLSF of ^{206}Po (green) and ^{210}Po (blue).

REFERENCES

[1] R. Dressler, et al., Ann. Rep. Labor Radio- & Umweltchemie, Univ. Bern & PSI (2005).

[2] S.Y.F. Chu, L.P. Ekström and R.B. Firestone: *WWW Table of Radioactive Isotopes*, database version 28.2.1999 (URL http://ie.lbl.gov/toi/index.htm).

FEASIBILITY TEST OF UTILIZING ORGANIC ZEOLITE AS ADSORBENT FOR COLLECTING TRACE IODINE FROM NATURAL WATER

K. Li, U. Krähenbühl (University of Bern)

A method which utilizes organic zeolite Tris(o-phenylenedioxy)cyclotriphsphazene as adsorbent for collecting trace iodine from water is tested regarding the compatibility of the zeolite with different acids, adsorbing efficiency at different concentration levels of iodine, ratio of oxidant/iodide, pH value, time dependency of dynamic adsorbing efficiency and the stability of I_2 adsorbed by the zeolite under different situation of elution.

1 INTRODUCTION

Considering the long half-life of 10^7 years, the big challenge for measuring ^{129}I in environmental samples comes from the low concentration, which makes it difficult to be determined either by mass spectrometry or by a radioactivity decay measurement. To solve the problem, a method which utilizes organic zeolite as adsorbent is tested for collecting trace level of iodine from water. The organic zeolite is Tris(*o*-phenylenedioxy)cyclotriphosphazene (TPP). According to Hertzsch [1], TPP with hexagonal configuration has high selectivity and efficiency for uptaking I_2 from water or gas. Previous tests with batch experiments also show that the adsorption is fast and efficient for ~20ppm I_2 in the water.

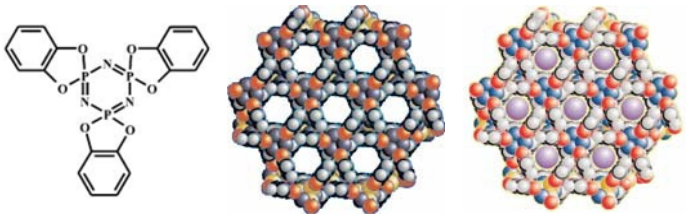

Molecular structure | Hexagonal channel topology | Hexagonal channel with I_2 molecules inside

Fig. 1: TPP zeolite and inclusion crystal of $TPP(I_2)_x$ (adapted from [1]).

The concentration of the total iodine in the fresh water is in the ppb range, with ^{129}I content of 10^{-11}-10^{-7} ppb. A pre-concentration to 10^{-2} ppb level of ^{129}I is preferred for a quadruple ICP-MS (ICP-QMS) measurement. Thus, at least 100L of water need to be processed to get the desired concentration of ^{129}I for a measurement with a detection limit of 1ppt. Considering the large amount of the sample which needs to be handled, dynamic procedure is preferred.

Batch experiments were firstly conducted to test the compatibility of the zeolite and acids, the adsorbing efficiency of the zeolite at ppb level of iodine. The zeolite column was then tested regarding the time dependency of the dynamic adsorbing efficiency and stability of I_2 adsorbed.

2 EXPERIMENTS AND RESULTS

The batch adsorbing efficiency of zeolite was tested regarding different concentrations of I_2, ratio of oxidant/iodide, and pH values. The concentration of I_2 was controlled by the amount of KI; KIO_3 was added as oxidant to form I_2; HNO3 was used to adjust the pH. The adsorbing efficiency was calculated from the difference of the concentrations of I (measured by ICP-QMS for ^{127}I) before and after the solutions were contacted with the zeolite. The results show that the adsorbing efficiency increases with increased concentration of iodate or iodide. On the other hand, the increase of pH causes peak efficiency at ~pH0.5 which implies that interference at 127AMU formed (possibly because of the decomposition of the zeolite) in HNO_3 solution with pH below 0.5.

The stability of the zeolite in the acidic solution was tested by leaving the zeolite in contact with different acids. The signal intensity of ^{127}I from the solutions with pH0 and pH2 acidified by HNO_3, H_2SO_4 or HCl respectively were monitored by ICP-QMS after different durations; 3 single zeolite crystals contact with 6M HNO_3 , 6M HCl and 6M HIO_3 respectively were visually checked during some time. It turns out that the TPP zeolite is sensitive to the oxidative effect of HNO_3 at pH < 1. Both high concentrated (6M) HNO_3 and HCl can totally dissolve the zeolite crystal given enough time. Whereas, HIO_3 can enhance the stability of the zeolite crystal because I_2 formed from the reaction between IO_3^- and remaining THF molecules in the zeolite crystal, filled into the cage of the hexagonal configuration.

For testing the time dependency of the dynamic adsorbing efficiency of the zeolite, columns (Ø=7mm) were set up using zeolite with particle size of 0.1mm-0.2mm. The sample solution was prepared in 50ml containing 0.06M HIO_3 and some NaI (spiked with ^{125}I) for controlling concentration of I_2 (~5ppb). The pH was adjusted to 1 by HCl. The mixture of HIO_3, HCl and NaI stood for 24h to ensure extensive formation of I_2. Sample was passed through the columns at different flow rates. The dynamic adsorbing efficiency was calculated from the difference of the ^{125}I activity (measured by γ spectrometer) before and after passing through the zeolite column. The adsorbing efficiency increases with increased contact duration. Efficiency of 70% can be obtained with contact duration of 40s. Considering 100L of sample needed to be processed within 10h, a flow rate of ~200ml/min is required, which means a zeolite column with diameter of 25mm should be at least 23cm in height despite the capacity of the zeolite.

The stability of I_2 adsorbed by zeolite is tested with the same procedures for sample and column preparation. After loading the column with I_2, it was washed with MQ H_2O followed by 0.1M NaI solution to check if formation of I_3^- could happen and release I_2 from the zeolite column. As results, 3 times higher radioactivity was found in the NaI washing comparing to the previous washing with MQ H_2O. This suggests a strong competition between I_2 diffusion into zeolite and formation of I_3^- in the solution.

REFERENCE

[1] T. Hertzsch et al., 2002, Angew.Chem., 41, 2282-2284 (2002).

METHOD DEVELOPMENT: ELIMINATION OF INTERFERENCES IODINE-ISOTOPES WITH THE NEW CRI-TECHNIQUE BY ICP-MS MEASUREMENTS

M. Zala, K. Li (Univ. Bern) Ch. Stenger (PSI & Univ. Bern), U. Krähenbühl (Univ. Bern)

For the interferencefree measurement of $1^{29}I$ by a quadrupole ICP-MS it is necessary to eliminate effectively ^{129}Xe ions from the plasma gas. The work for this method evaluation is based on the new CRI-technique for the ICP-MS technique.

1 HOW DOES CRI WORK

The ICP-MS Varian 820 is equipped with the new collision reaction interface (CRI) system. This system reduces spectroscopic interferences. The CRI system injects the collision gas directly into the plasma as it passes through the orifice of the cones. The reaction-interface allows an electrontransfer between the CRI gas and the disturbing interference. As the ion optics reflect only the ions into the mass analyzer system, the neutralized interferences do not reach the detector. This provides an interference free measurement.

The collision aspect of the CRI eliminates molecular interference breaking up molecular ions by collision with the CRI gas. This aspect was tested successfully by showing the removal of molecular interferences on Pd isotopes such as SrO or ZrO.

Figure 1 shows the skimmer cone, where the CRI gas is injected into the plasma. The red arrow shows the way of the aerosol.

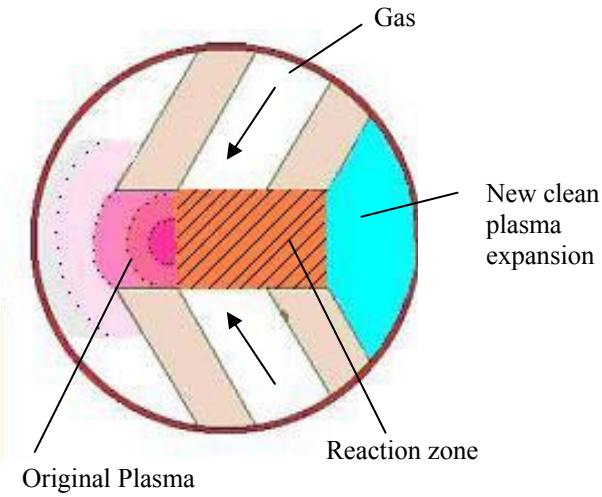

Fig. 1: Interface: Skimmer Cone [1]

2 ELIMINATION OF Xe IONS

For the elimination of ^{129}Xe several CRI gases were tested like hydrogen, helium, oxygen, methane and ethane. All gases except for ethane reduce iodine ions in the same degree as Xe ions. The preference of charge transfer among ions is dependant on the difference between the ionization energy of the gas and the element. The first ionization energy of iodine is 10.451 eV, of Xe 12.13 eV and of ethane 12.61 eV. The ionization energies of other gases were closer to the one of argon (15.759 eV), so that argon ions are preferentially in comparison to xenon. With ethane good results could be obtained. There was an efficient removal of Xe-Signal and only little reduction of the iodine-signal.

3 FURTHER EXPERIMENTS

For a further improvement of the sensitivity for iodine, experiments were made with an ultra sonic nebulizer (USN), desolvator and the combination thereof. Additives influencing the aerosol formation were tested as well. Tritone reduces surface tension, so different concentrations of tritone-solutions were tested. In addition the influence a the amine trimethylammoniumhydroxid (TMAH) was tested. These matrices were also tested in the combination with the different apparatus. Best results were obtained with a 0.05 % Tritone solution, coupled with the USN and by applying ethane as reaction gas. Results obtained by the desolvator are not useful, because the desolvator is eliminating also a fraction of the analyte in the aerosol.

Table 1 shows the data obtained by using different CRI-gases, different techniques and the different additives.

Matrix	Method	CRI-gas Skimmer	[ml/min]	^{127}I [cps]	^{129}Xe [cps]	Ratio $^{127}I/^{129}Xe$
HNO_3	Meinhard	He	0	229'274	122'670	1.87
			80	11'906	3'389	3.51
HNO_3	Meinhard	H_2	0	243'854	125'168	1.95
			70	13'058	6'497	2.01
HNO_3	Meinhard	Ethane	0	229'274	122'670	1.87
			150	10'192	37	275.46
Triton	Meinhard	Ethane	0	269'151	189'329	1.42
			140	10'396	107	97.16
Triton	Desolvator	no		183'051	20'740	8.83
Triton	USN-Desolvator	no		100'771	8'098	12.44
Triton	USN	Ethane	0	1'943'461	91'053	21.34
			140	400'071	919	435.33

Tab. 1: Results of measurements.

Further investigations are planned on the detection limit.

REFERENCE

[1] VARIAN ICP-MS Expert Help, version v2.0 b87.

LIST OF PUBLICATIONS

HEAVY ELEMENTS

J. Dvorak, W. Brüchle, M. Chelnokov, R. Dressler, Ch. E. Düllmann, K. Eberhardt, V. Gorshkov, E. Jäger, R. Krücken, A. Kuznetsov, Y. Nagame, F. Nebel, Z. Novackova, Z. Qin, M. Schädel, B. Schausten, E. Schimpf, A. Semchenkov, P. Thörle, A. Türler, M. Wegrzecki, B. Wierczinski, A. Yakushev, A. Yeremin
Doubly magic nucleus ^{270}Hs
Phys. Rev. Lett. 97, 242501 (2006).

R. Eichler, W. Brüchle, R. Buda, S. Bürger, R. Dressler, Ch. E. Düllmann, J. Dvorak, K. Eberhardt, B. Eichler, C. M. Folden III, H. W. Gäggeler, K. E. Gregorich, F. Haenssler, D. C. Hoffman, H. Hummrich, E. Jäger, J. V. Kratz, B. Kuczewski, D. Liebe, D. Nayak, H. Nitsche, D. Piguet, Z. Qin, U. Rieth, M. Schädel, B. Schausten, E. Schimpf, A. Semchenkov, S. Soverna, R. Sudowe, N. Trautmann, P. Thörle, A. Türler, B. Wierczinski, N. Wiehl, P.A. Wilk, G. Wirth, A. B. Yakushev, A. von Zweidorf
Attempts to chemically investigate element 112
Radiochim. Acta 94, 181-191 (2006).

R. Eichler, N.V. Aksenov, A.V. Belozerov, G.A. Bozhikov, V.I. Chepigin,R. Dressler, S.N. Dmitriev, H.W. Gäggeler, V.A. Gorshkov, F. Haenssler, M.G. Itkis, V.Ya. Lebedev, A. Laube, O.N. Malyshev, Yu.Ts. Oganessian, O.V. Petruschkin, D. Piguet, P. Rasmussen, S.V. Shishkin, A.V. Shutov, A.I. Svirikhin, E.E. Tereshatov, G.K. Vostokin, M. Wegrzecki, A.V. Yeremin.
Confirmation of the decay of $^{283}112$ and first indication for Hg-like behavior of element 112,
Nuclear Physics A (2006), doi: 10.1016/j.nuclphysa.2006.12.058.

SURFACE CHEMISTRY

T. Bartels-Rausch, D. J. Donaldson
HONO and NO_2 evolution from irradiated nitrate-doped ice and frozen nitrate solutions
Atmos. Chem. Phys. Discuss. 6, 10713-10731 (2006).

H. Franberg, M. Ammann, H.W. Gäggeler, U. Koester
Chemical investigations of isotope separation in on line target units for carbon and nitrogen beams
Rev. Sci. Instr. 77, Art. No. 03A708 Part 2 (2006).

T. Huthwelker, M. Ammann, T. Peter
The uptake of acidic gases on ice
Chemical Reviews 106, 1375-1444 (2006).

K. Stemmler, M. Ammann, C. Donders, J. Kleffmann, C. George
Photosensitized reduction of nitrogen dioxide on humic acid as a source of nitrous acid
Nature 440, 195-198 (2006).

A. Vlasenko, S. Sjogren, E. Weingartner, K. Stemmler, H.W.Gäggeler, M. Ammann
Effect of humidity on nitric acid uptake on mineral dust aerosol particles
Atmos. Chem. Phys. 6, 2147–2160 (2006).

ANALYTICAL CHEMISTRY

D. Bolius, M. Schwikowski, T. Jenk, H.W. Gäggeler, G. Casassa
A first shallow firn core record from Glaciar La Ollada on Cerro Mercedario in the Central Argentinian Andes
Annals of Glaciology 43, 14-22 (2006).

R. Fisseha, M. Saurer, M. Jäggi, S. Szidat, R.T.W. Siegwolf, U. Baltensperger
Determination of stable carbon isotopes of organic acids and carbonaceous aerosols in the atmosphere
Rapid Commun. Mass Spectrom. 20, 2343–2347, doi:10.1002/rcm.2586 (2006).

P. Ginot, Ch. Kull, U. Schotterer, M. Schwikowski, H. Gäggeler
Glacier mass balance reconstruction by sublimation induced enrichment of chemical species on Cerro Tapado (Chilean Andes)
Clim. Past 2, 21–30 (2006).

K.A. Henderson, A. Laube, M. Saurer, H.W. Gäggeler, S. Olivier, T. Papina, M. Schwikowski
Temporal variations of accumulation and temperature during the past two centuries from Belukha ice core, Siberian Altai
J. Geophys. Res. Atmospheres 111, D03104, doi:10.1029/2005JD005819 (2006).

T.M. Jenk, S. Szidat, M. Schwikowski, H.W. Gäggeler, S. Brütsch, L. Wacker, H.-A. Synal, M. Saurer
Radiocarbon analysis in an Alpine ice core: Record of anthropogenic and biogenic contributions to carbonaceous aerosols in the past (1650-1940)
Atmos. Chem. Phys. 6, 5381-5390 (2006).

S. Olivier, C. Blaser, S. Brütsch, N. Frolova, H.W. Gäggeler, K.A. Henderson, A.S. Palmer, T. Papina, M. Schwikowski
Temporal variations of mineral dust, biogenic tracers and anthropogenic species during the past two centuries from Belukha ice core, Siberian Altai
J. Geophys. Res. Atmospheres 111, D05309, doi:10.1029/2005JD005830 (2006).

M. Reth, A. Ciric, G.N. Christensen, E.S. Heimstad, M. Oehme
Short- and medium chain chlorinated paraffins in biota from the European Arctic – differences in homologue group patterns
Sci. Total Environ. 367, 252-260 (2006).

H. Reithmeier, V.Lazarev, W.Rühm, M.Schwikowski, H.W.Gäggeler, E.Nolte
Estimate of European ^{129}I releases supported by ^{129}I analysis in an Alpine ice core
Environ. Sci. Technol. 40, 5891-5896 (2006).

A. Schwerzmann, M. Funk, H. Blatter, M.P. Lüthi, M. Schwikowski, A.S. Palmer
Reconstruction of past accumulation rates in an alpine firn region: Fiescherhorn, Swiss Alps
J. Geophys. Res. Earth Surface 111, F01014, doi:10.1029/2005JF000283 (2006).

M. Schwikowski
Paleoenvironmental reconstruction from Alpine ice cores
PAGES News Vol. 14, N°1, 16-18 (2006).

M. Schwikowski, S. Brütsch, G. Casassa, A. Rivera
A potential high-elevation ice core site at the Southern Patagonian Icefield
Annals of Glaciology 43, 8-13 (2006).

M. Sigl, H. Strunk, H.-J. Barth
Dendroclimatic investigations in Asir Mountains – Saudi Arabia. Preliminary report
In: Heinrich, J., Gärtner, H., Montbaron, M. & Schleser G. (eds.): TRACE Tree rings in Archaeology, Climatology and Ecology. Vol. 4 – Schriften des Forschungszentrum Jülich, Reihe Umwelt/Environment 61, 92-98 (2006).

H. Sodemann, A.S. Palmer, C. Schwierz, M. Schwikowski, H. Wernli
The transport history of two Saharan dust events archived in an Alpine ice core
Atmos. Chem. Phys. 6, 667-688 (2006).

S. Szidat, T.M. Jenk, H.-A. Synal, M. Kalberer, L. Wacker, I. Hajdas, A. Kasper-Giebl, U. Baltensperger
Contributions of fossil fuel, biomass burning, and biogenic emissions to carbonaceous aerosols in Zürich as traced by ^{14}C
J. Geophys. Res. 111, D07206, doi:10.1029/2005JD006590 (2006).

RADWASTE ANALYTICS

J. Neuhausen, B. Eichler
Investigations on the thermal release of iodine from liquid eutectic lead-bismuth alloy
Radiochim. Acta 94, 239 (2006).

J. Neuhausen
Investigations on the release of mercury from liquid eutectic lead bismuth alloy under different gas atmospheres
Nucl. Instr. and Meth. A, 562, 702 (2006).

D. Schumann, R. Michel, G. Korschinek, K. Knie, J.-Ch. David
Excitation functions for the production of ^{60}Fe and ^{53}Mn in the reaction natPb(p,xn/yp)Z
Nucl. Instr. and Meth. A 562, 1057 (2006).

GEOCHEMISTRY UNIVERSITÄT BERN

A. Al-Kathiri, B.A. Hofmann, E. Gnos, O.Eugster, K.C. Welten, U. Krähenbühl
Shisr 043 (IIIAB medium octahedrite): the first iron meteorite from the Oman desert
Meteoritics & Planetary Science, 41 Nr 8 Supplement A217-230 (2006).

M. Ayranov, U. Krähenbühl, U. Schneider
Fast determination of uranium and radium in water of variable composition
Czechoslovak Journal of Physics, 56 Sup. D219-D227 (2006).

T. Barrelet, A. Ulrich, H. Rennenberg, U. Krähenbühl
Seasonal profiles of sulphur, Pphosphorus and potassium in Norway Spruce wood
Plant Biol. 462 469 (2006).

M. Döbeli, A.A.M. Gaschen, U. Krähenbühl
Fluorine analysis by ion beam techniques for dating applications
In Fluorine and the environment vol 2 ed. A. Tressaud
Elsevier ISSN 1872-0358 pages 215-252 (2006).

W. Finsinger, C. Bigler, U. Krähenbühl, A. Lotter, B. Ammann
Human Impact and eutrophication patterns during the past ˜200 years at Lago Grande di Avigliana (N. Italy)
J Paleolimnol 36 55-67 (2006).

A. A.-M. Gaschen, U. Krähenbühl, M. Döbeli, A. Markwitz, B. Barry
Artificial fluorine enrichment in bones: Diagenesis as restricting factor for exposure age dating by fluoreine diffusion
Proceedings 34th Symposium on Archaeometry, Zaragoza 2006
ISBN 84-7820-848-8 pages 61-64.

U. Krähenbühl, C. Fragnière, M. Haldimann
An environmental case history of platinum
Chimia 60 337 (2006).

W. Tinner, F. Sheng Hu, R. Beer, P. Kaltenrieder, B. Scheurer, U. Krähenbühl
Postglacial vegetational and fire history: pollen, plant macrofissil and charcoal records from two Alaskan lakes
Veget. Hist. Archeobot. 15 279-293 (2006).

REPORTS

P. Agostini, H. Glasbrenner, J.L. Courouau, A. Gessi, P. Turroni, A. Zucchini, J. Neuhausen, A. Ciampichetti, H. Jacobs, W. Leung, K. Woloshun, T. Cadiou, D. Pellini
Synthesis report on LBE technology for MEGAPIE
ENEA Report MP-A-R-001, Rev: 0, ENEA, Brasimone, Italy (2006).

F. Groeschel, J. Neuhausen, A. Fuchs, A. Janett
Beurteilung des all-einschliessenden Referenzstörfalls
Abschätzung der freigesetzten Aktivität zur Berechnung der maximalen Personendosis
MEGAPIE Report MPR-3-GF34-01/0, Paul Scherrer Institut, Villigen (2006).

CONTRIBUTIONS TO CONFERENCES, WORKSHOPS AND SEMINARS

HEAVY ELEMENTS

R. Eichler
Confirmation of the decay of ^{283}112 and evidence for Hg-like behavior of element 112
Nucleus-Nucleus Collisions, Rio de Janeiro, Brazil, 31 August 2006.

R. Eichler
Recent chemistry experiments with element 112 @ Dubna
Gas phase chemistry experiments @ TASCA
5-th Workshop on physical recoil separators dedicated for chemical experiments Garching, Germany, 20 September 2006.

R. Eichler
Bestätigung für die Bildung von ^{283}112 und dessen Zerfallseigenschaften.
Erste chemische Eigenschaften von Element 112.
Seminar für Kern- und Radiochemie, Universität Mainz, Germany, 30 October 2006.

H. W. Gäggeler
Gas chemical studies of 6d-elements
Seminar Labor für Radio- und Umweltchemie, Bern University, Switzerland, 13 January 2006.

H. W. Gäggeler
Gas chemical studies of transactinides
RadChem 2006, Marianske Lazne, Czec Republic, 23–28 April 2006.

H. W. Gäggeler
Chemistry of new elements
1st European Chemistry Conference, Budapest, Hungary, 27–31 August 2006.

H. W. Gäggeler
Confirmation of the decay of ^{283}112 and evidence for a behaviour of element 112 as a volatile metal
375. WE-Heraeus Seminar: Workshop on the Atomic Properties of the Heaviest Elements
Abtei Frauenwörth im Chiemsee, Germany, 24–27 September 2006.

SURFACE CHEMISTRY

M. Ammann
Oxidative processing and phase transfer properties of fatty acids on aerosol particles
Seminar at University of California, Irvine, USA, 4 February 2006.

M. Ammann
Photosensitized reduction of nitrogen dioxide to nitrous acid on humic acids
Seminar at University of California, Los Angeles, USA, 9 February 2006.

M. Ammann
Probing chemical composition at air – water
and air - ice interfaces by ambient pressure X-ray photoelectron spectroscopy
Seminar at Laboratory of Radio- and Environmental, University of Berne, Switzerland, 1 December 2005.

M. Ammann
Mechanisms and kinetics of aerosol chemical processing
Seminar at ETH Zürich, Switzerland, 22 June 2006.

M. Ammann, M. Kerbrat, T. Huthwelker, T. Bartels-Rausch, M. Birrer, T. Kaempfer, B. Pinzer, M. Schneebeli, D. J. Starr, H. Bluhm
(Co-) Adsorption of HONO et al. on ice
SCOUT-O3 Ice Meeting, Mainz, Germany, 7-8 December 2006.

M. Ammann, K. Stemmler, J. Kleffmann, C. George
Photoenhanced conversion of NO_2 on solid organic compounds: An important source of HONO.
Workshop "The routes for organics oxidation in the atmosphere and its implications to the atmosphere" Alpe d'Huez, France, 7-11 January 2006.

M. Ammann, J. Kleffmann, C. George, C. Donders, K. Stemmler
Photosensitized reduction of NO_2 on organic mimics of soil and atmospheric aerosol surfaces
AirUCI Workshop, Laguna Beach, USA, 26-27 January 2006.

H. Frånberg, R. AlvèsCondé, M. Ammann, J.C. Angélique, V. Dubois, F. Durantel, C. Eleon, G. Gaubert, H. W. Gäggeler, C. Huet-Equilbec, B. Jacquot, P. Jardin, U. Köster, R. Leroy, N. Orr, J.-Y. Pacquet, M.-G. Saint-Laurent, C. Stodel, J.-C. Thomas, A. C. C. Villari and the ISOLDE collaboration.
Developments for intensive short-lived carbon and nitrogen beams.
Colloque de GANIL in Giens, France 28 May-2 June 2006.

T. Huthwelker, M. Kerbrat, M. Ammann
Uptake processes of nitrous acid on ice studied with radioactively marked tracers
11th International Conference on the Physics and Chemistry of Ice PCI 2006 Bremerhaven, Germany, 23-28 July 2006.

T. Huthwelker, M. Kerbrat, M. Ammann
Investigation of the microphysics and kinetics of trace gas uptake into ice using radioactive tracers
SCOUT-O3 Meeting, Jülich, Germany, 20-23 March 2006.

T. Huthwelker, M. Kerbrat, T. Kaempfer, B. Pinzer, M. Schneebeli, M. M. Miedaner, and M. Ammann
Investigation of the microphysics and uptake kinetics of trace gas uptake into artificial snow using radioactive tracer and micro tomography
Frühjahrstagung der DPG, Heidelberg, Germany, 13-16 March 2006.

M.J. Krisch, M.A. Brown, J.C. Hemminger, R. D'Auria, K. M. Callahan, D.J. Tobias, M. Ammann, H. Bluhm, D.E. Starr
Impact of an alcohol on the depth profile of ion concentrations at the aqueous liquid-vapor interface
American Chemical Society Meeting, San Francisco, USA, 8 October 2006.

M.M. Miedaner, T. Huthwelker, F. Enzmann, M. Stampanoni, M. Kersten, M. Ammann
Characterization and distribution of soluble and insoluble impurities in ice depending on the mode of freezing by synchrotron computer tomography
Frühjahrstagung der DPG, Heidelberg, Germany, 13-16 March 2006.

M.M. Miedaner, T. Huthwelker, F. Enzmann, M. Kersten, M. Ammann, A. Groso, and M. Stampanoni
Trapping and mobility of soluble and insoluble impurities in ice monitored via cryo-synchrotron-tomography
European Crystallographic Meeting, Leuven, Belgium, 6-12 August 2006.

M.M. Miedaner, T. Huthwelker, F. Enzmann, M. Kersten, M. Ammann, A. Groso, and M. Stampanoni
Tomographic characterization of soluble and insoluble impurities and their transport in ice
11th International Conference on the Physics and Chemistry of Ice PCI 2006, Bremerhaven, Germany, 23-28 July 2006.

M.M. Miedaner, T. Huthwelker, F. Enzmann, M. Stampanoni, M. Kersten, M. Ammann
Tomographic characterization of soluble and insoluble impurities and their transport in ice
7th SLS Users' Meeting, Villigen, PSI, Switzerland, 28-29 September 2006.

M.M. Miedaner, T. Huthwelker, F. Enzmann, M. Stampanoni, M. Kersten, M. Ammann
Trapping and mobility of soluble and insoluble impurities in ice monitored via cryo-synchrotron-tomography
8th Biennial Conference on High Resolution X-Ray Diffraction and Imaging Karlsruhe/Baden-Baden, Germany, 19-22 September 2006.

M. Ndour, M. George, K. Stemmler, M. Ammann, J. Kleffmann, Y. Balkansky
Photoenhanced conversion of NO_2 on mineral dust
International Global Atmospheric Chemistry (IGAC) conference, Cape Town, South Africa, 17-23 September 2006.

D.E. Starr, M. Ammann, H. Bluhm
The adsorption and uptake of acetone on ice studied with ambient pressure photoemission spectroscopy
American Chemical Society Meeting, San Francisco, USA, 8 October 2006.

K. Stemmler, M. Ammann, J. Kleffmann, Y. Elshorbany, M. Ndour, B. D'Anna, C. George, C. Donders, K. Stemmler
Photosensitized chemistry of humic acids with nitrogen dioxide
Workshop on Humic Like Materials (HULIS) in the Atmosphere, Budapest, Hungary, 22-24 November 2006.

K. Stemmler, J. Kleffmann, M. Ammann, A, Vlasenko, C. George, M. Ndour
Reaction of HNO_3 and NO_2 with organic aerosol in flow tube experiments
International Global Atmospheric Chemistry (IGAC) conference, Cape Town, South Africa, 17-23 September 2006.

K. Stemmler, J. Kleffmann, M. Ammann, C. Donders, C. George
Photochemical reactions of nitrogen dioxide with humic matter and soil: A new source of nitrous acid
International Global Atmospheric Chemistry (IGAC) conference, Cape Town, South Africa, 17-23 September 2006.

K. Stemmler, M. Ammann, S. Vlasenko, C. Guimbaud, M. Birrer
Laboratory studies in multi-phase reactors on the heterogeneous reactions of NO_2 and HNO_3 with aerosol
Seminar at Laboratory of Radio- and Environmental Chemistry, University of Berne, Switzerland, 5 May 2006.

O. Vesna, S. Sjogren, V. Samburova, E. Weingartner, M. Kalberer, M. Ammann
The reactions of unsaturated fatty acids aerosol with O_3: Product formation and hygroscopic properties of the processed aerosol
7th International Aerosol Conference, St. Paul, USA, 11-15 September 2006.

O. Vesna, S. Sjogren, V. Samburova, E. Weingartner, M. Kalberer, M. Ammann
The reactions of unsaturated fatty acidsaAerosol with O_3: Product formation and hygroscopic properties of the processed aerosol
Seminar at Department of Chemistry, University of Toronto, Canada, 18 September 2006.

O. Vesna
Ozonolysis of UFA aerosol: application of ^{1}H NMR and GC-MS technique to hygroscopicity studies
Seminar at Laboratory of Radio- and Environmental, University of Berne, Switzerland, 1 December 2006.

ANALYTICAL CHEMISTRY

A. Ciric, M. Schwikowski, H.W. Gäggeler
An ice core record of ENSO related climate variability from Mercedario (32°S) in the Central Argentinean Andes
Research at Jungfraujoch – "Top of Science", Interlaken, Switzerland, 11-14 September 2006.

A. Ciric, D. Bolius, M. Schwikowski, H.W. Gäggeler
An ice core record of ENSO related climate variability from Mercedario (32°S) in the Central Argentinean Andes
7th Swiss Global Change Day, Bern, Switzerland, 20 April 2006.

A. Ciric
Climate reconstructions based on an ice core from South America
First year graduate symposium, University of Bern, Switzerland, 17 October 2006.

A. Ciric
First results of the deep ice core from Mercedario, Argentina
Seminar Radio- und Umweltchemie, Paul Scherrer Institut, Switzerland, 27 October 2006.

H. W. Gäggeler
Towards a table top accelerator mass spectrometry device – status and perspectives
Radiochemistry Conference, Saha Institute, Kalkutta, India, 23–27 January 2006.

H. W. Gäggeler
Development of a mini-AMS facility – Status and perspectives in environmental research
GENCO Festkolloquium, GSI-Darmstadt, Germany, 23 February 2006.

H. W. Gäggeler
Towards a table-top accelerator mass spectrometry device – status and perspectives in environmental research
RadChem 2006, Marianske Lazne, Czec Republic, 23–28 April 2006.

H. W. Gäggeler
Towards a table-top accelerator mass spectrometry device – status and perspectives
CERN/ISOLDE, Switzerland, 16 May, 2006.

H. W. Gäggeler
Forschung mit Gletschereis,
Schweizerischer Alpenclub, Sektion Zofingen, Zofingen, Switzerland, 3 November 2006.

H. W. Gäggeler
Recent developments in mini-accelerator mass spectrometry (AMS)
Seminar über aktuelle Themen aus Kosmochemie und Astrophysik, Mainz University, Germany, 13 November 2006.

T.M. Jenk, S. Szidat, M. Schwikowski, H.W. Gäggeler, H.-A. Synal, L. Wacker
Record of historical anthropogenic and biogenic contributions to carbonaceous aerosols from an Alpine ice core
19th International ^{14}C Conference, Oxford, U.K., 3-7 April 2006.

T.M. Jenk, H.W. Gäggeler, M. Schwikowski, S. Szidat
Rekonstruktion von Klima und anthropogenen Einflüssen im Alpenraum anhand eines Eisbohrkerns vom Fiescherhorngletscher
Phil. Alp (ICAS Swiss Alpine Studies), Die Alpen aus Sicht junger Forschender, Glarus, Switzerland, 23-24 March 2006.

C. Kamenik, B. Ammann, C. Bigler, A. Blass, A.L. Carnelli, J. Esper, M. Grosjean, T.M. Jenk, I. Larocque, R. Niederer, R. Schreier, M. Schwikowski, H. Wanner
Regional multi-proxy climate reconstruction – a calibration exercise
HOLIVAR 2006 – Natural Climate Variability and Global Warming, London, UK, 12-15 June 2006.

T. Kellerhals, L.Tobler, M. Schwikowski, H.W. Gäggeler
An improved set-up for the continuous analysis of trace elements in ice cores
39. Jahrestagung der Deutschen Gesellschaft für Massenspektrometrie, Johannes Gutenberg Universität Mainz, Germany, 5-8 March 2006.

V. Lanz, S. Szidat, A.S.H. Prévôt
^{14}C analyses and positive matrix factorization of organic aerosol mass spectra
AGU Fall Meeting, San Francisco, USA, 11-15 December 2006.

A.S.H. Prévôt, J. Sandradewi, M.R. Alfarra, K. Gäggeler, J. Dommen, S. Weimer, C. Mohr, M. Furger, E. Weingartner, S. Szidat, G. Legreid, M. Hill, S. Reimann, A. Caseiro, A. Kasper-Giebl, H. Puxbaum, A. Veres, Z. Bozoki, D. Gross, U. Baltensperger
Aerosols from wood combustion versus traffic in Alpine valleys (AEROWOOD project)
EGU, General Assembly, Vienna, Austria, 2-7 April 2006.

A.S.H. Prévôt, S. Szidat, M.R. Alfarra, J. Sandradewi, M. Furger, S. Weimer, C. Hueglin, V. Lanz, N. Bukowiecki, U. Baltensperger
The high PM10 episode in Switzerland in January and February 2006
10th ETH Conference on Combustion Generated Nanoparticles, Zürich, 21-23 August 2006.

A.S.H. Prévôt, M.R. Alfarra, S. Szidat, U. Baltensperger
Distinction of fossil and non-fossil particle carbon by ^{14}C analysis and distinction of primary and oxygenated organic aerosol by aerosol mass spectrometry
Advanced Atmospheric Aerosol Symposium, Milan, Italy, 12-15 November 2006.

M. Ruff, H.W. Gäggeler, M. Suter, H.-A. Synal, S. Szidat, L. Wacker
A gas ion source for low energy AMS
Frühjahrstagung der Deutschen Physikalischen Gesellschaft, Frankfurt, Germany, 13-17 March 2006.

M. Ruff, L. Wacker, H.W. Gäggeler, M. Suter, H.-A. Synal, S. Szidat, J. Thut
Simplifying radiocarbon measurements – a hybrid ion source at low beam energies
19th International ^{14}C Conference, Oxford, U.K., 3-7 April 2006.

M. Ruff
A gas ion source for low energy AMS
First year graduate symposium, University of Bern, Switzerland, 18 October 2006.

M. Ruff
Progress with the AMS gas ion source – First measurements
Seminar Radio- und Umweltchemie, Universität Bern, Switzerland, 1 December 2006.

M. Schwikowski
Results from Fedchenko snow pit samples
2nd CADIP meeting, Nagoya, Japan, 28-29 January 2006.

M. Schwikowski
High-alpine glaciers as archives of atmospheric pollution and climate
Seminar National Institute for Polar Research, Tokyo, Japan, 31 January 2006.

M. Schwikowski
High-alpine glaciers as archives of atmospheric pollution and climate
Workshop on "Prospects and Problems on Ice Cores Drilled at High Mountains, Institute of Low Temperature Science, Sapporo, Japan, 4 February 2006.

M. Schwikowski
Atmospheric and climate history of the past two centuries from Belukha ice core, Siberian Altai
Workshop on "Prospects and Problems on Ice Cores Drilled at High Mountains, Institute of Low Temperature Science, Sapporo, Japan, 4 February 2006.

M. Schwikowski
Chemie im Schnee von gestern: Kalte Gletscher als Umweltarchive
Festkolloqium anlässlich des 60. Geburtstag von H. Gäggeler, Paul Scherrer Institut, Villigen, Switzerland, 7 April 2006.

M. Schwikowski
High-alpine glaciers as archives of atmospheric pollution and climate
Seminar Centro de Estudios Científicos, Valdivia, Chile, 17 April 2006.

M. Schwikowski
Zeitreise durchs Eis: Gletscher als Klimaarchiv
Infotage Kernkraftwerk Leibstadt, Leibstadt, Switzerland, 6-7 May 2006.

M. Schwikowski
High-alpine glaciers as archives of atmospheric pollution and climate
Geowissenschaftliches Kolloquium, Universität Heidelberg, Heidelberg, Germany, 22 May 2006.

M. Schwikowski
Atmospheric and climate history of the past two centuries from Belukha ice core, Siberian Altai
TEM Kolloquium, Paul Scherrer Institut, Villigen, Switzerland, 29 June 2006.

M. Schwikowski, B. Rufibach, M. Rodriguez, A. Rivera, T. Jenk, G. Casassa, J. Wendt
Expedición Campo de Hielo Sur 2006: La Perforación
Seminar Centro de Estudios Científicos, Valdivia, Chile, 7 September 2006.

M. Schwikowski
Palaeo and present day atmosphere
Research at Jungfraujoch – "Top of Science", Interlaken, Switzerland, 11-14 September 2006.

M. Schwikowski, H.W. Gäggeler, T. Jenk, S. Brütsch, D. Bolius, G. Casassa, A. Rivera
Firn and ice core records from high-elevation sites in the mid-latitude Andes
Intern. Symposium on Reconstructing Past Regional Climate Variations in South America over the late Holocene: A new PAGES Initiative, Malargüe, Argentina, 4-7 October 2006.

M. Schwikowski
Chemie im Eis: auf Spurensuche in hochalpinen Gletschern
Seminar Department of Chemistry and Biochemistry, University of Berne, Berne, Switzerland, 23 November 2006.

M. Schwikowski
High-alpine glaciers as archives of atmospheric pollution and climate
Kolloquium Atmosphäre und Klima, IACETH, Zurich, Switzerland, 4 December 2006.

M. Sigl, D. Bolius, M. Schwikowski, H.W. Gäggeler, T.M. Jenk
A 1000-year climate history from an Alpine ice core?
7th Swiss Global Change Day, Bern, Switzerland, 20 April, 2006.

M. Sigl, D. Bolius, T.M. Jenk, M. Schwikowski, H.W. Gäggeler
A 1000-year climate history from an Alpine ice core?
HOLIVAR 2006 – Natural Climate Variability and Global Warming, London, UK, 12-15 June 2006.

M. Sigl, D. Bolius, M. Schwikowski, H.W. Gäggeler, T.M. Jenk
A 1000-year climate history from an Alpine ice core?
Rauriser Wissenschaftstage über Klimawandel in den Alpen, Rauris, Austria, 7-9 July 2006.

M. Sigl, D. Bolius, T.M. Jenk, M. Schwikowski, H.W. Gäggeler
A 1000-year climate history from an Alpine ice core?
Research at Jungfraujoch – "Top of Science", Interlaken, Switzerland, 11-14 September 2006.

M. Sigl
A 1000-year climate history from an Alpine ice core?
Seminar Radio- und Umweltchemie, University Bern, Switzerland, 5 May 2006.

M. Sigl
Reconstruction of past climate using an Alpine ice core
First year graduate symposium, University of Bern, Switzerland, 17 October 2006.

Ch.Stenger, U. Krähenbühl
Determination of the terrestrial age on the basis of uranium diffusion in L-Chondrites
69th Met. Soc. Meeting, ETH Zürich, Switzerland, 6-11 August 2006.

Ch. Stenger
Trace element analysis with CRI-ICP-MS
First year graduate symposium, University of Bern, Switzerland, 17 October 2006.

S. Szidat
Quellenzuordnung von anthropogenen und biogenen organischen Aerosolen mittels ^{14}C
Fachtagung "Feinstaub in der Schweiz", Dübendorf, Switzerland, 20 January 2006.

S. Szidat, A.S.H. Prévôt, H.-A. Synal, M. Hallquist, U. Baltensperger
Source apportionment of carbonaceous aerosols with ^{14}C
COST 633 (Particulate Matter) Workshop, Vienna, Austria, 3-5 April 2006.

S. Szidat, T.M. Jenk, H.-A. Synal, L. Wacker, A.S.H. Prévôt, U. Baltensperger
The importance of the elemental carbon (EC) fraction for source apportionment of carbonaceous aerosols with ^{14}C
19th International ^{14}C Conference, Oxford, U.K., 3-7 April 2006.

S. Szidat, A.S.H. Prévôt, J. Sandradewi, H.-A. Synal, H.W. Gäggeler, U. Baltensperger
Biomass burning: an underestimated source of carbonaceous aerosols in Switzerland
7th Swiss Global Change Day, Bern, Switzerland, 20 April 2006.

S. Szidat, T.M. Jenk, H.-A. Synal, L. Wacker, M. Kalberer, A.S.H. Prévôt, U. Baltensperger
Radiocarbon measurements in organic carbon (OC) and elemental carbon (EC) reveal unexpectedly high contributions from residential wood burning in Switzerland
7th International Aerosol Conference (IAC), St. Paul, USA, 10-15 September 2006.

S. Szidat, T.M. Jenk, L. Wacker, H.-A. Synal, S. Reimann, J. Cozic, E. Weingartner, A.S.H., Prévôt, U. Baltensperger
Source apportionment of carbonaceous aerosols with ^{14}C: I. Results from Jungfraujoch
Research at Jungfraujoch – "Top of Science", Interlaken, Switzerland, 11-13 September 2006.

S. Szidat
On the track of fine particulate matter with ^{14}C
Seminar at Laboratory of Ion Beam Physics, PSI & ETH Hönggerberg, Zurich, Switzerland, 6 December 2006.

F. Thevenon, F. Anselmetti, S. Bernasconi, M. Schwikowski, M. Sigl
Automated image analysis of pyrogenic products from Lake Lucerne sediments and glacier Colle Gnifetti (Switzerland)
4th Swiss Geoscience Meeting, Bern, Switzerland, 24-25 November 2006.

L. Tobler, M. Schwikowski, S. Eyrikh
Historische Entwicklung der Schwermetallkonzentrationen in einem Eisbohrkern des Belukha Gletschers im Sibirischen Altai
39. Jahrestagung der Deutschen Gesellschaft für Massenspektrometrie, Johannes Gutenberg Universität Mainz, Germany, 5-8 March 2006.

M. Viana, T.A.J. Kuhlbusch, A. Miranda, M. Vallius, A. Kasper-Giebl, S. Szidat, W. Winiwarter
Overview of source apportionment methods in use in European COST633 action member countries
COST 633 (Particulate Matter) Workshop, Vienna, Austria, 3-5 April 2006.

M. Wehrli, S. Szidat, H.W. Gäggeler, M. Ruff, L. Wacker, H.-A. Synal, J. Sandradewi, A.S.H., Prévôt, U. Baltensperger
Source apportionment of carbonaceous aerosols with ^{14}C: II. Results from the Swiss Plateau
Research at Jungfraujoch – "Top of Science", Interlaken, 11-13 September 2006.

RADWASTE ANALYTICS

J. Neuhausen
Practical aspects of radioisotopes extraction from Hg
EURISOL DS Task 2-5 Meeting, Padova, Italy, 20-21 March 2006.

J. Neuhausen
Recent results on the chemistry of liquid lead-bismuth and mercury targets
Seminar Labor für Radio- und Umweltchemie, Paul Scherrer Institute, Switzerland, 23 June 2006.

J. Neuhausen
EURISOL and the possibilities for nuclide production from liquid Hg-targets
1st Exploratory Workshop Exotic Radionuclides from Accelerator Waste for Science and Technology,
Paul Scherrer Institute, Villigen, Switzerland, 15-17 November 2006.

J. Neuhausen, S. Horn, D. Schumann
Mercury purification for the Megawatt Liquid Metal Spallation Target
EURISOL-DS Town Meeting, CERN, Geneva, Switzerland, 27-30 November 2006.

D. Schumann
ERAWAST - Exotic radionuclides from Acclerator Waste for Science and Technology,
Seminar, GANIL, Caen, France, 13 January 2006.

D. Schumann
ERAWAST - Exotic Radionuclides from Acclerator Waste for Science and Technology,
ISOLDE Annual User Meeting, Geneve, Switzerland, 6-8 February 2006.

D. Schumann, R. Weinreich, F. Atchison, M. Wohlmuther, H.-F. Beer
Determination of long-lived radionuclides in accelerator waste, talk
15. Radiochemical Conference, Marianske Lazne, Czech Republic, 23–28 April 2006.

D. Schumann
Gewinnung exotischer Radionuklide aus Beschleunigerabfällen
3. RCA workshop, Dresden, Germany, 15-16 June 2006.

D. Schumann
Accelerator waste at PSI
1st Workshop on Exotic Radionuclides from Accelerator Waste for Science and Technology (ERAWAST), Villigen, Switzerland, 15-17 November 2006.

D. Schumann
Chemical separation techniques
1st Workshop on Exotic Radionuclides from Accelerator Waste for Science and Technology (ERAWAST), Villigen, Switzerland, 15-17 November 2006.

D. Schumann, R. Weinreich, F. Atchison, M. Wohlmuther, H.-F. Beer
Radioanalytics of accelerator waste
1st EuCheMS Congress, Budapest, Hungary, 27-31 August 2006.

GEOCHEMISTRY UNIVERSITÄT BERN

A. Al-Kathiri, B.A. Hofmann, E. Gnos, O. Eugster, K.C. Welten, U. Krähenbühl
Shisir 043 (IIIAB Medium Octahedrite): First iron meteorite from the Oman Desert
Desert Meteorites Workshop: Casablanca, Morocco, 3-4 August 2006.

M. Ayranov, U.G. Schneider, U. Krähenbühl
Fast determination of uranium and radium in waters
15th Radiochemical Conference, Marianske Lazne, Czech Rep,. 23-28 April 2006.

I. Leya, M. Schönbächler, U. Wiechert, U. Krähenbühl, A. N. Halliday
Titanium isotopes in solarsystem objects
69th Meteoritical Society Meeting Zürich, Switzerland, 6-11 August 2006.

K. Li
Method development for the separation and determination of ^{129}I in environmental samples
Seminar AC- Labor Spiez, Switzerland, 23 March 2006.

Ch. Stenger, U. Krähenbühl, B.A. Hofmann
Time dependant enrichment of uranium in Oman Desert chondrites
69th Meteoritical Society Meeting Zürich, Switzerland, 6-11 August 2006.

PUBLIC RELATIONS

The following actions were taken to present the scientific work of our unit to the public:

Heavy Elements
Broadcast:

- Deutschlandfunk
  Superschwere Elemente unter der Lupe
  1 June 2006.

  Deutschlandfunk
  Chemische Untersuchung des Elements 112
  9 September 2006.

Printed media:

  Solothurner Zeitung und Mittelland Zeitung
  Sternstunde für Forscher des PSI-zwei schwere Elemente entdeckt
  1 February 2006.

  Neue Züricher Zeitung
  Bestätigung für die Existenz der Elemente 113 und 115
  8 February 2006.

  PSI media release
  Chemistry with two atoms of element 112
  31 May 2006.

- PSI media release
  Superschweres Element 112 chemisch untersucht
  31 May 2006.

- der BUND
  Superschwer und ultrakurz
  2 June 2006.

  geoscience
  Durchbruch auf der Insel der superschweren Elemente
  5 June 2006.

  Neue Züricher Zeitung
  Chemische Positionierung des Elements 112
  7 June 2006.

  Frankfurter Allgemeine Zeitung
  Flüchtige Chemie am Rande des Periodensystems
  7 June 2006.

  Die Botschaft
  Superschweres Element 112 chemisch untersucht
  12 June 2006.

Surface Chemistry

- PSI media release
  Sonne heizt die Chemie am Boden an
  09 March 2006.

- Aargauer Zeitung
  PSI untersucht Sommersmog
  10 March 2006.

- Die Botschaft
  Sonne heizt die Chemie am Boden an
  11 March 2006.

- NZZ am Sonntag
  Sonne produziert Smog
  12 March 2006.

- Chemical & Engineering News
  Nitrous acid from sun and soil
  13 March 2006.

- St. Galler TAGBLATT
  Sommersmog
  16 March 2006.

- Neue Züricher Zeitung
  Bildungsweg für salpetrige Säure indetifiziert
  22 March 2006.

Analytical Chemistry
Printed and online media:

- PSI media release
  2.5 Grad wärmer in 150 Jahren
  20 February 2006.

- 20 Minuten
  Sibirien schmilzt: Markanter Temperaturanstieg
  20 February 2006.

- Tagesanzeiger
  Eingefrorene Umweltgeschichte Sibiriens
  21 February 2006.

- planeterde-Portal – Welt der Geowissenschaften – online
  2,5 Grad wärmer in 150 Jahren - Markanter Temperaturanstieg im sibirischen Altai
  22 February 2006.

- ETH-Life
  Eis zeigt Klimaerwärmung
  23 February 2006.

- Tagesanzeiger
  Mit Leidenschaft im Gletschereis
  7 July 2006.

Broadcast:

- SF DRS MTV Menschen Technik Wissenschaft
  2,5 Grad wärmer im Altai, Kurzbeitrag
  23 February 2006.

- Radio DRS
  Kontext: Schweizerisch-Russische Klima- und Umweltforschung
  8 March 2006.

Demonstration and presentation:

Infotage Kernkraftwerk Leibstadt
Zeitreise durchs Eis: Gletscher als Klimaarchiv
6/7 May 2006.

- Nationaler Tochtertag am PSI
  Einblick in den Berufsalltag einer Chemikerin
  9 November 2006.

LECTURES AND COURSES

Prof. Dr. H.W. Gäggeler

Universität Bern, SS2006:

- Instrumentalanalytik II (with PD Dr. M. Schwikowski)
- Summer Course at the Paul Scherrer Institut. International Summer Student Programme. (3 month)
- Kolloquium Radio- und Umweltchemie in collaboration with Paul Scherrer Institut (organized by Dr. R. Eichler)
- Allgemeine Chemie: Einführung Radioaktivität
- Umweltradionuklide und nukleare Datierungen (with Dr. S. Szidat)

Universität Bern, WS 2006/2007:

- Biochemische Methoden I (with others)
- Biochemische Methoden I. Übungen (with others)
- Heavy Element Chemistry. (with Dr. Robert Eichler)
- Praktikum Physikalische Chemie II (with others)
- Physikalische Chemie IV: Radio- und Elektrochemie, inkl. Übungen
- Instrumentalanalytik II
- Nuclear / Radiochemistry.
- Nuclear and Radiochemistry – Lab. course
- Kolloquium Radio- und Umweltchemie in collaboration with Paul Scherrer Institut (organized by Dr. R.Eichler)

Prof. Dr. U. Krähenbühl

Universität Bern, SS2006:

- Analytische Ergänzungen für Pharmazeuten
- Analytisches Praktikum für Pharmazeuten
- Praktikum Physikalische Chemie II

Universität Bern, WS 2006/2007:

- Allgemeine Chemie für Veterinär Mediziner
- Umweltchemie
- Praktikum Physikalische Chemie II

PD Dr. M. Schwikowski

Universität Bern, SS2006:

- Instrumentalanalytik II (with Prof. H.W. Gäggeler)

Dr. Robert Eichler

Universität Bern, WS 2006/2007:

- Heavy Element Chemistry. (with Prof. H.W. Gäggeler)
- Kolloquium Radio- und Umweltchemie in collaboration with Paul Scherrer Institut

MEMBERS OF SCIENTIFIC COMMITTEES EXTERNAL ACTIVITIES

Dr. Markus Ammann:

- PSI Research Commission.
- Member of the Editorial Board of Atmospheric Chemistry and Physics.

Prof. Dr. Heinz W. Gäggeler:

- Schweizerische Vereinigung für Atomenergie (SVA), executive board.
- Astronomische Kommission der Stiftung Jungfraujoch & Gornergrat.
- Jungfraujoch-Kommission der SANW.
- Member of the working group on the discovery of new elements (IUPAC).
- International Union of Pure and Applied Chemistry (IUPAC), Fellow.
- Member of the Steering Committee of EURISOL.
- Chairman of the Organizing Committee, TAN 07 Conference.

Prof. Dr. Urs Krähenbühl:

- Member of the Meteoritical Society.
- Meteoritics & Planetary Science; associate editor.
- Eidgenössische Kommission für Strahlenschutz und Überwachung der Radioaktivität.

PD Dr. Margit Schwikowski:

- Expert of the Matura Examination of Kantonsschule Baden.
- Member of the Coordinating Committee of the Pages/IGBP initiative LOTRED SA (Long-Term climate REconstruction and Diagnosis of (southern) South America).
- Scientific Editor Annals of Glaciology Volume 43 containing Papers from the International Symposium on High-Elevation Glaciers and Climate Records, held in Lanzhou, China, 5-9 September 2005.
- Schweizerische Gesellschaft für Schnee, Eis und Permafrost (SEP), board member.

DOCTORAL THESIS

Alexander Vlasenko

Aerosol flow tube study of the heterogeneous interaction between submicron mineral dust particles and gaseous nitric acid
Dr. M. Ammann / PSI
Prof. Dr. H. W. Gäggeler / PSI & Uni Bern
January 18, 2006

Timothée Barrelet

Norway spruce as an environmental archive for sulphur dioxide.
Prof. Dr. U. Krähenbühl / Uni Bern
January 26, 2006

David Bolius

Paleo climate reconstructions based on ice cores from the Andes and the Alps
PD Dr. M. Schwikowski / PSI
Prof. Dr. H. W. Gäggeler / PSI & Uni Bern
May 04, 2006

Theo M. Jenk

Ice core based reconstruction of past climate conditions and air pollution in the Alps using radiocarbon
PD Dr. M. Schwikowski / PSI
Prof. Dr. H. W. Gäggeler / PSI & Uni Bern
November 23, 2006

DIPLOMA THESIS

Christian Stenger

Bestimmung des terrestrischen Alters von Meteoriten der Gruppe L-Chondriten anhand von Urandiffusion
Prof. Dr. U. Krähenbühl / Uni Bern
February 07, 2006

Manuel Schläppi

Analyse von Quecksilber in Firn- und Eisproben vom La Ollada-Gletscher Argentiniens
PD Dr. M. Schwikowski / PSI
Prof. Dr. H. W. Gäggeler / PSI & Uni Bern
November 14, 2006

Miriam Wehrli

Source apportionment of carbonaceous aerosols for the winter smog episode 2006 in Switzerland based on radiocarbon (^{14}C) analysis
Dr. S. Szidat / Univ. Bern & PSI
Prof. Dr. H. W. Gäggeler / PSI & Uni Bern
December 19, 2006

BACHELOR THESIS

Renato Baumgartner

Nachweisgrenze und Messmöglichkeit von Palladium mittels ICP-MS
Prof. Dr. U. Krähenbühl / Uni Bern
March 06, 2006

Beat Muther

Niederschlagsbestimmung mittels ^{210}Pb-Methode anhand von Schneeproben vom Jungfraujch
PD Dr. M. Schwikowski / PSI
Prof. Dr. H. W. Gäggeler / PSI & Uni Bern
June 04, 2006

SUMMER STUDENTS

Biner Sarah
Herstellung von Targets mit Potential für hochintensive Schwerionenstrahlen
Universität Bern
July – October 2006

Pfaffen Chantal
Untersuchung der Mobilität von Halogenid-Ionen in einem Temperaturgradienten in polykristallinem Eis
Universität Bern
August – September 2006

Roost Caroline
Analyse von ionischen Spurenstoffen und stabilen Isotopen in einem Eisbohrkernstück vom Belukha Gletscher aus dem sibirischen Altai-Gebirge
Universität Bern
July – October 2006

Von Rohr Fabian
Über das Verhalten von ^{210}Po in Blei-Wismut
ETH Zürich
June – October 2006

Damine Chiffelle
3-wöchiges Berufspraktikum zur Analyse von Gletschereis mit ICP-MS
Kantonsschule Wettingen
October 2006

Corinna Müller
Schnupper-Woche, Analyse von Gletschereis
Klettgau-Gymnasium, Waldshut-Tiengen
October 2006

PATENTS

G. Beyer, R. Catherall, A. Hohn, U. Koester, J. Lettry, J. Neuhausen, H. Ravn, A. Tuerler,L. Zanini
Method for production of radioisotope preparations and their use in life science research, medical application and industry
International patent No. PCT/EP2006/000324 (2006).

VISITING GUESTS AT PSI 2006

13 January:
Th. Bartels, University of Toronto, Canada
Photolyse in Eis und Schnee und Charakterisierung der Eisoberfläche mit „laser induced fluorescence“

C. Fragnière, Philip Morris International, Neuchâtel, Switzerland
Anthropogenic platinum emission – investigations in food and environmental samples

U. Köster, Isolde / Cern, Switzerland
Summary of the results of the TARGISOL projects

13–17 February:
J. Kleffmann, Universität Wuppertal, Germany
Collaborative experiments (Univ. Wuppertal, Univ. Lyon, PSI) on the photochemical reaction of NO_2 on aerosol surfaces

13-24 February:
M. Ndour, University of Lyon, France
Collaborative experiments (Univ. Wuppertal, Univ. Lyon, PSI) on the photochemical reaction of NO_2 on aerosol surfaces

20 June:
C. Barbante, J. Gabrieli, University of Venice
Claude Boutron, Laboratoire de Glaciologie et Géophysique de l'Environnement, Grenoble, France
Chemical analysis of the Colle Gnifetti ice cores recovered in 2003

23 June:
C. E. Düllmann, GSI Darmstadt, Germany
Toward a new compound class of trans-actinides - Studies of volatile group 4 metal complexes with hexafluoroacetyl-aceton

C. Schlüchter, University Bern, Switzerland
Rekonstruktion der holozänen Gletscher-Stände in den Alpen

2 August:
T. Papina, Institute for Water and Environmental Problems, Barnaul, Russia
Future collaborative studies on ice cores from the Altai mountains

02 August – 29 September:
N. Aksenov, Joint Institute for Nuclear Research, Dubna, Russia
Theoretical and experimental studies on the behaviour of metals in liquid eutectic lead bismuth alloy

24 October – 11 November:
B. D’Anna, University of Lyon, France
Experiments on the photochemical reaction of ozone on humic acid aerosol surfaces

Transformation of organic material in the atmosphere: uptake of trace gases and light induced aging

24 October – 03 November:
A. Jamoul, University of Lyon, France
Experiments on the photochemical reaction of ozone on humic acid aerosol surfaces

13 November:
T. Baer, The University of North Carolina at Chapel Hill, USA
Studies of aerosol nucleation and gas surface reactions using synchrotron radiation mass spectrometry

15–17 November:
U. Köster, ILL Grenoble, France
Multi-neutron-capture for gamma-ray spectroscopy and more

^{39}Ar and ^{42}Ar: too valuable for ventilation!

15 November:
M. Avrigeanu, University Bucharest, Romania
α-particle semi-microscopic optical potential for low energies and medium-mass nuclei

L. Fraile, CERN, France
Mass separation at CERN ISOLDE

C. Geppert, GSI, Germany
Spectroscopy of ^{10}Be on the search for the beryllium halo nuclei charge radii

A. Krasznahorkay, ATOMKI, Hungary
Proton-neutron interaction at the proton dripline near 44V

S. Lahiri, Chemical Science Division Saha Institute, India
Possible role of "Saha Institute of Nuclear Physics - Radiochemistry group" in ERAWAST project

K. Wendt, Uni Mainz, Germany
Laser based investigations and analytics of ultra rare trace isotopes

16 November:
C. Angulo, UCL, Belgium
^{10}Be and ^{26}Al beams at UCL

L. Gialanella, INFN, Italy
Production and Applications of a ^{7}Be radioactive beam using a 3 MV Tandem Accelerator

M. Hass, Weizmann Institute, Israel
^{7}Be for measuring the cross section of the ^{7}Be(p,γ)^{8}B reaction

M. Heil, FZ Karlsruhe, Germany
Branchings in the s-process path

F. Kaeppeler, FZ Karlsruhe, Germany
^{60}Fe(n,gamma)^{61}Fe at stellar energies: Astrophysical quests and experimental challenges

A. Mengoni, CERN, France
Perspectives for measurements of neutron reaction cross sections of rare radioactive isotopes at CERN n_TOF

A. Murphy, Uni Edinborough, United Kingdom
^{44}Ti abundance as a probe of nucleosynthesis in core collapse supernovae

R. Reifarth, Los Alamos, USA
Neutron capture on radioactive isotopes for astrophysics

17. November:
G. Korschinek, TU München, Germany
AMS and radionuclides from a beam dump

F. Rösch, Uni Mainz, Germany
New radionuclide generators based on long-lived parent radionuclides

G. Rugel, TU München, Germany
Half-life measurement of ^{60}Fe

A. Wallner, Uni Wien, Austria
Availability of radionuclides for AMS – from calibration to applications

06–15 December:
M. Hutterli, British Antarctic Survey, United Kingdom
Participation on μ-tomographic measurementc on frostflowers at the SLS

20-22 December:
R. Rüegg, VAW ETH Zürich, Switzerland
C. J.L. Wilson, University of Melbourne, Australia
Preparation of thin slides of ice samples from Gornergletscher for crystal size analysis

PAUL SCHERRER INSTITUT

LABOR FÜR RADIO- UND UMWELTCHEMIE
DES PAUL SCHERRER INSTITUTS UND DER UNIVERSITÄT BERN
31. 12. 2006

UNIVERSITÄT BERN

PSI — Prof. Dr. Heinz W. Gäggeler — Uni Bern

Angela Blattmann (Secretary / 80 %)

Catrina Veraguth (Secretary / 40 %)

PD Dr. Margit Schwikowski (Deputy)

SURFACE CHEMISTRY
Dr. Markus Ammann (80 %)
Dr. Thomas Huthwelker
Dr. Konrad Stemmler
Dr. Thorsten Bartels-Rausch
Mario Birrer (80 %)
Hanna Frånberg [1]
Olga Vesna [1]
Michael Kerbrat [1]
Yulia Sosedova [1]

ANALYTICAL CHEMISTRY
PD Dr. Margit Schwikowski
Leonhard Tobler
Dr. Anja Eichler (50%)
Thomas Aemmer
Sabina Brütsch
Silvia Köchli
Theo Jenk [1]
Michael Sigl [1]
Anita Ciric [1]
Thomas Kellerhals [1]
Christian Stenger [1]
Manuel Schläppi [2]

RADIOCHEMISTRY
Dr. Sönke Szidat
Matthias Ruff [1]
Myriam Wehrli [2]

GEOCHEMISTRY
Prof. Dr. Urs Krähenbühl
Edith Vogel
Kaizhen Li [1]
Meena Zala [2]

HEAVY ELEMENTS
Dr. Robert Eichler
Dr. Rugard Dressler
Dave Piguet
Andreas Laube
Florian Haenssler [1]
Alexey Serov [1]
Lidija Josic

RADWASTE ANALYTICS
Dr. Dorothea Schumann
Dr. Jörg Neuhausen
Susanne Horn

[1] Graduate student
[2] Diploma student

AUTHOR INDEX

AFFILIATION INDEX

ATOMKI Debrecen	Institute of Nuclear Research of the Hungarian Academy of Sciences, Debrecen, Bem ter 18/C, H-4026, Hungary
CERN (ISOLDE/CERN)	Organisation (Conseil) Européenne pour la Recherche Nucléaire, CH-1211 Genève 23
CECS	Centro de Estudios Cientificos, Valdivia, Chile
EAWAG Dübendorf	Eidgen. Anstalt für Wasserversorgung, Abwasserreinigung und Gewässerschutz, Überlandstrasse 133, 8600 Dübendorf, Switzerland
ETHZ	Eidgen. Technische Hochschule Zentrum, CH-8092 Zürich, Switzerland
FLNR Dubna	Flerov Laboratory of Nuclear Reactions, Joliot Curie 6, 141980 Dubna, Russia
FZ Jülich	Forschungszentrum Jülich GmbH, Leo-Brandt-Str., D-52428 Jülich, Germany
FZ Karlsruhe	Forschungszentrum Karlsruhe, Hermann-von-Helmholtz-Platz 1, D-76344 Eggenstein-Leopoldshafen, Germany
ILL, Grenoble	Institut Laue-Langevin, 6, Rue Jules Horowitz, BP 156 - 38042 Grenoble Cedex 9, France
IWEP	Institute for Water and Environmental Problems, Siberian Branch of the Russian Academy of Sciences, 105 Papanintsev Str., RU-Barnaul 656099, Russia
JINR	Joint Institute for Nuclear Research, Joliot-Curie 6, 141980 Dubna, Moscow region, Russia
KUP	Climate and Environmental Physics, Physics Institute, University of Bern, Sidlerstrasse 5, 3012 Bern, Switzerland
LBNL	Lawrence Berkeley National Laboratory, Berkeley, CA 94720, USA
LGGE	Laboratoire de Glaciologie et Geophysique de l'Environnement, 38402 Saint Marin d'Hère, Cedex, France
NCCR Climate	NCCR Climate Management Centre, University of Bern, Erlachstrasse 9a, CH-3012 Bern, Switzerland
PSI	Paul Scherrer Institut, CH-5232 Villigen PSI, Switzerland
SLF	Institut für Schnee- und Lawinenforschung, Flüelastr. 11, CH-7260 Davos, Switzerland
TU / TUM	Technische Universität München, Physik Department E 15, James-Franck-Strasse, D-85748 Garching, Germany
UCI	University of California, Chemistry Departement, Irvine, CA 92697, USA
Univ. Bern	Departement für Chemie und Biochemie, Universität Bern, Freiestr. 3, CH-3012 Bern, Switzerland
Univ. Erlangen	Friedrich-Alexander Universität Erlangen-Nürnberg, Physikalische Chemie II, Egerlandstrasse 3, D-91058 Erlangen, Germany
Univ. Lyon	IRCELYON - Institut de Recherches sur la Catalyse et l'Environnement de Lyon UMR5256 CNRS-Université LYON 1, Domaine Scientifique de la Doua, Batiment J. Raulin - 4eme Etage, 43 Bd du 11 Novembre 1918, F-69622 Villeurbanne Cedex, France
Univ. Mainz	Universität Johann Gutenberg, Institut für Kernchemie, 55128 Mainz, Germany
Univ. Venice	University of Venice, 30123 Venice, Italy
Univ. Wuppertal	Physikalische Chemie/FB C, Bergische Universität Wuppertal, 42097 Wuppertal, Germany
ZSR Hannover	Zentrum für Strahlenschutz und Radioökologie, Universität Hannover, Hannover, Germany